CHLORIDE SIGNATURE AND TRANSPORT IN AN URBAN-AGRICULTURAL WATERSHED

Andrew Oberhelman

80 pages

Manual and high frequency observations (n = 535) of chloride (Cl^-), bromide (Br^-), nitrate (NO_3-N), sodium (Na^+), calcium (Ca^{2+}), and potassium (K^+) of stream and tile-drain waters were conducted in an urban-agricultural watershed (8% urban, 87% agriculture) to investigate the importance of stormflow to Cl^- transport and to explore potential differences in the signature of Cl^- originating from an urban source as compared to an agricultural source. The study was conducted in Evergreen Lake Watershed (ELW) located in central Illinois. Manual samplings were conducted on a weekly interval from February 2018 to February 2019 at three station along Six Mile Creek (SMC), the main drainage of ELW. All storm events were sampled at high frequency at the most downstream station while select storm events were sampled at an upstream station to compare how export changes along the stream. Nearly all surface water and tile water samples had Cl^- concentrations above the calculated background threshold of 18 mg/l. Mann-Whitney U test show ratios of Cl^- to Br^- ($p = 0.045$), NO_3-N ($p < 0.0001$), Ca^{2+} ($p < 0.0001$), and Na^+ ($p < 0.0001$) to statistically significantly different between urban and agricultural waters. Cl^- ratios indicate that road salt is the dominant source of Cl^- in ELW while KCl fertilizer is an important secondary source. Total Cl^- export during the study period was 777055.8 kg. Storm events are vital to Cl^- export in ELW, accounting for 57.64% of total Cl^- load during only 19% of the study period. The importance of storm events varies seasonally with winter and spring storms accounting for nearly half of total Cl^- export, while summer and fall storm event account for only 10% of total export. Results imply two periods of Cl^- flushing in ELW. The first is associated with flushing of road salt

from impervious surfaces following the cold season and second is associated with flushing salt build up from the dry season. When road salt is present on watershed surfaces increased discharge always corresponds with increased Cl^- load. During storm events when road salt is not present on watershed surfaces increased in discharge corresponds with increased Cl^- load at lower discharges. At higher discharges the relationship reaches an asymptote where further increases in discharge do not correspond with increased Cl^- load. Tile drains do not appear to impact the asymptotic behavior of Cl^- load-discharge relationship. This study demonstrates that deicing in watersheds where urban land use is minimal can have a profound impact on Cl^- dynamics.

KEYWORDS: Road Salt, Chemical Ratios, Land Use, High Frequency Sampling, Tile Drain

CHLORIDE SIGNATURE AND TRANSPORT IN AN URBAN-AGRICULTURAL WATERSHED

Andrew Oberhelman

A Thesis Submitted in Partial
Fulfillment of the Requirements
For the Degree of

MASTER OF SCIENCE

Department of Geography, Geology, and the Environment

ILLINOIS STATE UNIVERSITY

2019

CHLORIDE SIGNATURE AND TRANSPORT IN AN URBAN-AGRICULTURAL WATERSHED

Andrew Oberhelman

COMMITTEE MEMBERS:

Eric W. Peterson, Chair

Catherine M. O'Reilly

Walton R. Kelly

ACKNOWLEDGMENTS

I would like to thank my committee chair, Dr. Eric Peterson, for his continuous support and guidance during the course of this work. I would also like to thank my other committee members Dr. Catherine O'Reilly and Dr. Walton Kelly for their advice and feedback. This work was funded by the Illinois Groundwater Association and Illinois State University. Special thanks to the City of Bloomington, McLean County, and Rick Twait for the usage of equipment, advice, and assistance with field work. Analysis of samples would not have been possible without the help of Tony Ludwig from the Illinois State Department of Chemistry. Thanks to Kathy Alt for permission to sample and gauge Six Mile Creek on her land.

CONTENTS

ACKNOWLEDGMENTS i

CONTENTS ii

FIGURES iv

TABLES vi

CHAPTER I: INTRODUCTION 1

Road Salt and Freshwater Salinization 1
Objectives, Questions, and Hypotheses 4
CHAPTER II: METHODS 6

Study Area 6
Fertilizer Use 8
Field Methods 9
Weekly Sampling 9
Storm Event Sampling 10
Tile Drain Sampling 10
Groundwater Chemistry 10
Data Collection 11
Sample Analysis 11
High Frequency Data 11
Data Analysis 12
Discharge and Load 12
Background Concentrations 15
Box Plots and Chemical Ratios 15
CHAPTER III: RESULTS 16

Overview 16
Water Chemistry and Chloride Ratios 21
Anions 21
Cations 25
Chloride Ratios and Ratio Plots 30
Chloride Transport 38
Event and non-event load 38

Seasonal Load 41
CHAPTER IV: DISCUSSION 44
Overview 44
Water Chemistry and Chloride Source 45
Impact of Storm Events on Chloride Load and Concentration 51
CHAPTER V: CONCLUSION 56
REFERENCES 59
APPENDIX A: WEEKLY FIELD AND MAJOR ION DATA 64
APPENDIX B: EVENT SAMPLE MAJOR ION DATA 69

FIGURES

Figure		Page
1.	Map of Evergreen Lake Watershed.	7
2.	Rating curves for Six Mile Creek at WS1 and WS1.5.	13
3.	(A) Daily precipitation, (B) calculated discharge at WS1, and (C) calculated discharge WS1.5 during the study period.	14
4.	Cumulative probability plots for (A) NO_3-N, (B) Cl^-, (C) Na^+, and (D) K^+ with background threshold concentration labeled.	19
5.	Boxplots for NO_3-N, Cl^-, and Br^- using data from all samples grouped by location or type (tile or well).	23
6.	Timeseries of Cl^- concentration.	24
7.	Timeseries of NO_3-N concentration.	24
8.	Boxplots for Ca^{2+}, Na^+, and K^+ using data from all samples grouped by location or type.	27
9.	Timeseries of K^+ concentration.	28
10.	Timeseries of Na^+ concentration.	28
11.	Timeseries of Ca^{2+} concentration.	29
12.	Na^+ vs. Cl^- with 1:1 line in red.	34
13.	Cl^- vs. NO_3-N with samples grouped by (A) sample location/type and (2) season.	35
14.	Cl^-/Br^- ratios vs. Cl^- concentration of all samples with measurable Br^-.	36
15.	K^+ vs. Cl^- with 1:1 in in red.	37
16.	Ca^{2+} vs. Cl^- with 2:1 line in red.	37

17.	(A) Cumulative load by season and seasonal storm during the calculation period at WS1 (TCL –Total cumulative load, SCL – Total storm cumulative load, PoTCL – Percent of total cumulative load, PoSCL – Percent of total storm cumulative load).	39
18.	Cumulative load (solid line) and hydrograph (dotted line) at WS1 for the study period.	40
19.	Cumulative load (solid line) and discharge (dotted line) for a spring storm at WS1 and WS1.5.	40
20.	Plot of instantaneous Cl^- flux against discharge with data sorted by season.	43
21.	Combination Cl- concentration timeseries (dashed red) and hydrograph (black) at WS1.	56

TABLES

Tables		Page
1.	Maximum, minimum, and median values for select ions in mg/l.	20
2.	WS2 and tile drain molar chloride ratio Mann-Whitney U test results.	33

CHAPTER I: INTRODUCTION

Road Salt and Freshwater Salinization

Natural salinity in freshwaters originates from rock weathering, sea spray, and rainfall. Anthropogenic activities such as irrigation, resource extraction, wastewater treatment, land clearing, industry, and road deicing have greatly increased the salt concentration in freshwaters around the world (Schulz and Cañedo-Argüelles, 2018; Dugan et al., 2017; Cañedo-Argüelles et al., 2016; Gutchess et al., 2016; Kaushal et al., 2005). Increased freshwater salinity is a growing environmental problem linked to biological degradation, reduced ecosystem functioning, and threatens water resource security (Schulz and Cañedo-Argüelles, 2018; Cañedo-Argüelles et al., 2016; Cañedo-Argüelles et al., 2013).

In northern regions salinization, represented by increased chloride (Cl^-) concentration, is associated with a dramatic increase in the use of deicing salts since 1940 (Ledford et al., 2016; Jackson and Jobbágy, 2005; Kaushal et al., 2005). The most common deicing salt is sodium chloride, but magnesium and calcium chloride are used when the freeze point of water needs to be depressed further (below -18 °C). The United States alone applied 24.5 million megagrams of rock salt for driver safety in 2014, accounting for 45% of total salt consumed in the U.S. that year (Lilek, 2017). While deicing salts are vital to driver safety under winter conditions, elevated Cl^- concentrations can damage ecosystems, infrastructure, and drinking water supplies (Rivett et al., 2016; Kushal et al., 2005).

Cl^- is a conservative and highly mobile ion that is not easily removed from aquatic systems. Its harmful impacts at elevated levels are well documented (Wyman and Koretsky, 2018; Prosser et al., 2017; Cañedo-Argüelles et al., 2013; Nelson et al., 2009; Kushal et al., 2005). These include invasion of saltwater species into previously freshwater ecosystems, altered lake chemistry and

mixing, stream acidification, altered mortality and reproduction of aquatic plants and animals, and altered wetland communities (Kushal et al., 2005). Even at relatively low concentrations (~100 mg/l) Cl^- can alter microbial communities and inhibits denitrification (Kushal et al., 2005). Seasonal Cl^- fluctuations related to deicing also harm freshwater aquatic life because they cannot adjust to the resultant changes in osmotic potential (Cañedo-Argüelles et al., 2013; Kushal et al., 2005).

Another impact of deicing salts is the degradation of water supplies (Stets et al., 2017). A salty taste is imparted at 250 ppm Cl^- and waters become toxic to humans at higher concentrations. The U.S. Environmental Protection Agency (USEPA) has set the acute and chronic water quality limits for Cl^- of 860 mg/l and 250 mg/l respectively (Ledford et al., 2016, USEPA 2011). Cl^- rich waters have also been shown to mobilize soil bound heavy metals such as cadmium and lead and leach lead from pipes (Nelson et al., 2009; Edwards and Triantafyllidou, 2007). Furthermore, the cations associated with deicing salts, particularly sodium, also have the potential to harm aquatic ecosystems and humans (Kushal et al., 2005). Sodium concentrations above 20 mg/l have been labeled harmful by the EPA to those suffer from hypertension. Tyree et al. (2017) found that even small increases in the concentration of sodium (7-14 mg/l) can be harmful to detritivores, which could alter stream processes.

The magnitude of salinization in northern regions has a strong relationship with land use, with urban land use associated with largest increase in Cl^- concentration (Dugan et al., 2017; Lax et al., 2017; Kushal et al., 2005; Herlihy et al., 1998). Overland flow during precipitation and melt events is the primary transport mechanism for deicing salt to streams and shallow groundwater (Ledford et al., 2016; Rivett et al., 2016; Cañedo-Argüelles et al., 2013). Elevated baseflow salinity is attributed to storage of road salt derived Cl^- in groundwater (Cañedo-Argüelles et al., 2013;

Kelly et al., 2008; Kushal et al., 2005). Wind and spray form vehicle tires also play a role in movement of salt off roads and into freshwater systems (Cañedo-Argüelles et al., 2013). Compounds used in water softeners and to treat wastewater are other sources of Cl^- in urban areas that have been shown to contribute to salinization (Hubbart et al., 2017; Lax et al., 2017).

Even small increases in the amount of impervious surface cover have resulted in salinization (Dugan et al., 2017; Kushal et al., 2005). A recent study found that urban or rural lakes surrounded by >1% impervious surface cover exhibit increasing Cl^- trends (Dugan et al., 2017). However, to a lesser degree, agricultural land use is also associated with elevated Cl^- concentration (Hubbart et al., 2017; Lax et al., 2017; Ludwikowski, 2016). The relationship between land use and salinization is thus complicated in urban-agricultural watersheds. While urban Cl^- sources are dominant, agricultural Cl^- has the potential to contribute to unanticipated levels of salinization in rural and urban-rural watersheds.

The threat posed by salinization to aquatic ecosystems and drinking water supplies make the study of Cl^- dynamics imperative. While many studies have explored the residence time of Cl^- at stream and basin scales few have explored Cl^- load dynamics at high resolution in salt impacted streams (Hubbart et al., 2017; Ludwikowski, 2016; Gutchess et al., 2016; Rivett et al., 2016; Kelly et al., 2008). High intensity sampling of base and storm flows is needed to shed light on the dynamics of acute and chronic Cl^- concentrations as well as the role of storms in flushing salt from the subsurface. Understanding these dynamics is essential in evaluating the risk of salinization to specific aquatic ecosystems and water supplies. Thus, a study that explores the importance of storm events to Cl^- transport dynamics is warranted.

Furthermore, it is not clear why salinization has been seen in rural watersheds where the impacts of urbanization are minimal and impervious surface cover is low (Lax and Peterson, 2009,

Kushal et al., 2005). A portion can be attributed to road salts, but few studies have explored the potential of an agricultural Cl^- sources to contribute to salinization. The primary agricultural source of Cl^- is potash (KCl), a potassium fertilizer (David et al., 2016; Panno et al., 2006a; Böhlke 2002). Nitrification inhibitors represent another potential agricultural source of Cl^-. Nitrapyrin (2-Chloro-6-(trichloromethyl)pyridine, $C_6H_3Cl_4N$) is a common nitrification inhibitor applied to fields with anhydrous ammonia fertilizer after harvest to inhibit ammonia oxidation thereby preserving the fertilizer for crop uptake (Redemann et al., 1964). Nitrapyrin in the soil degrades into 6-chloro-picolinic acid ($C_6H_4ClNO_2$), which is thought to break down through microbial action or plant uptake during which a portion is dehalogenated (Meikle and Redemann, 1966; Redemann et al., 1964). When this biota breaks down, mobile Cl^- may be released into the soil and shallow groundwater (Meikle and Redemann, 1964).

Objectives, Questions, and Hypotheses

Salinization of freshwater represents a significant threat to aquatic ecosystems and water supplies in northern regions. It is important to further understand stream and basin scale Cl^- dynamics to address the problems posed by salinization. Along with sources related to roads and urban centers, agricultural Cl^- sources are poorly understood and could represent a significant contribution to rising background Cl^- levels. This project: (1) investigates the importance of storm events to Cl^- transport and (2) identifies and assess Cl^- signatures in an urban-agricultural watershed.

1. Differentiate the signature of urban and agricultural Cl^- with chemical ratios in a multi-land use watershed:

(a) Urban and Agricultural Cl^- signature

H_0: Waters from Urban and Agricultural sources have the same $[Cl^-]$:[X] ratios (where X is either Ca^{2+}, K^+, NO_3-N, Na^+, or Br^-)

H_a: Urban and Agriculture sources have the different $[Cl^-]$:[X] ratios

(b) Cl^- source identification

Can chloride sources be identified?

2. Investigate the contribution of storm events to Cl^- transport in multi-land use watershed:

(a) Individual event and total event Cl^- load

H_0: Storm Event Cl^- Load = Non-event Cl^- Load

H_{a1}: Storm Event Cl^- Load > Non-event Cl^- Load

H_{a2}: Storm Event Cl^- Load < Non-event Cl^- Load

(b) Seasonal Cl^- load

H_0: Total seasonal storm event load will be the same among the seasons

H_a: Total seasonal event load will be different among the seasons

CHAPTER II: METHODS

Study Area

The Evergreen Lake watershed (ELW), contained within the greater Mackinaw River Basin, encompasses 106.4 km^2 in central Illinois and is part of both McLean and Woodford Counties (Fig. 1). The ELW is situated in 46 to 137 meter thick end moraine and till deposits of the Wisconsinan glaciation. (ISGS Staff, 2005; McLean et al., 1997). Agriculture and rural grassland represent the dominant land use (>87%) in the watershed (Evergreen Lake Watershed Planning Committee, 2006). Agriculture primarily consists of rotation between corn and soybean row crop. The Village of Hudson and the northern edge of the town of Normal are the main urban centers of the watershed (Fig. 1). Real estate listing in 2019 for Hudson Illinois show residences to have private septic systems. Major roads include I-39 and I-55, which respectively run north-south through the middle of the watershed and along its southeastern edge (Fig. 1).

Urban land and paved roads made up 8% of total ELW acreage in 2000 (Evergreen Lake Watershed Planning Committee, 2006). However, commercial and residential developments along I-39, the northern edge of Normal, and southern edge of Hudson have increased urban land use in ELW by approximately 2% between 2000 and 2019. Winter and summer have average temperatures of 2.2 °C and 19.4°C respectively. Average annual rainfall is 96.5 cm with the majority (61%) falling in April through September. Major sources of Cl^- rich road runoff are Normal, Hudson, and the two interstates (Fig. 1). NaCl sprayed with a 32% calcium chloride solution is the primary deicing agent used in Mclean County (Jerry Stokes, Mclean County Engineer, personal communication, 2018).

Six Mile Creek (SMC) is the largest of three major tributaries (two remain unnamed) for Evergreen Lake, one of two reservoirs serving as the source of water for the City of Bloomington (Evergreen Lake Watershed Planning Committee, 2006). The lake was created by damming SMC in 1971. The headwaters of SMC are rooted in the northern outskirts of the town of Normal. SMC flows 18.0 km from southeast to northwest crossing I-39, paralleling it along the western edge of Hudson before draining into Evergreen Lake (Fig. 1). Fields in the study area are heavily tiled and, as a result, tile discharge to SMC is a main water source.

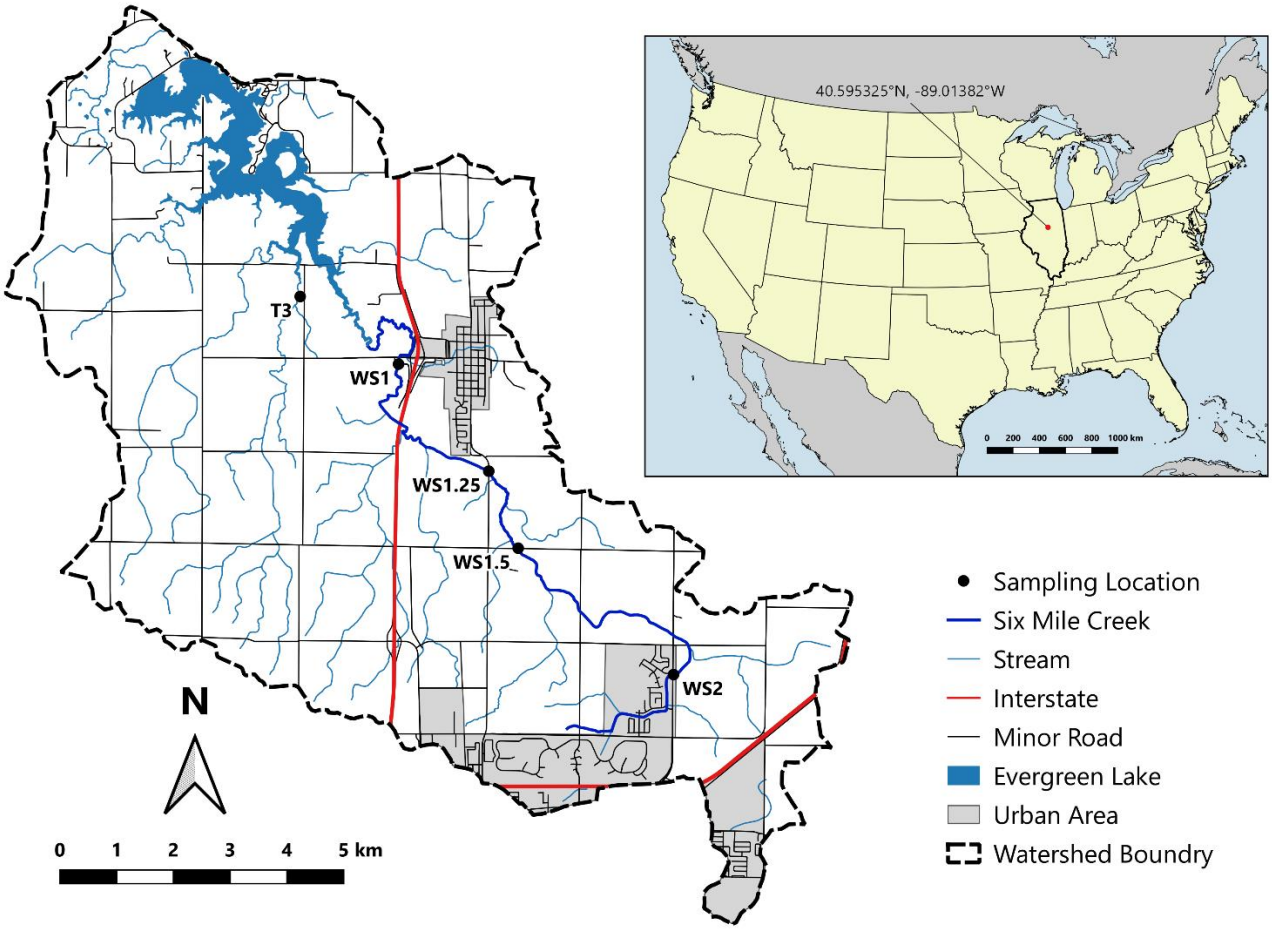

Figure 1. Map of Evergreen Lake Watershed.

Fertilizer Use

Nitrogen (N) and Phosphorus (P) are the main nutrients added to fields in ELW (Michael Ruffatti, personal communication, 2019). N is applied in the form of anhydrous ammonia or urea ammonium nitrate (Ruffatti, 2019). P is applied in the form of diammonium phosphate, which also supplies a small amount of N (Ruffatti, 2019). Timing of fertilizer application in the ELW depends on if a field is in corn-corn or corn-soybean rotation (Ruffatti, 2019). N application for farmers in a corn-corn rotation is 27% apply in the fall while 73% apply in the spring (survey). Application for corn-soybean rotation is a more even split with 45% of farmers applying N in the fall and 55% applying N in the spring (Ruffatti, 2019). In recent years (2014-2016) farmers in ELW (~2/3) have moved toward supplying nitrogen in multiple applications over the growing season (Ruffatti, 2019).

Information on the use of K^+ fertilizers is less available, and the application schedule likely varies between farmers based on soil needs and crop type. The dominant form of K^+ applied to fields in Illinois is KCl (David et al., 2016; Kelly et al., 2010; Panno et al., 2006a). In 2008 the U.S. Department of Agriculture (USDA) reported that about 80% of corn fields and 30% of soybean fields in Illinois receive annual KCl treatment (Kelly et al., 2010). Corn and soybean planted acreage in McLean county in 2018 was 314500 and 312000 respectively (USDA, 2018). Panno et al. (2006b) state based on a 2001 personal communication that ~90% of Illinois farmers apply KCl and that the KCl application rate for Illinois cropland is ~90 kg/acre every 2 years. David et al. (2016) reported application of potash every 3 to 4 years on fields owned by the University of Illinois over the course of their study.

Field Methods

Weekly Sampling

Grab samples were collected at three stream stations each week between February 16, 2018 and February 17, 2019 (Fig. 1). WS1 was chosen as the furthest downstream station because instrumentation was already in place and because it is located beneath where SMC crosses the interstate and the town of Hudson. WS2 is located at the discharge point of a stormwater retention pond receiving drainage from two subdivisions and a golf course on the northern edge of Normal. It was chosen to capture the signature of urban input to SMC. WS1.5 and WS1.25 were chosen as intermediate stations between WS1 and WS2 where flow would be continuous with WS1 to illustrate how water evolved with more agricultural input from tile drains. WS1.5 was only sampled until June 1, 2018, when permission to sample at the site was withdrawn. Sampling was shifted to WS1.25, about 1.6 km downstream. Overland flow between WS2 and the intermediate sampling sites was only continuous during high flow events because of dry conditions or complete infiltration of flow along the upper reach of SMC.

Samples were drawn directly from stream and passed through a 0.42 µm syringe filter into an acid washed 30 ml sample bottle and frozen on return to the lab. Discharge, water level, temperature, pH, dissolved oxygen, and specific conductivity were measured at each location during weekly samplings. Discharge (ft^3/s) was measured with a Stontek Flowtracker following the Six-Tenths-Depth method. These values were converted to m^3/s for load calculations. A YSI Sonde was used to measure temperature (°C), pH, dissolved oxygen (mg/l), and specific conductance (µS/cm). A weighted measuring tape was used to measure water level (m) from a fixed reference point at each site.

Storm Event Sampling

Two 24 bottle ISCO auto samplers were used to sample storm events and tile drains. One is permanently in place at WS1 and is triggered by a DTS-12 Digital turbidity sensor (Fig. 1). Select storm events at WS1.5 or WS1.25 were sampled with the second transportable ISCO auto sampler that sampled on a specified time interval. WS1 storm samples were acidified with H_2SO_4 at the time of collection while storm samples from WS1.25 and WS1.5 were not. All storms were sampled at WS1 until January 25, 2019 when in-stream instrumentation had to be removed for maintenance and due to freezing weather conditions. Storm samples were selected for processing to achieve a representative set along an event hydrograph. Samples selected for processing were filtered through a 0.42 µm glass fiber syringe filter into an acid washed 30 ml sample bottle and then frozen. ISCO bottles were acid washed between use.

Tile Drain Sampling

Tile drains were located near each stream station and were sampled on rotation each week. Samples were drawn directly from the drain if flowing and passed through a 0.42 µm syringe filter into an acid washed 30 ml sample bottle and frozen on return to the lab. Tile-drain water samples from the adjacent Lake Bloomington watershed were used to supplement tile water samples collected in ELW. The tile these samples were taken from will be referred to as T1. These samples were collected with an in place 24 bottle ISCO auto sampler that collects multiplex samples based on flow volume through the drain. These samples were filtered in the lab through a 0.42 µm glass fiber filter into an acid washed 30 ml sample bottle and then frozen.

Groundwater Chemistry

Five samples from a shallow well (< 5 meters) installed in the T3 riparian buffer zone (Fig. 1) were selected for analysis to assess the major ion composition of non-tile drain shallow

grounwater in ELW. These samples were filtered in the lab through a 0.42 µm glass fiber filter into an acid washed 60 ml sample bottle and then frozen.

Data Collection

Sample Analysis

Grab and storm samples were analyzed for major anions and cations at Illinois State University (ISU). Cation concentrations (Na^+, Ca^{2+}, K^+, Mg^{2+}) were measured on a PerkinElmer Optima 8300 Inductively Coupled Plasma Optical Emission Spectrometer. All samples were acidified with sulfuric acid before cation analysis. Anions concentrations (Cl^-, Br^-, NO_3-N, PO_4-P, SO_4^{2-}) were measured on a Dionex ICS-1100 Ion Chromatograph. Anion standards were made from salts at ISU, while cation standards were made by diluting a purchased stock solution. Data quality assurance and quality control procedures consisted of a series of matrix spikes, sample duplicates, independent standard calibration verification, and sample blanks. Raw weekly sample data can be found in Appendix A and raw storm event sample data can be found in Appendix B.

High Frequency Data

High frequency data were collected at all stream stations. At WS1 there is an RG-T Precision Tipping Bucket Rain Gauge, Meter Environment CTD, an SDI Pressure transducer, and a DTS-12 Digital turbidity sensor. Temperature (°C), stage (m), turbidity (NTU), and rainfall (mm) data are recorded on an Axiom H2 data logger while the CTD logs conductivity (mS/cm) as a separate unit. Conductivity data at WS1 are incomplete due to equipment malfunction. Stage (m) and temperature (°C) were logged on an Onset MX2001-04 level logger and sensor set at WS1.5 and WS1.25. Stage (m), temperature (°C), and conductivity (mS/cm) are logged using a Meter Environment CTD at WS2. Data were logged on a 15-minute interval on all instruments except the CTDs, which logged on a 5-minute interval.

Data Analysis

Discharge and Load

High frequency stage, manual discharge measurements, and chemical data were used to assess the importance of storm events to chloride export in SMC. The stage-discharge relationship built from weekly discharge measurements (Fig. 2) was used to create a hydrograph (Fig. 3) for each station that was paired with a 15-minute timeseries of Cl^- concentration created by assuming a constant concentration between samples. Load was estimated along a 15-minute interval by multiplying the Cl^- concentration by the calculated discharge (eq. 1).

$$\text{Load}\left(\frac{\text{kg}}{\text{s}}\right) = \text{Concentration}\left(\frac{\text{mg}}{\text{l}}\right) \times \text{Discharge}\left(\frac{\text{m}^3}{\text{s}}\right) \times \frac{1}{10^6}\left(\frac{\text{kg}}{\text{mg}}\right) \times 10^3\left(\frac{\text{l}}{\text{m}^3}\right) \quad eq.1$$

Cumulative Cl^- load was determined by multiplying the average of two subsequent load estimates by the time difference between the two, then taking the summation for all previous estimates (eq. 2). Load calculation were only performed at WS1 and WS1.5 as a reliable discharge stage relationship was unable to be determined at WS2 and WS1.25 due to sensor placement (Figs 3). Further, load was only calculated over the majority of the study period at WS1, while at WS1.5 load was calculated for only two storm events that had good sample coverage (Fig. 3B and 3C). Load at WS1 was not calculated after January 25th, 2019 as sample and stage data coverage was not good enough due to the removal of instrumentation.

$$\text{Cumulative Load(kg)} = \sum_{\text{i=1}}^{\text{n}} \left(\frac{\text{load}_\text{i} + \left(\frac{\text{kg}}{\text{s}}\right) + \text{load}_{\text{i+1}}\left(\frac{\text{kg}}{\text{s}}\right)}{2} \right) \times \left(\text{Time}_{\text{i+1}}(\text{s}) - \text{Time}_\text{i}(\text{s})\right) \quad eq.2$$

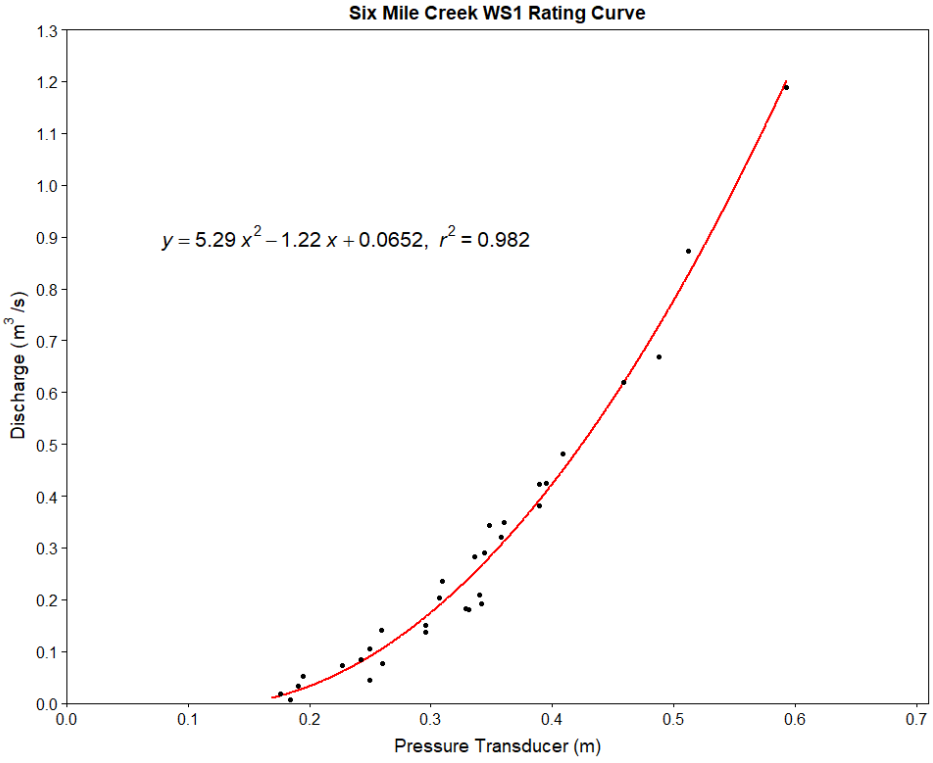

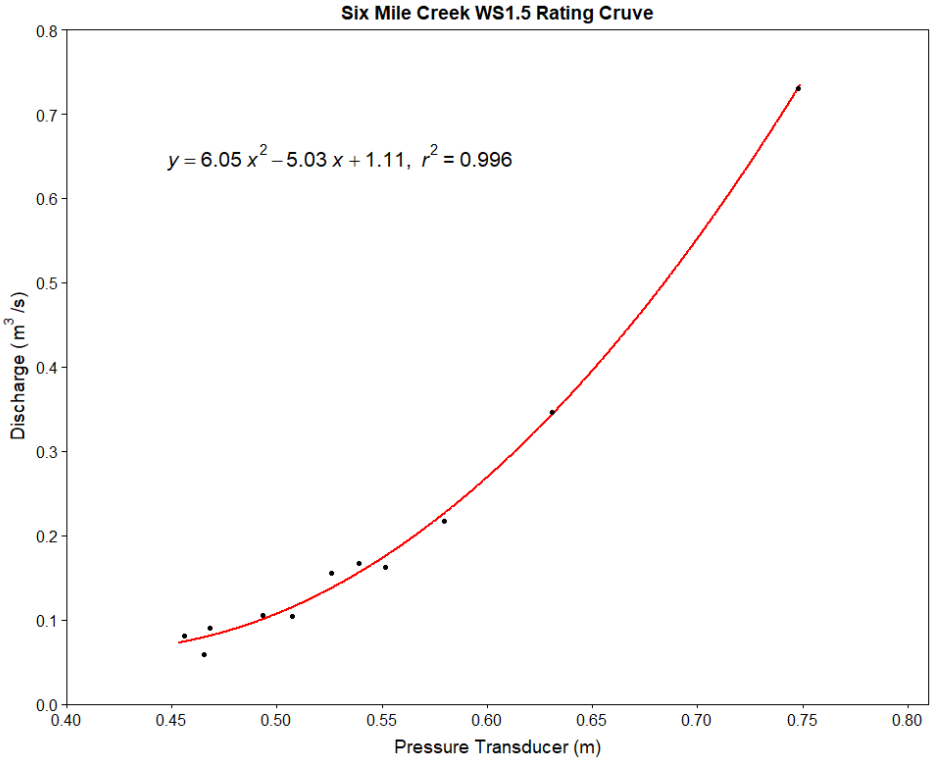

Figure 2. Rating curves for Six Mile Creek at WS1 and WS1.5.

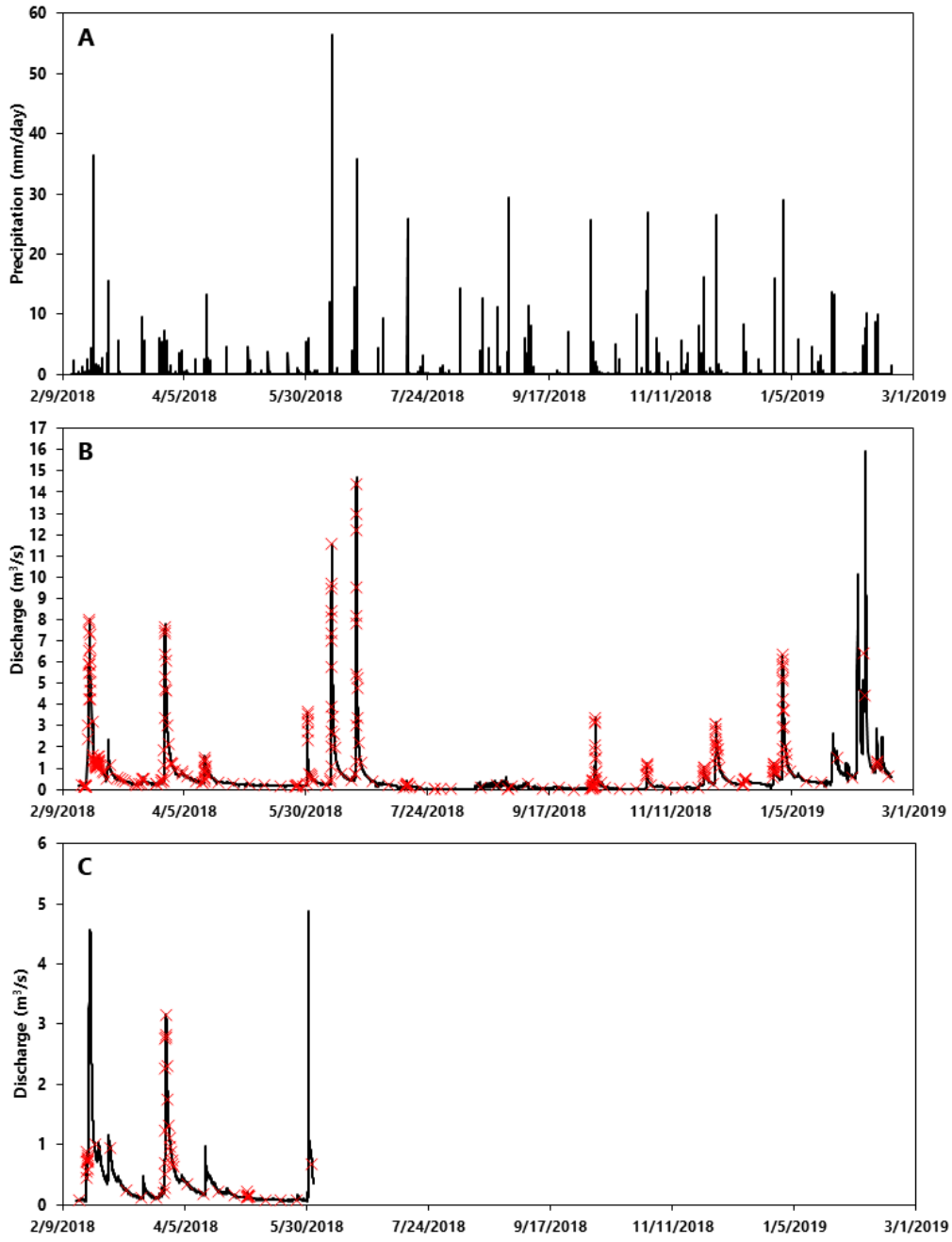

Figure 3. (A) Daily precipitation, (B) calculated discharge at WS1, and (C) calculated discharge WS1.5 during the study period. Precipitation data were collected using a rain gage at WS1. Sample collection points are marked with a red "x".

Background Concentrations

In order to assess the impact deicing and agricultural practice in SMC background concentrations of Cl^-, NO_3-N, K^+, and Na^+ were estimated using cumulative probability plots (Panno et al., 2006b). This technique operates on the idea that the chemical composition of a water contains one or more populations (e.g. different source contributions). These source contributions vary over time and space. By plotting the probability of a sample concentration relative to a sample set ($n > 100$) these sources can be defined by different slopes on a cumulative density curve. The inflection points between slopes are called "threshold" values and represent the boundary between populations with one population assumed to represent the natural background.

Box Plots and Chemical Ratios

Molar ratio plots ([X]:[Cl^-]) and box plots with data categorized by location, season, and event or non-event sample were used to assess the difference between urban and agricultural waters as well as to identify Cl^- source. In particular, the ratios of Cl^- to Br^-, NO_3-N, and Na^+ are good indicators when assessing the source of Cl^- in a water (Panno et al., 2006a; Panno et al., 2006b). Timeseries of the concentration of each major ion were also created to help assess seasonal differences between urban and agricultural waters as well as the role of storm events in movement of ions through SMC. A Mann-Whitney U test was performed to determine which [Cl]:[X] ratios differed significantly ($p < 0.05$) between urban (WS2 samples) and agricultural waters (tile drain water samples).

CHAPTER III: RESULTS

Overview

A total of 533 samples were collected and analyzed during the study period (Appendices A and B). Number of samples, maximum, minimum, and median concentrations for select major ions (Cl^-, Br., NO_3-N, Ca^{2+}, Na^+, K^+) sorted by sample location and type are shown in Table 1. These ions were chosen because they best exhibit the differences between agricultural and urban waters as well as indicate Cl^- source. Due to the sample interval at both mid-stream stations, WS1.5 and WS1.25, not representing the entire study period, thus causing the statistics to be more biased toward seasonal concentration trends, these stations were considered together when discussing major ion trends along SMC. Total precipitation in ELW during the study period was 81.25 cm. In the proceeding sections, seasons are defined as follows: winter is December 1st to February 28th, spring is March 1st to May 31st, summer is June 1st to August 31st, and fall is September 1st to November 30th.

Cumulative probability plots and estimated threshold concentrations using data collected during this study (n = 533) can be seen in Figure 4. The background threshold concentrations for NO_3-N, Cl^-, Na^+, and K^+ were estimated to be 2.5, 18.0, 4.5, and 0.5 mg/l respectively (Fig. 4). The NO_3-N threshold concentration estimate agrees with the estimates made in Panno et al. (2006b) at 2.1-2.5 mg/l and in Peterson and Benning (2013) at 2.5 mg/l for Little Kickapoo Creek, an urban-agricultural stream in a larger watershed 20 km south of ELW. Further, the Cl^- threshold concentration also agrees with previous the estimates in Panno et al. (2006b) at 15 mg. Previous threshold estimates for Na^+ and K^+ were unable to be found.

At WS1, a total of 51 weekly sampling events were completed during the study period. The maximum and minimum measured discharge during sampling events were 1.19 and 0.001 m^3/s respectively. A total of 21 storm events were sampled at WS1 until instrumentation was

removed from the stream. There were 6 events during the winter, 5 events during the spring, 4 events during the summer, and 6 events during the fall. The maximum calculated discharge of 15.95 m^3/s occurred during the winter of 2019 (Fig. 3).

At WS1.25, a total of 26 weekly sampling events were completed from July 27th, 2018 to February 17th, 2019. A single storm was sampled during the fall at this station. The maximum and minimum measured discharge during sampling events were 0.606 and 0.012 m^3/s respectively.

At WS1.5, a total of 22 weekly sampling events were competed from February 16th, 2018 to June 1st, 2018. The maximum and minimum measured discharge during sampling events were 0.730 and 0.058 m^3/s respectively. There was 1 winter, and 2 spring storm events sampled at this station, with only the two spring events having sample coverage along the entire event hydrograph (Fig. X1). One of these two events did not create a hydrograph at WS1 making an upstream-downstream comparison impossible. The maximum calculated discharge of 5.89 m^3/s occurred during the spring of 2018 (Fig. 3).

At WS2, a total of 49 weekly sampling events were completed during the study period. No storms were sampled at this station. The maximum and minimum measured discharge during sampling events were 0.248 and 0.001 m^3/s respectively. A sample of road salt impacted road run off was collected at this location during the 2019 winter. This sample had the highest measured Cl^-, Br^-, and Na^+ concentrations during the study period (Table 1).

Discharge from tile drains sampled in the ELW during the study period ranged from 0.05 l/s to 1.8 l/s. Sampled tile drains in the ELW ceased flow during the late summer and began flowing again in late fall or early winter. There were 9 tile-drain water samples collected at WS1, 5 at WS1.25, 8 at WS2, 5 at T3, and 37 at a tile in the adjacent Lake Bloomington Watershed. The 5

samples drawn from a shallow T3 well represent part of a monthly sampling regime from May to September of 2018.

Weekly discharge measurements show that discharge increased with increasing stream distance when SMC was flowing. There was an extended period of no discharge at each stream station from mid-July to early October 2018. At downstream stations (WS1.5, WS1.25, and WS1) this was the result of the loss of tile input (observed at sampled tiles in ELW) in the summer and fall. At WS2, the dry period was a result of increased evaporation from the storm water retention pond and reduced rainfall intensity during summer and fall months (Fig. 3A and B). Summer storms did cause short periods of minimal flow in SMC, although none restored tile input (Fig. 3A and B). Late summer and fall tile samples were all drawn from the tile in the adjacent Lake Bloomington watershed as there was intermittent flow from this tile during the dry period. The stream partially froze over at all stations in early February 2019 due extreme cold (< -25°C) during a polar vortex.

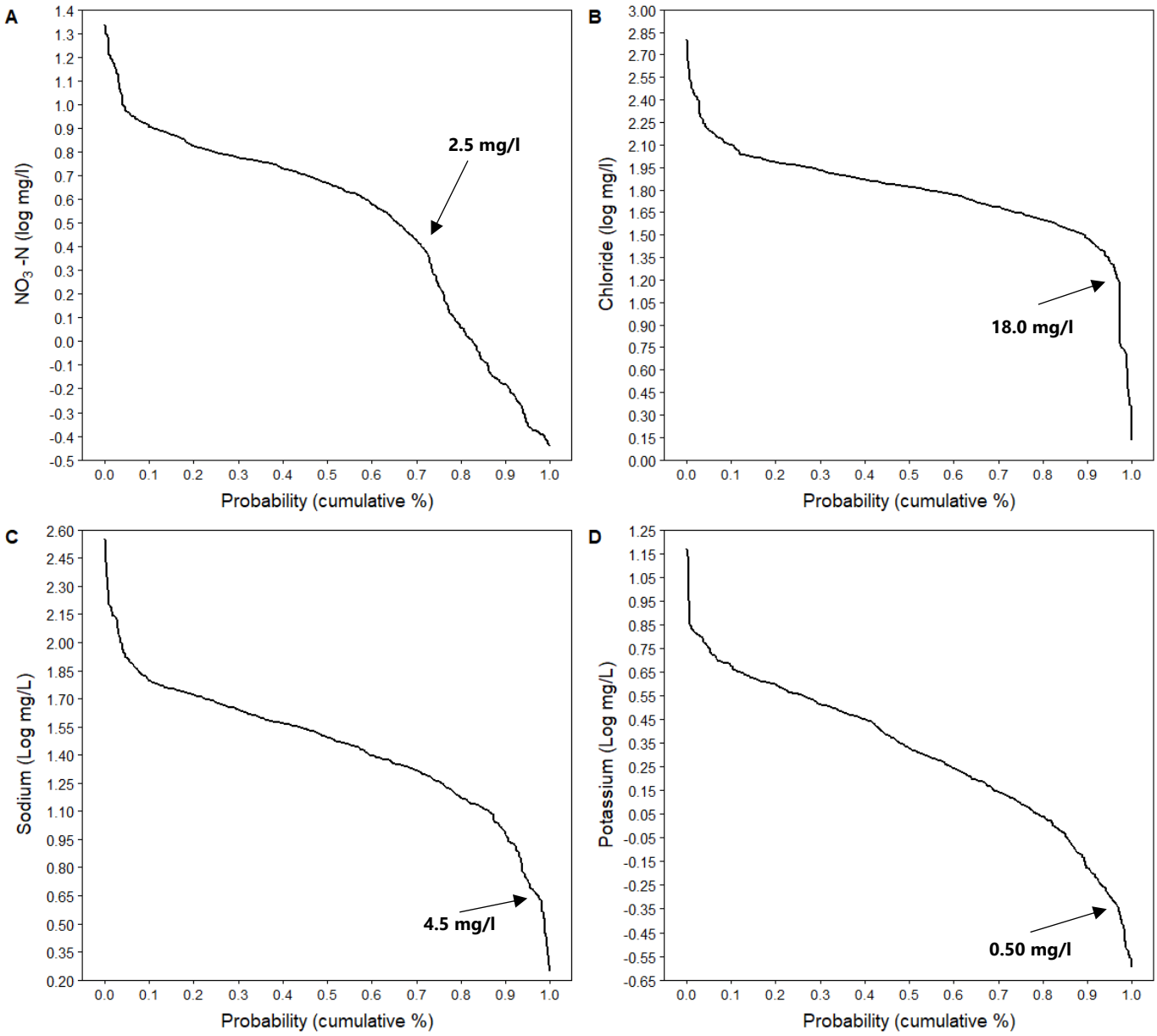

Figure 4. Cumulative probability plots for (A) NO_3-N, (B) Cl^-, (C) Na^+, and (D) K^+ with background threshold concentration labeled. The first inflection points for NO_3-N, Cl^-, Na^+, and K^+ are located at log mg/l concentrations of 0.40, 1.25, 0.65, and -0.30 respectively.

Table 1. Maximum, minimum, and median values for select ions in mg/l. Data are sorted by location/type. n indicates the number of samples

Location		Cl^-	Br^-	NO_3-N	Ca^{2+}	Na^+	K^+
WS1	Median	62.49	0.041	4.91	71.84	26.63	2.77
n = 315	Maximum	345.64	0.276	9.87	241.67	192.93	7.31
	Minimum	15.56	0.001	0.39	23.98	4.43	0.17
WS1.25	Median	65.73	0.035	0.64	70.44	37.85	2.81
n = 40	Maximum	161.45	0.143	8.38	122.51	100.28	9.00
	Minimum	36.01	0.007	0.36	17.62	12.83	1.07
WS1.5	Median	77.80	0.065	5.98	76.69	38.23	1.43
n = 52	Maximum	346.64	0.172	8.38	109.11	220.44	6.13
	Minimum	47.06	0.054	0.42	43.43	11.05	0.25
WS2	Median	84.41	0.063	1.72	56.23	42.93	2.00
n =52	Maximum	636.77	0.313	5.80	157.35	356.85	4.80
	Minimum	27.80	0.009	0.00	6.90	20.00	0.61
Tile	Median	49.05	0.020	6.92	90.43	15.28	0.64
n = 64	Maximum	464.01	0.154	21.68	210.53	268.84	14.76
	Minimum	4.45	0.001	0.92	33.04	2.17	0.28
Well	Median	2.33	0.124	0.46	105.25	3.68	0.39
n = 5	Maximum	3.02	0.296	0.75	126.72	5.95	1.80
	Minimum	1.34	0.104	0.38	95.95	2.83	0.18
Road Salt Runoff		30997.97	2.115	4.71	73.55	17491.24	62.87

Water Chemistry and Chloride Ratios

Anions

Cl^- concentration exhibited a seasonal trend during the study period (Fig. 6). Concentrations were highest during the winter and early spring, particularly during periods of high flow associated with snowmelt or precipitation (Figs. 3 and 6). These concentrations never exceeded the EPA acute toxicity limit of 860 mg/l, although the chronic limit of 230 mg/l was exceeded for short time periods (hours to days) at WS1, WS1.5, WS2, and in tile discharge (Table 1). Late spring, summer, and fall precipitation, in contrast, caused dilutions of Cl^- concentration (Figs. 3 and 6). Median Cl^- concentration was highest at WS2 at 84.41 mg/l and lowest in well water at 2.33 mg/l (Table 1). Median well Cl^- concentration was the only one to fall below the calculated background threshold. In tile drains the median Cl^- concentration was 49.05 mg/l, which is lower than median value observed at any SMC station. Median Cl^- concentration decreased downstream from WS2 to WS1 (Fig. 5). Tile drains had the second highest maximum Cl^- concentration at 464.02 mg/l after WS2 at 636.77 mg/l. Small spikes in Cl^- concentration that likely result from evaporation were observed in SMC and tile waters in the late summer and early fall (Fig. 6). Downstream Cl^- concentrations fall between those measured at WS2 and in tile drains (Fig. 6).

Over the course of this study, median NO_3-N concentrations were highest in tile drain water at 6.92 mg/l and lowest in well water at 0.46 mg/l. (Table 1 and Fig. 5). Intermediate NO_3-N concentrations were observed in SMC with median values ranging from 4.91 mg/l at WS1 to 1.72 mg/l at WS2 (Table 1 and Fig. 5). Median NO_3-N concentration generally increased downstream from WS2 to WS1 (Figs. 5 and 7). Figure 5 appears to contradict this downstream trend as WS1.5 has higher median NO_3-N concentration than WS1 while WS1.25 has a lower median concentration than WS2. NO_3-N concentrations were highest through the spring and early summer

(Fig. 7). NO_3-N concentration was lowest during the late winter and through summer and early Fall. Elevated NO_3-N concentrations were also observed in the late Fall (Fig. 7). Mirroring Cl^-, downstream NO_3-N concentrations at WS1, WS1.25, and WS1.5 tended to fall between those measured at WS2 and in tile drains (Fig. 7). NO_3-N concentrations were diluted by storm events (Figs. 3 and 7).

For many of the samples, Br^- concentrations were below detection limit. These samples were not included on ratio or boxplots. Median Br^- concentration of samples that had measurable Br^- was highest in well water at 0.12 mg/l and the lowest in tile water at 0.02 mg/l (Table 1). Intermediate median Br^- concentration ranged from 0.04 mg/l at WS1 to 0.06 mg/l at WS2. Median Br^- concentration decreased downstream from WS2 to WS1 (Fig. 5).

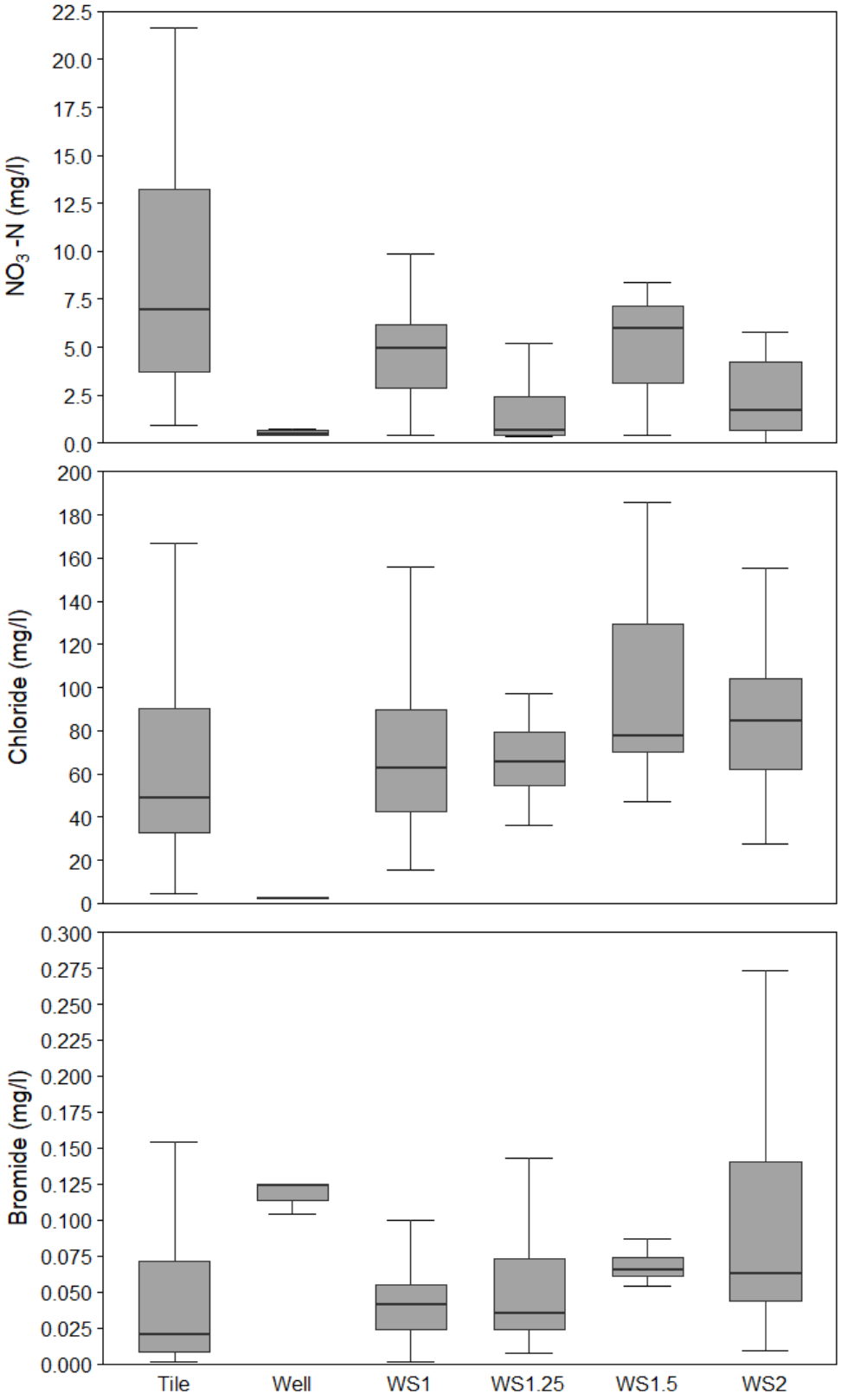

Figure 5. Boxplots for NO_3-N, Cl^-, and Br^- using data from all samples grouped by location or type (tile or well). Boxplots follow the standard Tukey definition.

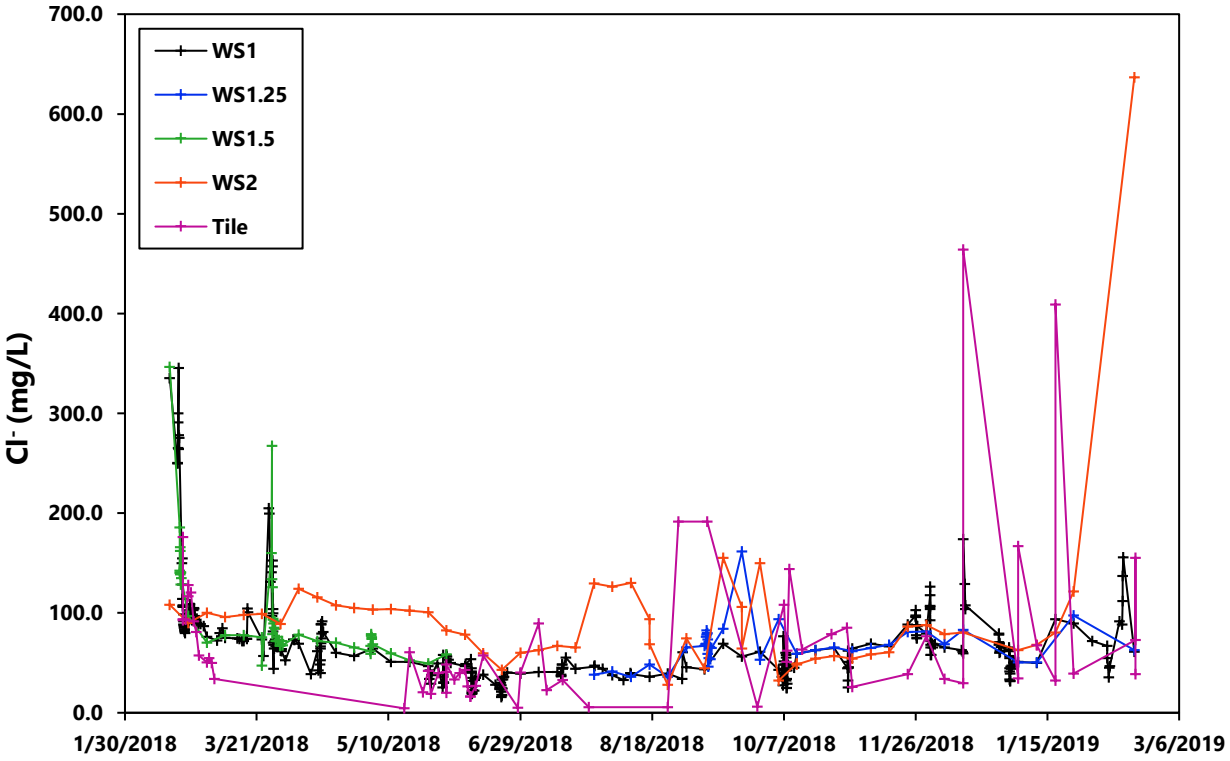

Figure 6. Timeseries of Cl^- concentration.

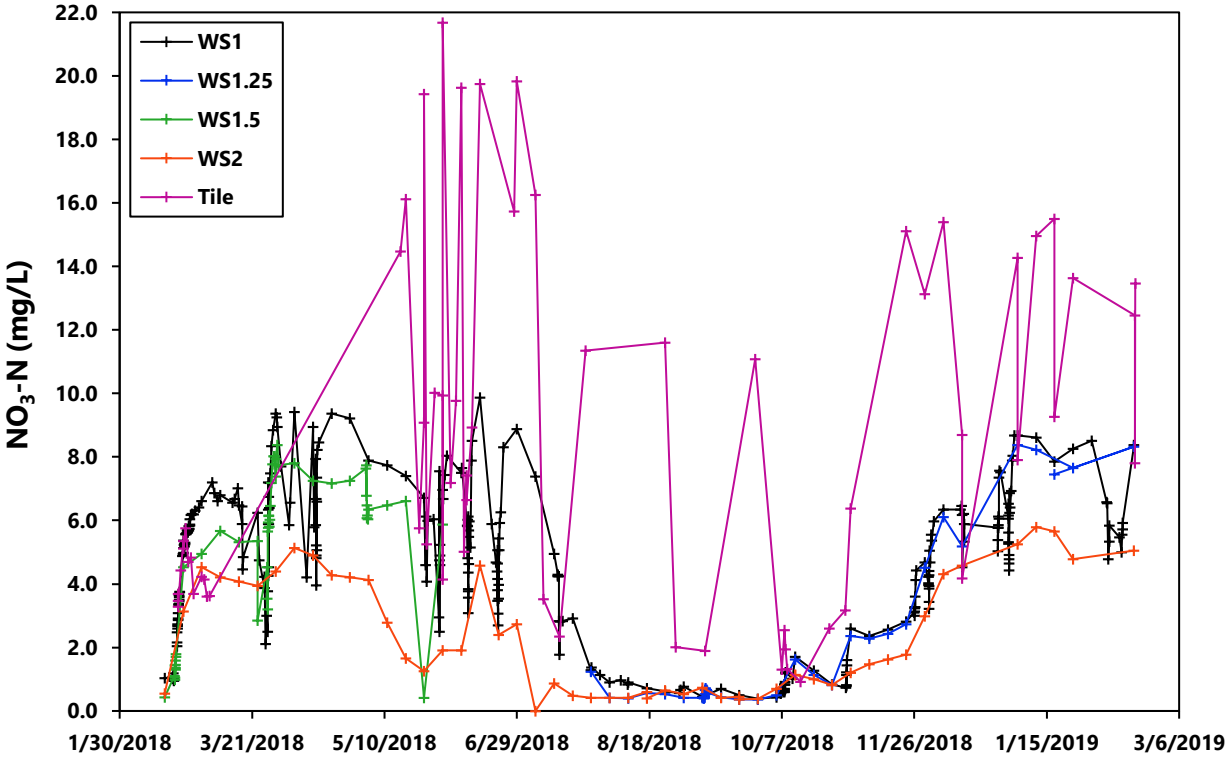

Figure 7. Timeseries of NO_3-N concentration.

Cations

Median K^+ concentration was highest at WS1.5 at 2.81 mg/l, but when WS1.25 and WS1.5 are considered together the highest median concentration is at WS1 at 2.77 mg/l (Table 1). The lowest median K^+ concentration was observed at in well water at 0.39 mg/l. Median K^+ concentration increased downstream (Fig.8), with the concentrations at intermediate station fall between that observed at WS2 and in tile drains (Fig. 9) The highest K^+ concentrations were observed during the summer and fall and are likely the result of evaporation (Fig. 9). Elevated K^+ concentrations were also seen during the winter. Spikes in K^+ concentration was observed during high flow events regardless of season (Figs. 3 and 9).

The concentration of Na^+ followed the same patters as Cl^-. Concentrations were highest during the winter and early spring, particularly during periods of high flow due to snowmelt or precipitation (Figs. 3 and 10). Late spring, summer, and fall precipitation, in contrast, caused dilutions of Na^+ concentration (Figs. 3 and 10). The highest median Na^+ concentration was at WS2 at 42.93 mg/l while the lowest was in well water at 3.68 mg/l. WS2 had the highest maximum Na concentration at 356.85 mg/l, followed by tile-drain waters at 268.84 mg/l. An increase in Na^+ concentration due to evaporation was seen in the summer and early fall (Fig. 10). Median Na^+ concentration decreased downstream from WS2 (Fig. 8), with concentrations at WS1, WS1.25, and WS1.5 falling between concentrations measured at WS2 and in tile waters (Fig. 10).

Median Ca^{2+} concentration was highest in well water at 105.25 mg/l and lowest at WS2 at 56.23 mg/l (Table 1). The median concentration of Ca^{2+} was higher in tile drain water at 90.44 mg/l than at any stream station. Tile waters also exhibited the largest maximum Ca^{2+} concentration at 210.53 mg/l (Table 1). Median Ca^{2+} concentration tended to increase downstream from WS2 (Fig. 8). Strom events caused a dilution of Ca^{2+} concentration, with select storm events in the

spring and early summer causing an increase in Ca^{2+} concentration after the initial dilution (Figs. 3 and 11). As with the other ions, WS2, WS1.25, and WS1.5 waters plot between WS2 and tile waters with respect to Ca^{2+} (Fig. 11). Evaporation appeared not to increase Ca^{2+} concentrations in the late summer and fall except for WS2 waters, which showed an increase during those months (Fig. 11).

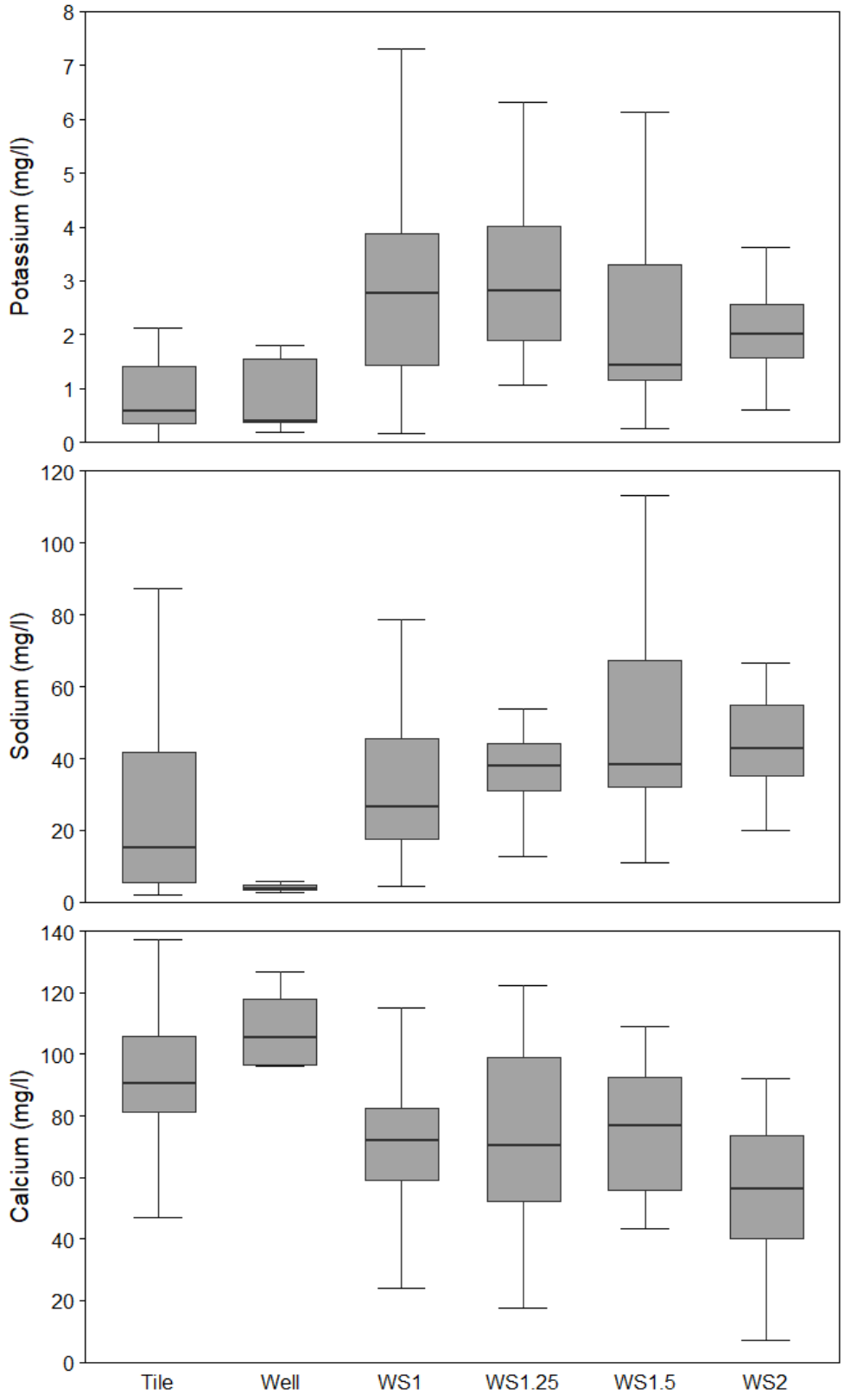

Figure 8. Boxplots for Ca^{2+}, Na^{+}, and K^{+} using data from all samples grouped by location or type. Boxplots follow the standard Tukey definition.

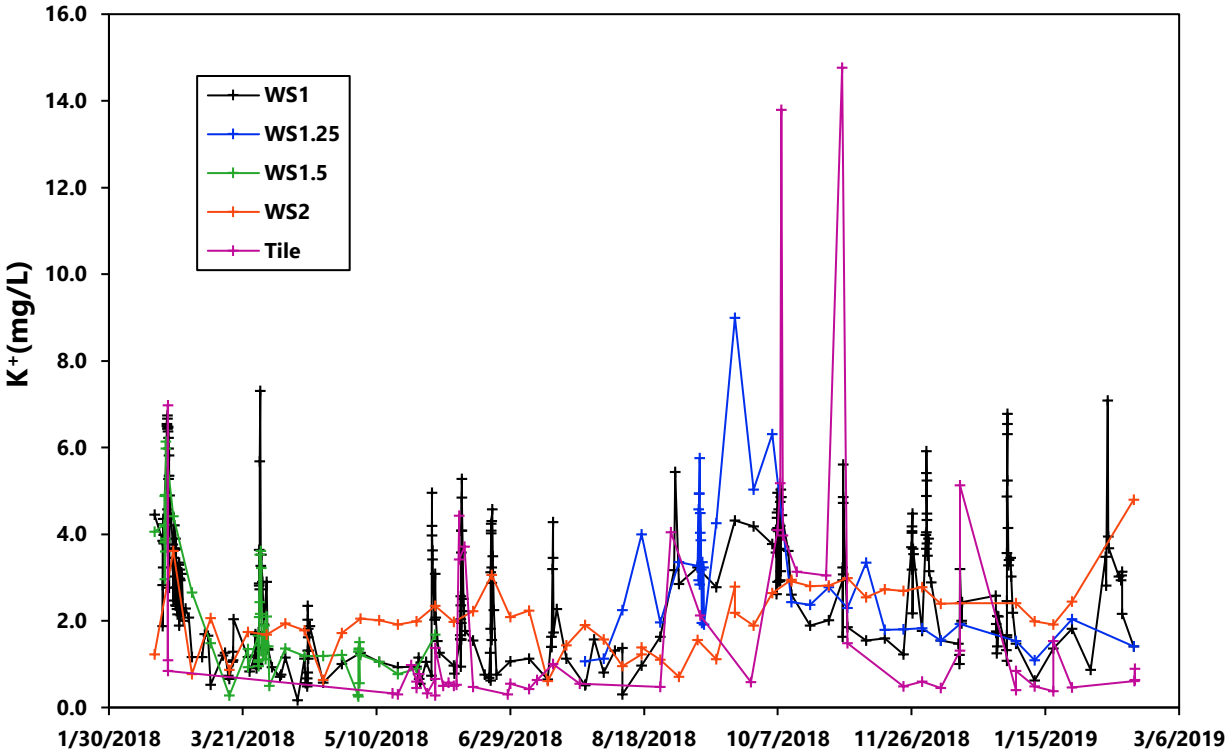

Figure 9. Timeseries of K^+ concentration.

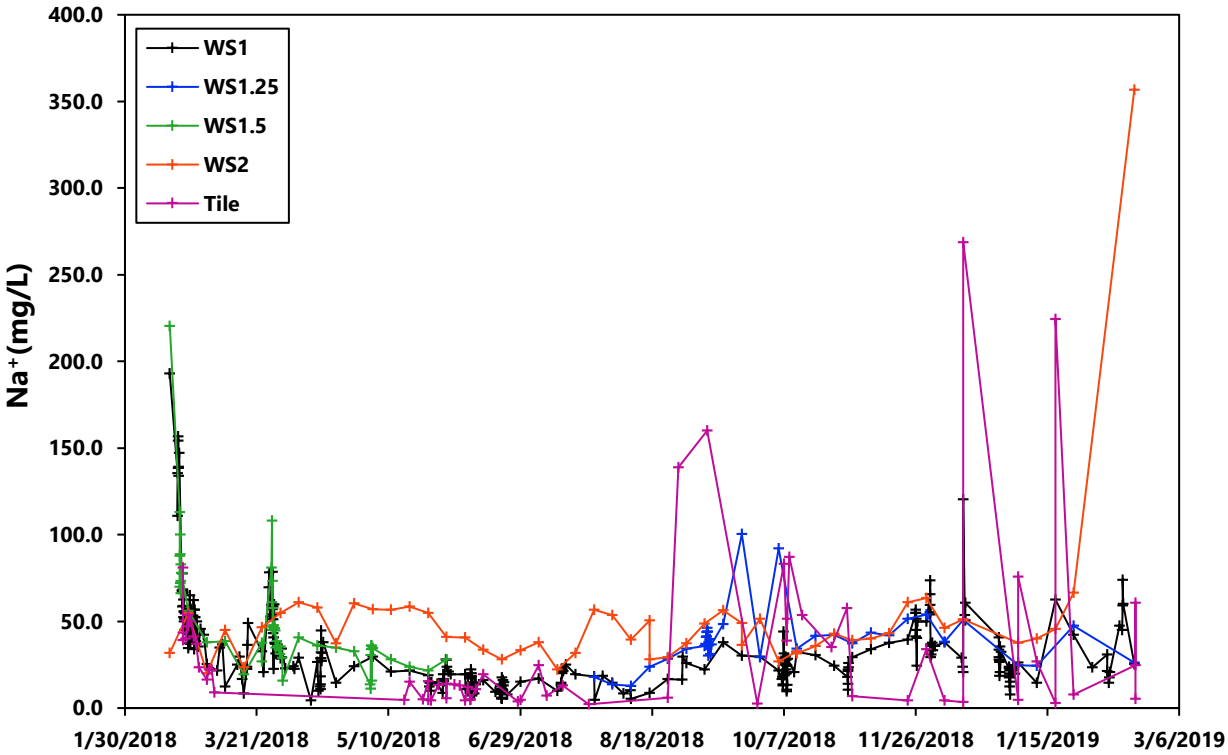

Figure 10. Timeseries of Na^+ concentration.

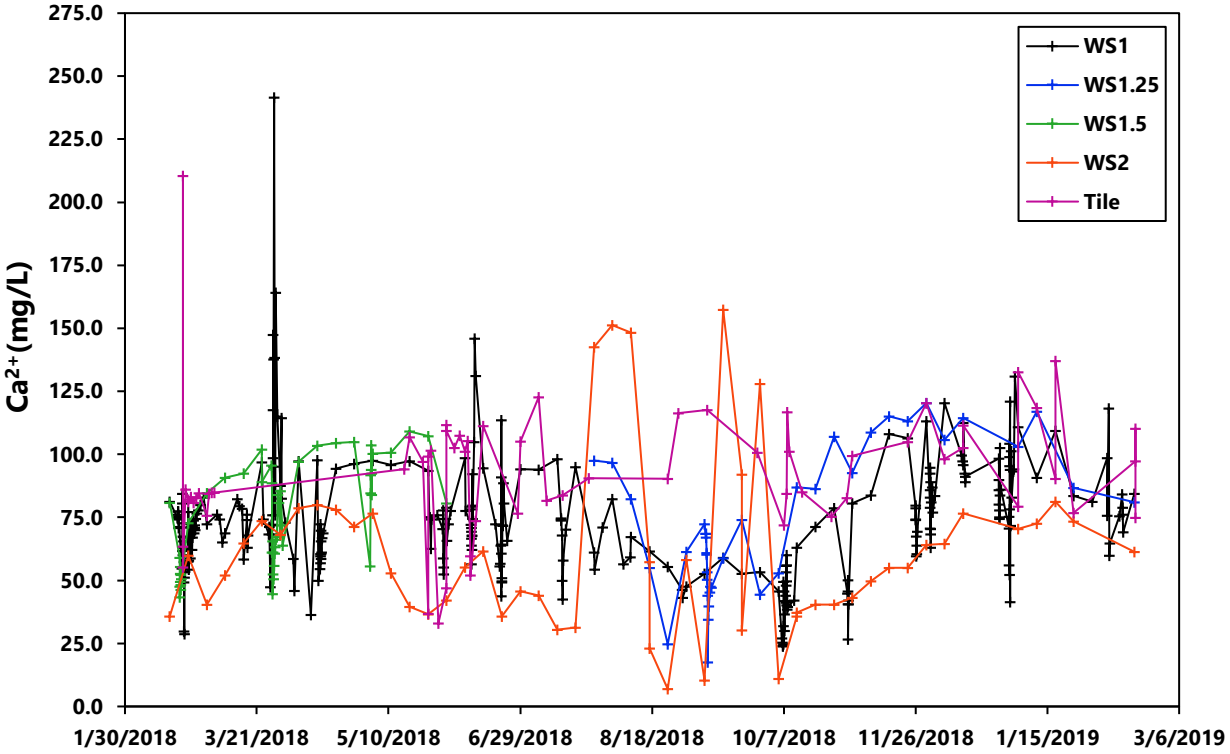

Figure 11. Timeseries of Ca^{2+} concentration.

Chloride Ratios and Ratio Plots

None of the Cl^- ratio populations were normally disturbed. Normality was assessed by visual inspection of a density plot, Shapiro-Wilk test, and with Q-Q plots. Median, maximum, and minimum ratio values for WS2 and tile-drain waters can be found in Table 2. Mann-Whitney U tests reveal that the $[Cl^-]$:[X] is significantly different ($p < 0.05$) between urban (WS2) and agricultural waters (tile drain) for all ratios except $[Cl^-]$:$[K^+]$ (Table 2). The median ratio value was higher urban water than in tile water for $[Cl^-]$:$[Ca^{2+}]$, $[Cl^-]$:$[Br^-]$, and $[Cl^-]$:$[NO_3\text{-}N]$, while tile drain water exhibited a higher median ratio value for only $[Cl^-]$:$[Na^+]$ (Table 2).

Ratios plots comparing the molar concentration of Na^+ to Cl^- reveals that most samples plot on or just below the 1:1 line (Fig. 12). Spread along the 1:1 line and drift away from it vary by season (Fig 12A). Winter samples exhibit the most spread along the 1:1 line and only minimal drift below it. Fall samples also exhibit minimal drift below the 1:1 line, but do not spread as wide as winter samples do along it. Spring samples display the second widest spread along the 1:1 line. Spring and summer samples exhibit the most drift below the 1:1 line, but separate along the line with springs samples plotting higher up the line than summer samples. Large drift below the 1:1 line occurs in some samples between 0.50 and 0.60 mg/l Cl^-. Grouping samples by location/type reveals these samples are from tile drains, although many tile-drain waters plot closer to the 1:1 line at higher Cl^- concentrations. (Fig 12B). Well water plots above the line with the lowest Na^+ and Cl^- concentrations (Fig. 12B).

On Cl^- vs NO_3-N ratio plots (Fig. 13), the rectangle in the bottom left corner defined by the threshold concentrations lines represents the domain for pristine unimpacted waters (Fig. 4). These plots indicate that almost all samples exceed the estimated background threshold Cl^- concentration of 18 mg/l while a large portion of samples are still below the estimated 2.0 mg/l background threshold concentration for NO_3-N (Fig. 13). Well water samples are the only ones to plot within

the zone for natural waters. Most tile-drain waters plot along the vector that indicates influence form nitrogen and anhydrous ammonia fertilizers, but several tile samples exhibit elevated Cl^- concentrations and plot along the road salt or animal waste/septic effluent vectors (Fig. 13A). Stream samples tend to plot on the low end of the road salt or nitrogen and anhydrous ammonia fertilizer vectors (Fig. 13A). Tile and stream samples that plot high along the road salt vector were all collected in the winter (Fig. 13B). Overall, winter samples plot along an arc between the road salt vector and the nitrogen and anhydrous ammonia Spring and summer samples make up the majority of stream samples that plot along the low end of the nitrogen and anhydrous ammonia fertilizer vector, while fall samples make up the majority of stream samples that plot along the low end of the road salt vector (Fig 13B). A few spring samples do, however, exhibit elevated Cl^- concentrations (Fig. 13B).

Most samples with measurable bromide were collected during storm events and plot in the road salt and septic effluent zone on a Cl^-/Br^- vs Cl^- plot (Fig. 14A). Tile drain are spread throughout the data cluster (Fig. 14A). Of samples that plot outside the road salt zone, some fall in the basin brine and animal waste field below the main cluster while a larger number plot above the main cluster passing through the field tile zone into an undefined area on the plot. Only one tile sample plots in the field tile zone (Fig. 14A). All well samples and 5 tiles are classified as pristine aquifer water. Spring and winter samples tend to plot further into the road salt and septic effluent zone and trend towards the sample of road salt runoff (Fig. 14A/B). Fall and summer samples overlap with the tail end of the winter and spring sample cluster and plot more towards the field tile zone (Fig. 14B).

A K^+ vs Cl^- molar ratio plot shows that nearly all samples collected during this study plot far below a 1:1 line (Fig. 15). Well water and some tile samples are the only ones to approach the

1:1 line (Fig.15). Stream samples from WS1 plot the closest to the 1:1 line of all stream stations (Fig. 15). The molar ratio plot of Ca^{2+} vs Cl^{-} shows most samples lie above a 2:1 line (Fig.16). A subset of samples plots or below the 2:1 line (Fig. 16). These samples, most of which were collected during the winter and spring, form a trend away from the main data cluster (Fig. 16).

Table 2. WS2 and tile drain molar chloride ratio Mann-Whitney U test results. $P < 0.05$ denotes a significant difference between WS2 and tile drain sample populations. Median, maximum, and minimum $[Cl^-]$:[x] values are included.

Ratio / p-value		WS2 (Urban)	Tile Drain
$[Cl^-]$:$[Na^+]$	Median	1.17	1.61
$p < 0.0001$	Maximum	3.25	7.74
	Minimum	0.59	0.58
$[Cl^-]$:$[K^+]$	Median	50.43	68.24
$p = 0.059$	Maximum	554.08	295.74
	Minimum	13.37	4.02
$[Cl^-]$:$[Ca^{2+}]$	Median	1.56	0.64
$p < 0.0001$	Maximum	11.72	4.70
	Minimum	0.94	0.05
$[Cl^-]$:$[Br^-]$	Median	1530.00	450.50
$p = 0.045$	Maximum	17961.00	11534.00
	Minimum	1093.75	63.00
$[Cl^-]$:$[NO_3^-]$	Median	16.73	2.13
$p < 0.0001$	Maximum	153.18	43.82
	Minimum	4.65	0.12

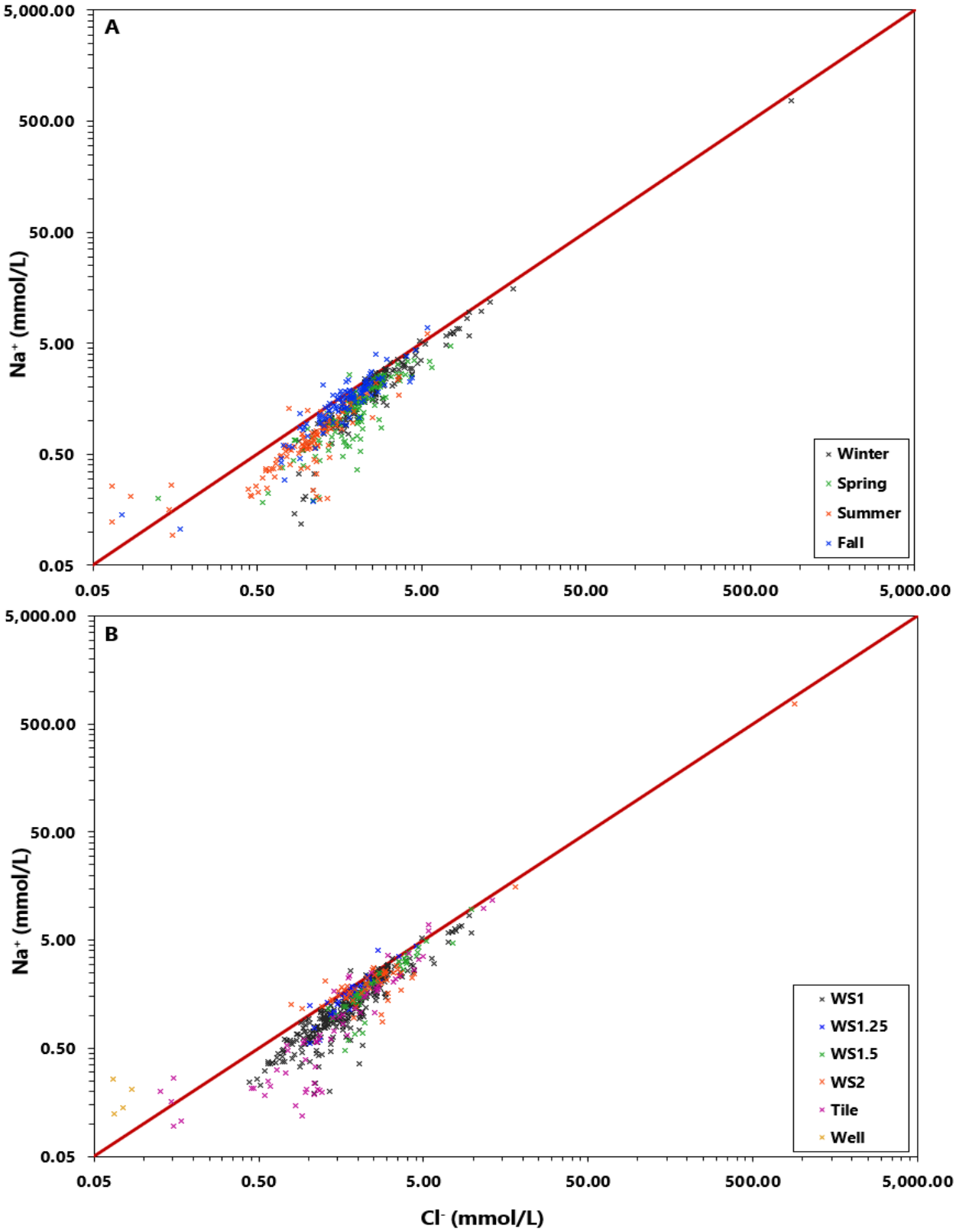

Figure 12. Na^+ vs. Cl^- with 1:1 line in red. (A) Samples are grouped by season. (B) Samples grouped by location/type.

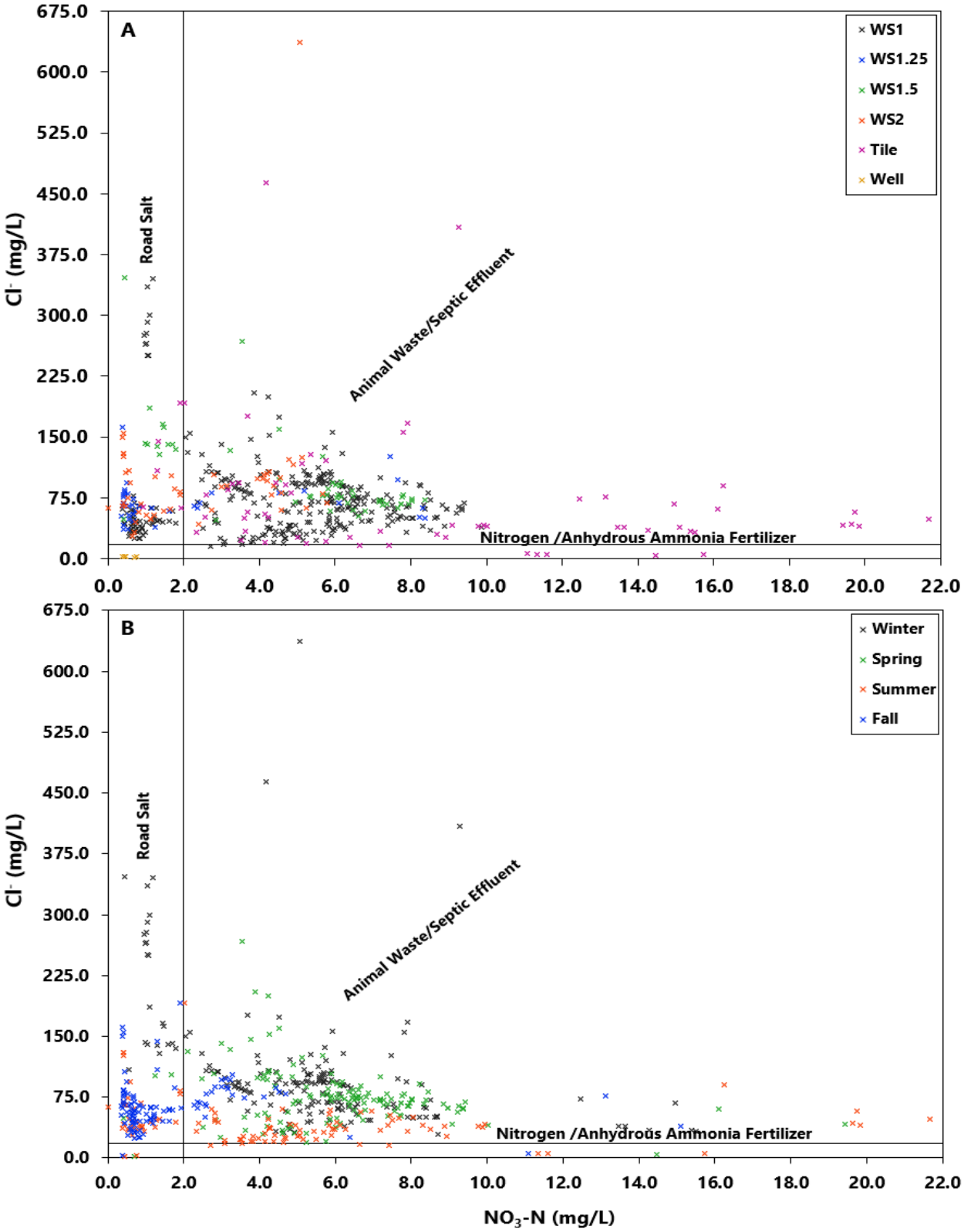

Figure 13. Cl^- vs. NO_3-N with samples grouped by (A) sample location/type and (2) season. Endmember vectors are labeled. Horizontal and vertical lines represent background threshold concentrations.

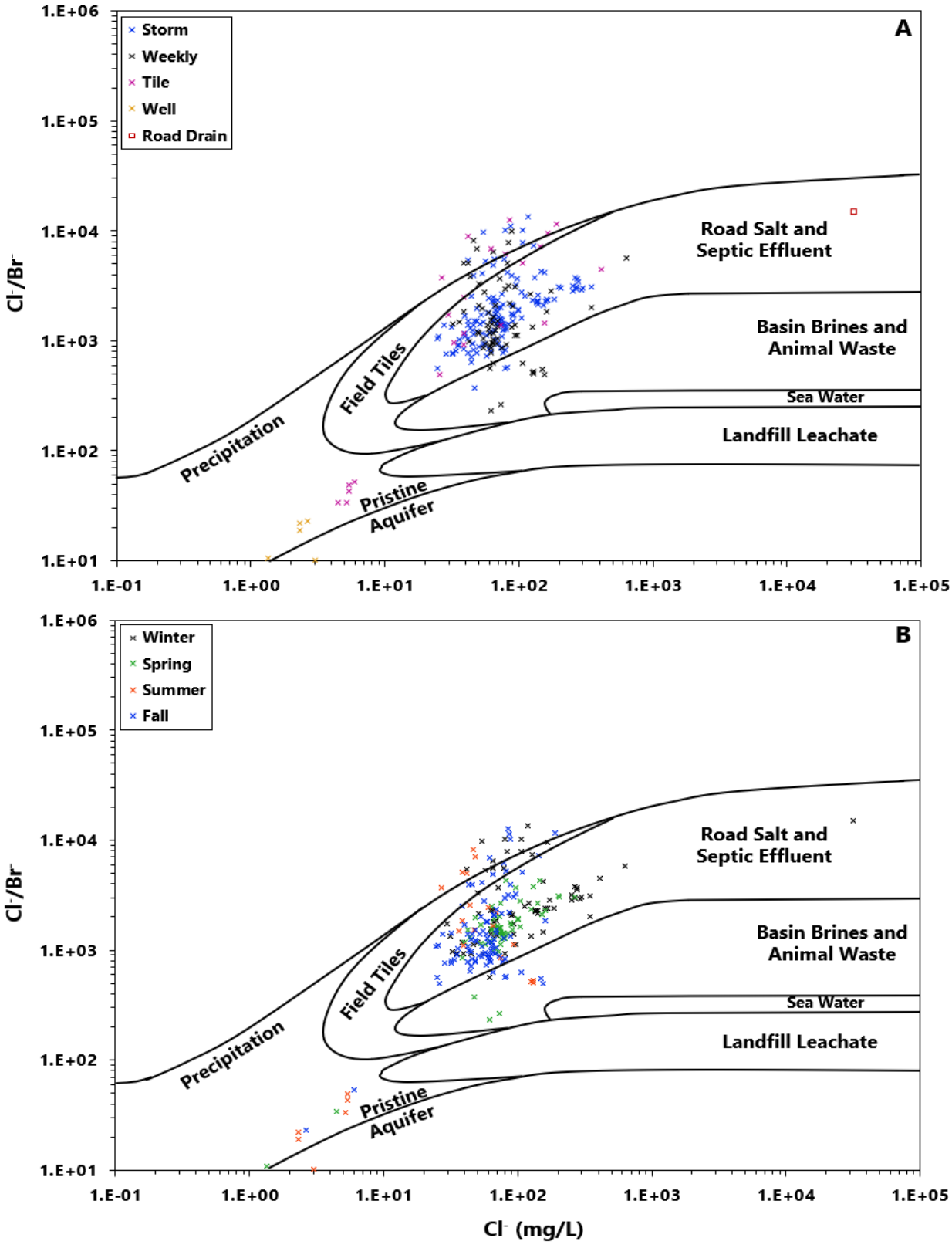

Figure 14. Cl^-/Br^- ratios vs. Cl^- concentration of all samples with measurable Br^-. Samples are grouped by (A) storm/weekly and (B) season. Endmember zones based off Panno et al. (2006a) are labeled.

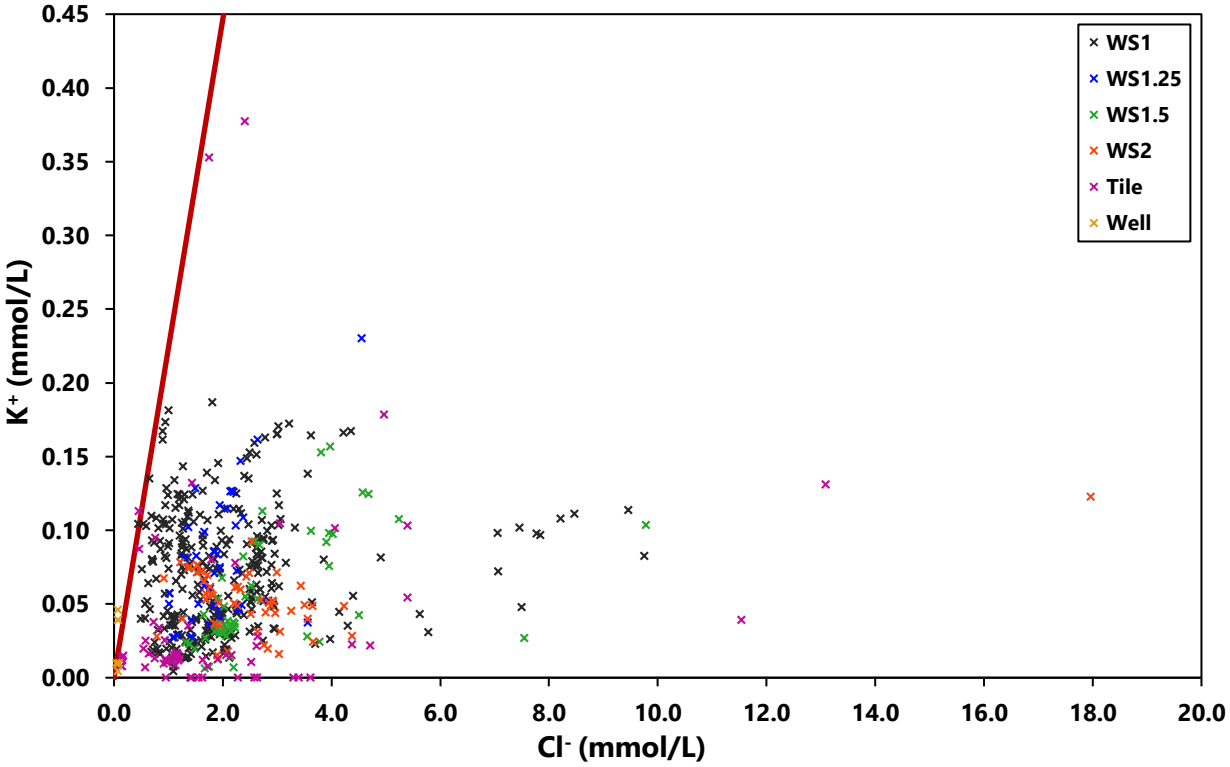

Figure 15. K^+ vs. Cl^- with 1:1 in in red. Samples grouped by location/type.

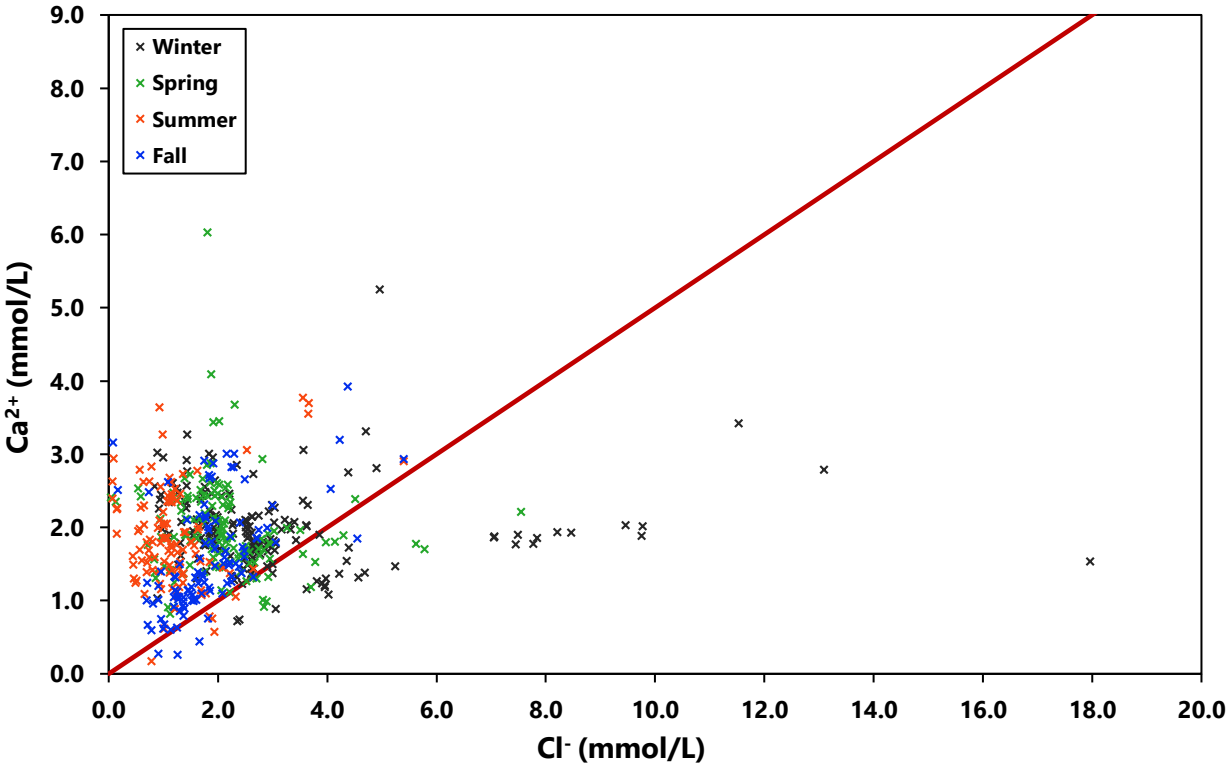

Figure 16. Ca^{2+} vs. Cl^- with 2:1 line in red. Samples are grouped by season.

Chloride Transport

Event and non-event load

Tables that contain cumulative load and flow volume quantities and percentages during event and non-event periods can be found in Appendix C. Total chloride export for the calculation period (Feb. 16th, 2018 to Jan. 25th, 2019) at WS1 was 7.77×10^5 kg (Fig. 17A). Cl^- export during storm events totaled 4.48×10^5 kg, which makes up 57.6% of the total Cl^- export. The total volume of water that flowed through SMC at WS1 for the calculation period was 1.25×10^7 m^3 (Fig. 17B). Water volume attributed to storm events was 7.25×10^6 m^3, which makes up 58.0% of the total flow volume (Fig. 17B).

A cumulative load plot illustrates that the largest contributions to Cl^- load in SMC occur during storm events (Fig. 19). This is shown as a step pattern with brief and sharp upward steps during storm events followed by a period of gradual upward slope during non-event flow (Figs. 18 and 19). The cumulative load comparison for a spring storm at WS1 and WS1.5 indicates that load in SMC grows with increasing stream distance (Fig. 19). Total export for this event at WS1 was 8.82×10^4 kg while at WS1.5 it was 5.03×10^4 kg. Most export occurred during the period of peak discharge when loading was the greatest (Fig. 19). At all points during the event cumulative load was greater at WS1.

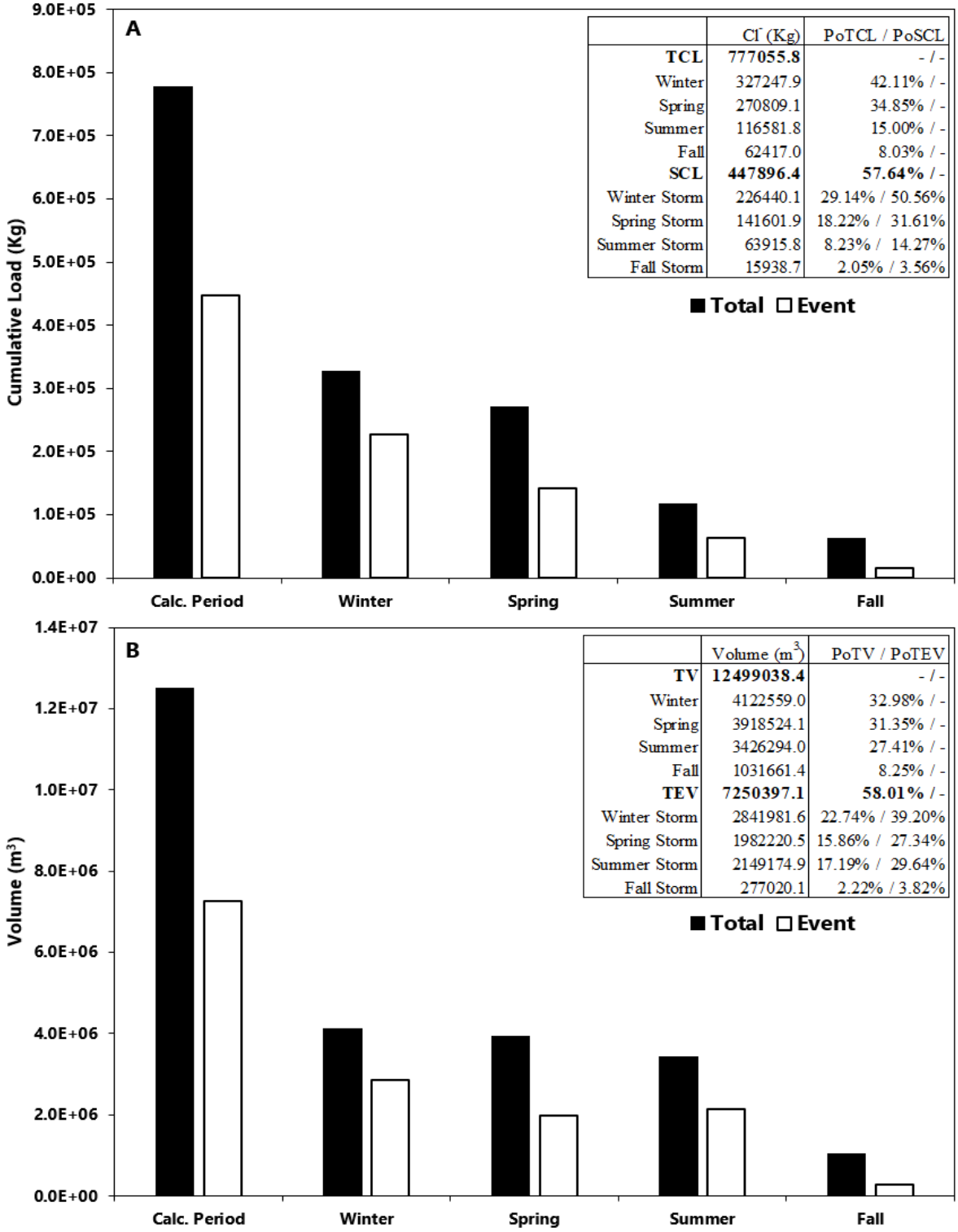

	Cl⁻ (Kg)	PoTCL / PoSCL
TCL	**777055.8**	- / -
Winter	327247.9	42.11% / -
Spring	270809.1	34.85% / -
Summer	116581.8	15.00% / -
Fall	62417.0	8.03% / -
SCL	**447896.4**	**57.64%** / -
Winter Storm	226440.1	29.14% / 50.56%
Spring Storm	141601.9	18.22% / 31.61%
Summer Storm	63915.8	8.23% / 14.27%
Fall Storm	15938.7	2.05% / 3.56%

	Volume (m^3)	PoTV / PoTEV
TV	**12499038.4**	- / -
Winter	4122559.0	32.98% / -
Spring	3918524.1	31.35% / -
Summer	3426294.0	27.41% / -
Fall	1031661.4	8.25% / -
TEV	**7250397.1**	**58.01%** / -
Winter Storm	2841981.6	22.74% / 39.20%
Spring Storm	1982220.5	15.86% / 27.34%
Summer Storm	2149174.9	17.19% / 29.64%
Fall Storm	277020.1	2.22% / 3.82%

Figure 17. (A) Cumulative load by season and seasonal storm during the calculation period at WS1 (TCL –Total cumulative load, SCL – Total storm cumulative load, PoTCL – Percent of total cumulative load, PoSCL – Percent of total storm cumulative load). (B) Discharge volume by season and seasonal storms during the calculation period at WS1 (TV – Total volume, TEV – Total event volume, PoTV – Percent of total volume, PoTEV – Percent of total event volume).

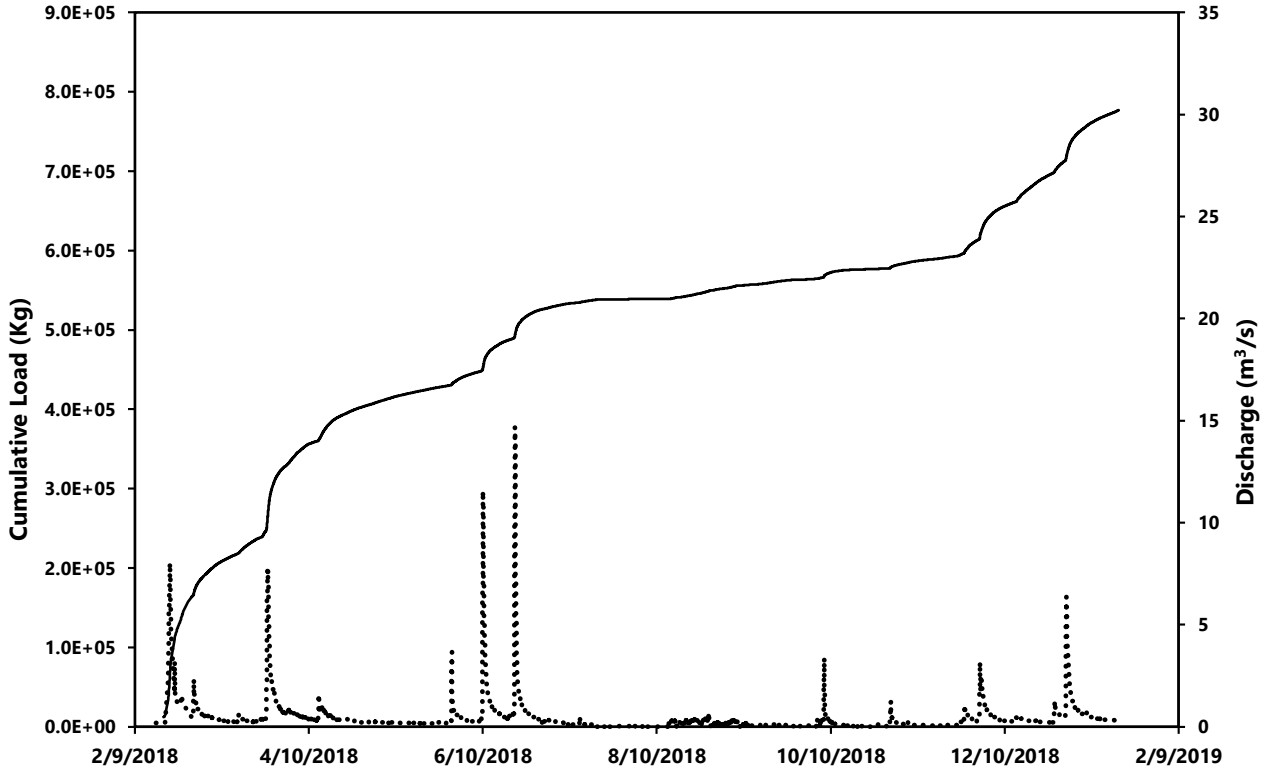

Figure 18. Cumulative load (solid line) and hydrograph (dotted line) at WS1 for the study period.

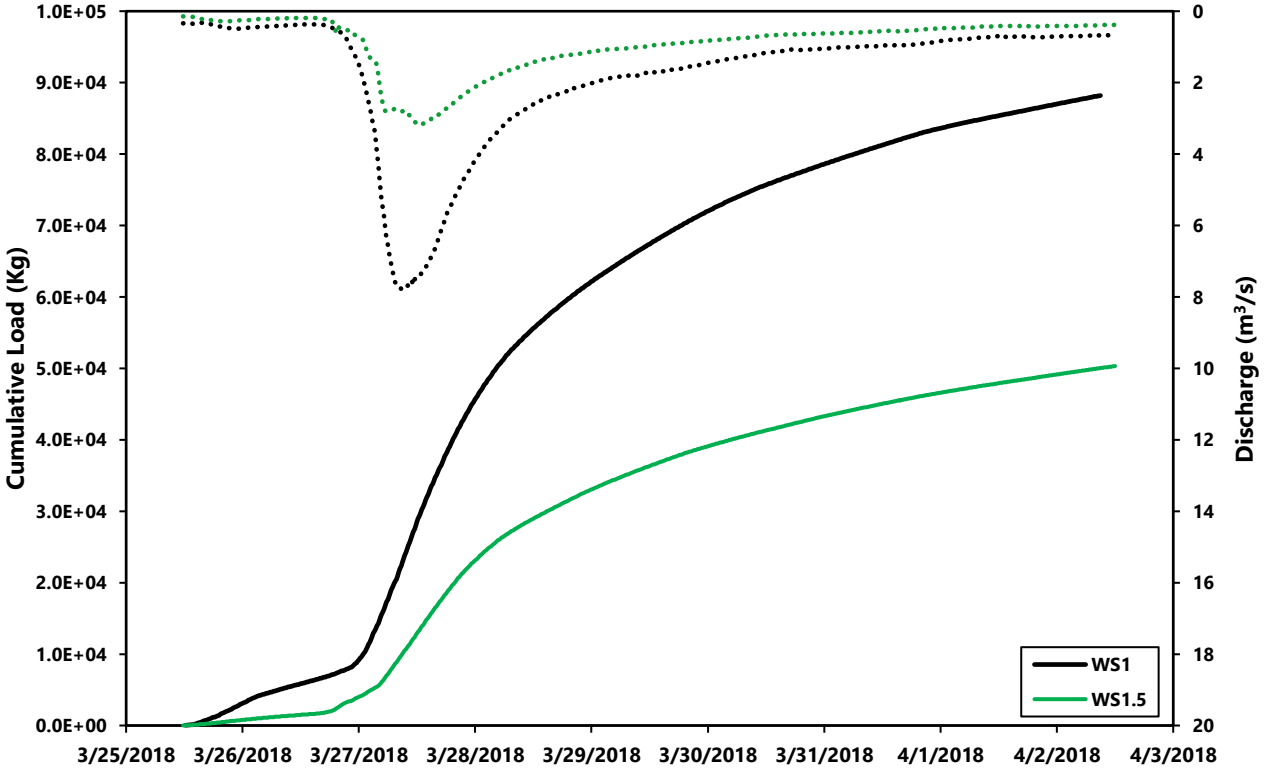

Figure 19. Cumulative load (solid line) and discharge (dotted line) for a spring storm at WS1 and WS1.5.

Seasonal Load

Results show a distinct loading difference between the seasons and seasonal storm events during the calculation period. Winter, spring, summer, and fall account for 42.11%, 34.85%, 15.00%, and 8.03% of total cumulative Cl^- load respectively (Fig.17A). Winter storms alone account for 29.14% of total cumulative load and 50.56% of total cumulative storm load (Fig. 17A). Cumulative spring Cl^- load contributes the next most to total Cl^- load at 34.85% (Fig.17A). Spring storm events account for 31.61% of total storm Cl^- load and 18.22% of total Cl^- load. Summer and fall storm events account for a small portion of total Cl^- load at 8.23% and 2.05% respectively (Fig. 17A). Regarding total storm event Cl^- load, summer accounts for 14.27% and fall accounts for 3.56% (Fig. 17A).

Results show a more even distribution of flow volume over the seasons. Approximately a third of total flow can be attributed to winter (32.98%), spring (31.35%), and summer (27.41%) (Fig.18). Event flow volume during every season except fall makes up greater than half of total flow during that season (Fig.17B). Winter storms account for 22.74% of total flow and 39.20% of flow during storm events (Fig.17B). Spring storms make up 15.86% of total flow and 27.34% of total event flow (Fig. 17B). Summer storms account for 17.19% of total flow and 29.64% of total event flow (Fig. 17B). Percentages by flow volume and Cl^- load are close to equal during the fall (Fig. 17A/B). Winter and early spring events, although smaller in discharge magnitude than late spring and summer events, made up a comparable or much larger contribution (i.e. a greater step) to total cumulative load (Fig. 18).

A load vs discharge plot reveals a branching trend (Fig. 20). This pattern is best described when data are categorized by season. The base of the trend is made up of samples from all seasons (Fig. 20). The upper branch has the steepest slope and consists of winter and spring samples (Fig. 20). The second branch has a shallower slope the appears to reach a plateau. This branch consists

of mostly samples collected during the summer, but it does contain multiple samples from the other seasons at lower discharges. Regression lines for data from each season show that the summer trend line fits best for the lower branch while the winter trend line fits best for the upper branch (Fig. 20).

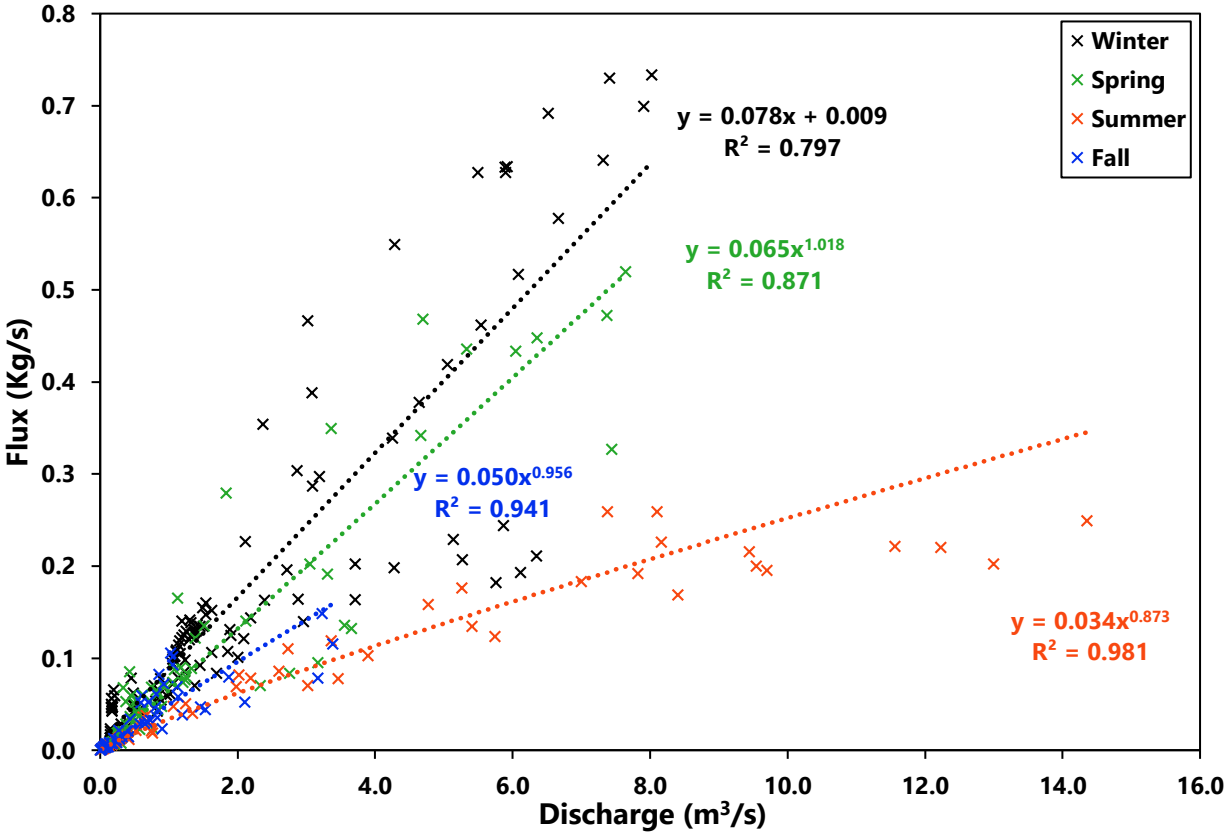

Figure 20. Plot of instantaneous Cl^- flux against discharge with data sorted by season. Data points represent those where samples were collected. Each regression considers data only from that season.

CHAPTER IV: DISCUSSION

Overview

The following text will address the hypotheses stated in the introduction:

1a: Urban and Agricultural Cl^- signature

Statistically significant variation was observed in $[Cl^-]$:[X] ratios between urban and agricultural waters. The hypothesis that ratios of Cl^- are the same between urban and agricultural water with respect to the Na^+, Ca^{2+}, Br^-, and NO_3-N is rejected. The alternate hypothesis that urban and agricultural waters have different Cl^- ratios is rejected with respect to K^+.

2a: Individual event and total event Cl^- load

Over the calculation period, 57.64% of total Cl^- load occurred during storm events (Fig. 17A). Thus, the null hypothesis that event load will be equal to non-event load is rejected and the first alternate hypothesis that storm event load is greater that non-event load is accepted.

2b: Seasonal Cl^- load

Seasonal event load calculations reveal that a disproportion amount of Cl^- export during winter and spring events compared to summer and fall events (Fig. 17A). Winter and spring events also made up a large portion of total Cl^- load during the calculation period (Fig. 17A). The alternate hypothesis that total seasonal event load will differ among the seasons is accepted.

Water Chemistry and Chloride Source

Major ion concentrations of stream water (i.e. WS1, WS1.25, WS1.5) fall between those measured in tile drains and at WS2 for all six ions. This indicates that the mixing of these two waters generate the composition of water in SMC. Low flow and stagnant conditions in the stream that coincide with a loss of tile input in the late summer through most of the fall show that tile input is the main water source to SMC. Substantial difference exists between median ion concentrations in well and tile waters, except with respect to K^+. Although the single well sampled in this study is unlikely representative of ELW groundwater, it supports that SMC does not receive any substantial input from groundwater unimpacted by agriculture as stream waters are more similar to tile water than to well water. Groundwater and tile water should thus be considered compositionally different.

Urban waters appear to be the main source of Cl^- and Na^+ to SMC while tile waters act as the main source of Ca^{2+} and NO_3-N. Fertilizer applied to fields is the source of NO_3-N while Ca^{2+} is both a byproduct of agricultural practices (liming of fields) and the result of water interacting with local soils as it flows to tiles (Kaushal et al., 2018; Kopáček et al., 2014). The data show Cl^- concentration deceases along SMC as tile inputs acts to dilute higher Cl^- concentration water exiting the headwaters of SMC. However, load calculations illustrate that Cl^- export in SMC increases downstream, indicating the presence of additional Cl^- sources to SMC along its reach. Ratios of Cl^- to Na^+ and Br^-, and the graphical relationship between Cl^- and NO_3-N concentrations indicate road salt as the main Cl^- source for SMC.

The molar ratio of Na^+ to Cl^- (Fig. 12) in water where NaCl is the main Cl^- source has a value at or close to 1. Waters impacted by deicing salt where NaCl was the deicing agent would thus have a ratio close to 1 (Lax et al., 2017). Most ELW samples have excess Cl^- compared to Na^+ (Fig. 12), but the ratio is still close to one except for several tile water samples and summer

stream samples. This "excess" Cl^- is likely due to Na^+ removal by cation exchange (Kaushal et al., 2018; Cooper et al., 2014) and extra Cl^- from the 32% $CaCl_2$ solution that road salt is pre-treated with in Mclean County before application (Stokes, Personal Communication).

Panno et al. (2006a) defined the relationship between Cl^-/Br^- ratio and Cl^- concentration in relation to potential Cl^- sources (Fig. 14). Only one tile sample plots in the appropriate domain for field tiles while most of the rest exhibit elevated chloride consistent with the influence of road salt or septic effluent. Seasonal trends on this plot also support road salt as the main source of Cl^-. Winter and early spring samples plot more towards the sample of road salt runoff reflecting the flushing of road salt through SMC. In contrast, by late spring the majority road salt runoff has moved through SMC allowing stream Cl^- concentrations return to more normal levels reflecting the Cl^- concertation in tiles rather than urban runoff. Consequently, late spring, summer, and fall samples plot closer to the field tile domain.

Vectors on Cl^- vs NO_3-N plots (Fig. 13) are based on relations described in Angel and Peterson (2015) and Böhkle (2002) and can be used to identify the influence of various anthropogenic sources of NO_3-N and Cl^- on a water. This graph can also be used to illustrate where a set of samples plot in relation to both NO_3-N and Cl^- background concentration thresholds. Excluding the 5 well samples, only 7 tile samples, 5 of which were from the T3 site, and 3 stream samples from WS1 had Cl^- levels below the background threshold. In contrast, many stream samples and several tile samples had NO_3-N concentrations below the background threshold. Samples from all seasons, particularly those collected in the winter and fall, show clear road salt influence, but a number of these samples have an elevated nitrate concentration shifting them away from the road salt vector to the animal waste and septic effluent vector.

The animal waste and septic effluent vector is not suitable for ELW. Animal waste use is minimal in ELW (Ruffatti, 2019) and can be ruled out as a Cl^- source. Sewage or septic effluent is unlikely to make a large contribution to the elevated Cl^- levels observed in SMC and tile water due to the low density of houses and lack of a waste water treatment plant in ELW. The village of Hudson could be significant source of Cl^- derived from septic effluent, but the signature and contribution from these systems would be overshadowed by that from road salt used in Hudson and along the adjacent Interstate. Kelly et al. (2008) support this conclusion as they found that sewage and water softeners accounted for less than 10% of Cl^- input to a rural stream in New York. Samples plot along the animal waste and septic effluent vector (Fig. 13) because the influence of tile discharge and road salt overlap to elevate both NO_3-N and Cl^- making samples appear to be influenced by septic effluent or animal waste.

After most road salt was flushed from surfaces during late winter and early spring in the ELW, tile drains still provided most of the non-event flow water to SMC until mid-July. Stream chemistry reflect this as waters plot along the fertilizer vector (Fig. 13A) and fall away from the 1:1 $[Cl^-]$:$[Na^+]$ line (Fig. 12). Tile input stopped in the late summer through most of the fall where low flow and stagnant conditions persisted. During low flow conditions most water in the stream was groundwater inflow and overland flow from storm events. Multiple studies support subsurface retention of Cl^- and Na^+ associated with road salt runoff in soil and groundwater near impacted streams, retention ponds, and roads (Hubbard et al. 2017; Ledford et al., 2016; Casey et al., 2013; Kelly et al., 2008). Retained Cl^- then serves as a source to the stream after during the late spring, summer, and fall. Groundwater entering SMC during the fall reflects legacy road salt contamination, with storm events acting to dilute impacted groundwater waters flushing it from

the subsurface. When tile flow resumes in the late fall, water composition moves back toward the nitrogen fertilizer vector and exhibits more drift from the $[Cl^-]$:$[Na^+]$ 1:1 line.

This process was observed during weekly samplings at WS2 in the late summer and fall. Groundwater was observed to be discharging into the stream just below the stormwater pond outlet allowing a small but flowing pool to form and persist for the entire dry season. This water had elevated Cl^- and Na^+ concentrations (Figs. 6 and 10) with $[Cl^-]$:$[Na^+]$ ratios close to 1 (Fig. 12). During these periods of base flow, evaporation likely plays a role in the elevated concentration of ions during the late summer and fall, although it would only impact concentrations and not ratios.

Seasonal patterns in Cl^- load also support road salt being the main source of Cl^- in ELW. December through March in ELW accounts for 63% of total chloride load. Hubbart et al. (2016) conducted a study in the 230 km^2 Hinkson Creek Watershed (HCW), a multi land use watershed (34% forest, 38% agriculture, 25% urban) located in Missouri, and calculated that on average (n = 3.5 years) December through March account for 64% of total Cl^- export. In both cases approximately two-thirds of Cl^- export occurs during the third of the year when road salt would be applied and is flushed from surface through the watershed, illustrating its role as a principal Cl^- source. This result is somewhat surprising given the difference in percentage urban land use and watershed area between ELW and HCW, but could be attributed to differences in the severity and frequency of events requiring road deicing between studies as well as different salt application rates.

While road salt is a major Cl^- source in ELW, the contribution of potash fertilizers cannot be ignored. David et al. (2016) observed Cl^- concentrations rise from 5-10 mg/l to 25-30 mg/l in tile drainage from a corn plot in Illinois following potash treatment. Lax et al. (2017) reported a $[Cl^-]$:$[Na^+]$ ratio between 2.2 and 2.9 and above background Cl^- concentration between 36 and 95

mg/l in tile-drain waters thought to be impacted by KCl fertilizer. The median $[Cl^-]$:$[Na^+]$ ratio of 1.61 (Table 2) in tile-drain waters during this study is not consistent with the reported Lax et al. (2017) values. Ratios of $[Cl^-]$:$[Na^+]$ ranged from 7.74 to 0.58 in tile waters with only a minority of tile water samples (8 of 64) exhibiting a ratio within the range reported in Lax et al. (2017) for KCl influence (Table 2). Median Cl^- concentration in sampled tiles (49.05 mg/l**)** is consistent with Cl^- concentrations reported in the literature for KCl impacted tile waters. The only tile that always exhibited chemistry consistent with KCl influence was the one sampled at WS1, while only a few samples from the tile at WS2 and T1

The $[Cl^-]$:[K+] ratio plot (Fig. 15) did not identify the presence of potash using the sample principal as $[Cl^-]$:$[Na^+]$ ratio plots. This is probably due to where and why these salts are applied. KCl is applied to fields where crops take up the K^+ as a nutrient and free K^+ has a much more interaction with soil particles allowing it to adsorb becoming less mobile than the conservative Cl^- left behind (Ávila et al., 1992). Storm events appear to mobilize K^+ as spikes in concentration occur in all sampled waters during events. The behavior of K^+ during storm events contrasts with Ca^{2+} and NO_3-N, which are initially diluted in tile and stream water during storm events, although NO_3-N concertation increases in the stream after the dilution. This indicates that K^+ is also mobilized from a source within the stream channel and in the urban headwaters while NO_3-N is only mobilized from fields after a lag between precipitation and increase tile discharge to SMC.

A similar K^+ dynamic was observed by Ávila et al. (1992) in a study of storm solute behavior in a montane Mediterranean watershed. They attributed low baseflow concentrations to biologic uptake, cation exchange, and fixation into clay lattices. Spikes in K^+ concentration during storm events were attributed to leaching of K^+ from surfaces, organic soil layers, flushing of subsurface accumulation.

Moderately elevated Cl^- concentration and $[Cl^-]$:$[Na^+]$, ratios much greater than 1, and in field tiles along with widespread use in Illinois support contribution of Cl^- from potash fertilizer. Tile drains where these chemical traits were not observed were likely draining fields where potash was not applied during the study period. In tiled watershed elevated Cl^- from potash fertilizer has been shown to move rapidly from the shallow surface to streams with concentrations returning to pre application levels within 1-2 years (David et al., 2016). Due to the irregular nature of KCl application, the amount of fertilizer derived Cl^- discharged to SMC would vary from year to year. Both road salt and KCl fertilizer are important Cl^- sources to SMC and contribute to above background Cl^- concentrations observed in ELW, but data support road salt as the main Cl^- contributor. Fertilizer derived Cl^- was unable to elevate Cl^- level above the EPA chronic and acute limits, whereas road salt was able to raise Cl^- levels above the chronic limit in ELW for short periods of time. The Cl^- from tile waters plays a part in the 'excess' Cl^- that causes the $[Cl^-]$:$[Na^+]$ to be slightly greater than 1.

KCl can explain moderately elevated Cl^- concentrations in tile waters but cannot account for the highly elevated concentrations (> 100 mg/l). Chemical data suggest the tiles where high Cl^- concentrations were observed were impacted by road salt runoff, which could mask the smaller potash signature. In the winter and spring, the tile drain at WS1.25 and T1 in the adjacent watershed exhibited high Cl^- concentration and $[Cl^-]$:$[Na^+]$ ratios close to 1. The WS1.25 tile discharges into SMC next to a main road that connects Hudson to Normal and receives deicing treatment in the winter. The tile in the adjacent watershed also discharges near a road and is in an area near I-55 likely to be contaminated by road salt. These tiles receive direct road salt runoff or water contaminated by road salt runoff and discharge it to streams. This may act to reduce salt build up in the subsurface near roads and enhance flushing by storm events.

Nitrification inhibitors are another potential source of agricultural Cl^-. Their contribution, however, is unlikely to be significant or noticeable when compared to road salt and KCl inputs. The Cl^- originating from nitrification inhibitors is also not readily mobile as only minimal dehalogenation occurs after the inhibitor byproduct is taken up by the crops (Meikle and Redemann, 1966). Further, the byproducts are organic chlorine (Meikle and Redemann, 1966), which is thought to be more easily retained in soils (Kopáček et al., 2014).

Near pristine groundwater and the signature of road salt in only select tile drains near roads highlights the more point source nature of road salt contamination in low urban land use watershed like ELW. That is, contamination is only present in streams receiving road salt runoff and in the near vicinity of salted roads. The rest of the watershed may remain relatively unaffected by road salt application. Even in streams receiving road salt runoff stretches between salted roads or far from developed areas may remain relatively unimpacted. Baseflow Cl^- concentrations reported by Stripe et al. (2017) were 200-230 mg/l year-round in a watershed with 44% urban land use. ELW (8% urban land use) had Cl^- concentration from ground and tile waters, excluding tiles that received direct road salt runoff in the winter, that ranged from 1 to 95 mg/l.

Impact of Storm Events on Chloride Load and Concentration

Storms play an important role in Cl^- export in ELW. The load calculation period was approximately 336.5 days, with event flow making up approximately 64.3 days or 19.1% of that period. Thus, 57.6% of Cl^- load and 58.0% of flow volume occurred during 19.1% of the calculation period. Storms are particularly important to load during the winter, where they accounted for almost a 1/3 of total Cl^- load and 1/2 of total storm event load. Spring and winter combined account for 80% of event Cl^- load and almost half of total Cl^- load.

Figure 21 illustrates the impact of storm events on Cl^- concentration. Winter and early spring storm events result in large spikes in Cl^- concentration after a brief initial dilution illustrating the role of storms in flushing salt from impervious surfaces. Once salt has been flushed from surfaces storms act to dilute Cl^- concentration, but the rate of export still increases as a result of increased discharge (Fig. 18 and 21). The first major storm event after the summer dry season in late September also resulted in a smaller scale increase in Cl^- concertation and represents a second flushing event. The subsequent storm in October saw a return to dilution by storm events (Fig. 21). Variable Cl^- concentration dynamics during storm events in ELW highlights the need for high frequency sampling regimes to make accurate load estimates.

Kinoshita et al. (2014) conducted a study to understand the role of storm dynamics on stream water chemical viability in an urban-fringe watershed located in southern California. They found a similar flushing dynamic after the dry season, where the first storm resulted in a Cl^- concentration spike with following storms causing dilution. The initial dry season Cl^- spike was attributed to the flushing of salt that built up in the basin by atmospheric deposition and agricultural activity. In watersheds where road salt is applied there are two periods of flushing instead of one. The initial storm following a dry period may also mobilize road salt trapped in the subsurface near salted roads and the interstates as well as that concentrated by evaporation. In both cases, storm events are important in preventing Cl^- build up on watershed surfaces.

The magnitude of a storm event as defined by peak discharge appears to have a different impact of Cl^- load depending season (Fig. 20). Increased discharge in winter and spring result in a larger increase in Cl^- load than higher discharge does for the same magnitude increase in the summer or fall. A closer examination of the lower branch reveals that the pattern cannot fully be explained as seasonal because, while it is mostly made up of summer and fall water samples, it

also contains samples from the winter and spring. The steep upper branch, which only contains samples from the winter and sprint, more likely represent the period when road salts are being flushed through SMC, while the lower branch represents the Cl^- load-discharge relationship after road salt is flushed from watershed surfaces.

The lower branch (Fig. 20) appears to reach an asymptote, which suggests that Cl^- load no longer increases after discharge reaches a certain level when road salt is not being flushed SMC. Storms would increase Cl^- load in three ways: flushing from watershed surfaces, increased tile flow (i.e flushing to the near subsurface), and wet deposition. Surficial flushing is minimal after winter until the first storm after a prolonged dry period. Thus, the asymptotic behavior implies that wet deposition and tile discharge reach a constant mass flux into SMC regardless of storm intensity, as measured by peak discharge. Stripe et al. (2017) also observed asymptotic behavior in Cl^- export for spring and summer (April – August) storms at higher discharge volumes in the 31 km^2 Casperkill watershed (44% urban, 35% open vegetated, 18% forested, 3% wetland), a tributary to the Hudson River.

Stripe et al. (2017) explains this behavior as the result of the relative contribution to stream storm flow from surface runoff increasing during more intense precipitation events while the contribution from increased baseflow due to infiltration remains static once soil become saturated. A static contribution from baseflow is important because this water contains high Cl^- concentrations from legacy road salt and KCl fertilizers. This conclusion supports the upper branch (Fig. 20) being related to the presence of road salts rather than being purely seasonal. Interestingly, the presences of tile drains, which expedite the movement of infiltration to streams, do not prevent this asymptotic behavior. Instead tile drains may only push the occurs of the asymptote out to

higher discharge or facilitate the flushing of Cl^- from only the soil above the drain while preventing or slowing flushing of the soil below the drain.

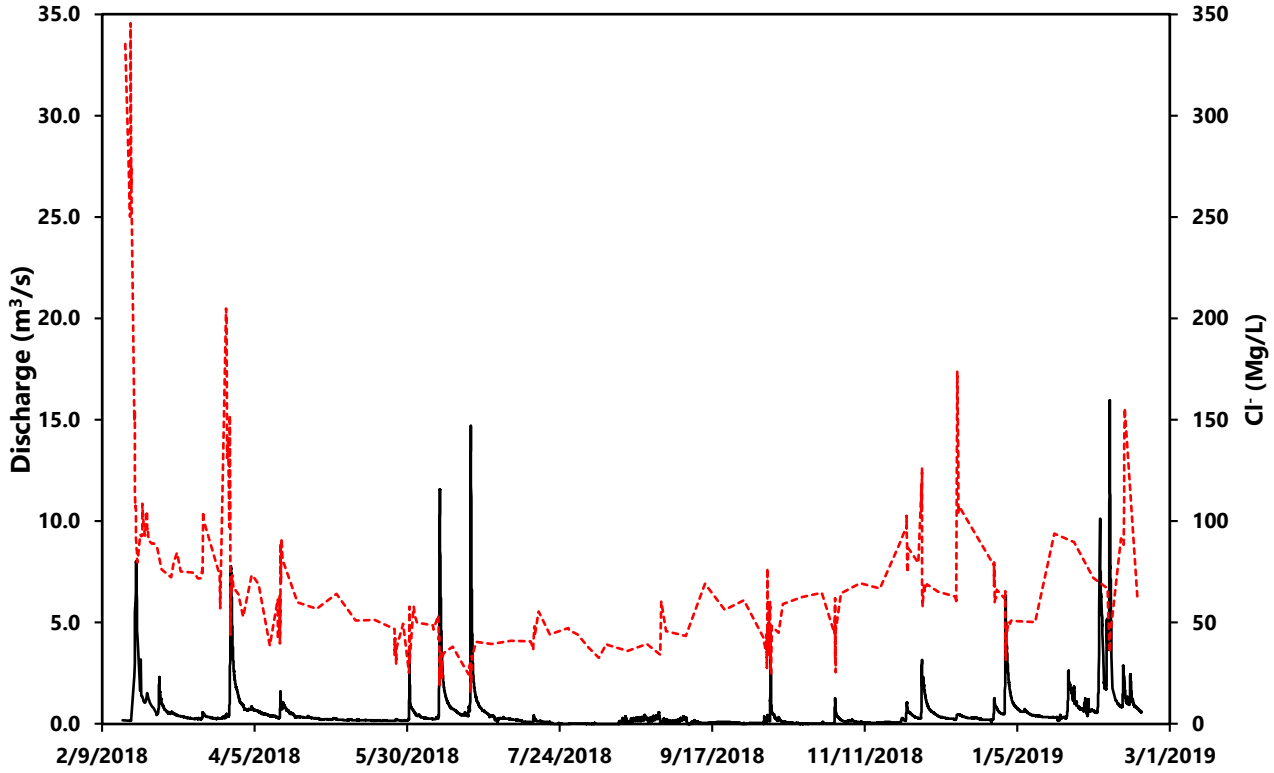

Figure 21. Combination Cl- concentration timeseries (dashed red) and hydrograph (black) at WS1.

CHAPTER V: CONCLUSION

Manual and high frequency sampling of a low order urban-agricultural stream and surrounding field tiles located in central Illinois was conducted to investigate the importance of stormflow to Cl^- transport and to explore potential differences in the signature of Cl^- originating from an urban source as compared to an agricultural source. Samples were collected on a weekly interval from February 2018 to February 2019. All storm events were sampled at high frequency at the most downstream station while select storm events were sampled at an upstream station to compare how export changes along the stream. Key findings from this study include:

a. Nearly all surface water and tile water samples had Cl^- concentrations above the background threshold. In ELW, where the dominant land use is agricultural and urban land use is low the combination of road salt application on only a small portion of impervious surfaces and the use of KCl fertilizer is enough to elevate Cl^- concentrations in surface water above background year-round.

b. Major ion ratios are statistically significantly different between urban and agricultural waters. Ratios indicate that road salt is the dominant source of Cl^- in ELW while KCl fertilizer is an important secondary source. $[Cl^-]$:$[K^+]$ ratios were unable to identify the impact of KCl fertilizers. $[Cl^-]$:$[Na^+]$, $[Cl^-]$:$[Br^-]$, and $[Cl^-]$:$[NO_3\text{-}N]$ ratios were the most useful for identifying Cl^- sources and the influence of agricultural waters on stream chemistry.

c. Large spikes in Cl^- concentration (>100 mg/l) appear to only be associated with areas receiving road salt contaminated runoff. The rest of the watershed appears to remain relatively

unimpacted by the use of road salt, but does show the influence of KCl fertilizers. When road salts are not present on ELW surfaces storm events dilute in stream Cl^- concentration, but the mass flux still increases downstream.

d. Storm events are vital in flushing Cl^- form ELW, a low order urban-agricultural watershed. Results imply two periods of Cl^- flushing in ELW. The first is associated with flushing of road salt from impervious surfaces following the cold season and second is associated with flushing salt build up from the dry season. Some of this second flush is likely associated with legacy road salt contamination

e. Two relationships between Cl^- load and discharge. When road salt is present on watershed surfaces increased discharge always corresponds with increased Cl^- load. During storm events when road salt is not present on watershed surfaces increased in discharge corresponds with increased Cl^- load at lower discharges. At higher discharges the relationship reaches an asymptote where further increases in discharge do not correspond with increased Cl^- load. Tile drains does not appear to impact the asymptotic behavior of Cl^- load-discharge relationship

REFERENCES

Angel, J. and Peterson, E., 2015, Nitrates in Karst systems: comparing impacted systems to a relatively unimpacted system: Journal of Geography and Geology, v. 7, no. 1, p. 65-76, doi 10.5539/jgg.v7n1p65.

Ávila, A, Piñol, J., Rodá, F., and Neal., C., 1992, Storm Solute behavior ina montane Mediterranean forested catchment: Journal of Hydrology, v 140, no. 1-4, p. 143-161, doi 10.1016/0022-1694(92)90238-Q.

Böhlke, J.K., 2002, Groundwater recharge and agricultural contamination: Hydrogeology Journal, v. 10, no. 1, p. 153-179, doi 10.1007/s10040-002-0210-z.

Cañedo-Argüelles, M., Sala, M., Peixoto, G., Prat, N., Faria, M., Soares, A.M.V.M., Barata, C., and Kefford, B., 2016, Can salinity trigger cascade effects on streams? A mesocosm approach: Science of the Total Evironment, v. 540, no. 1, p. 3-10, doi 10.1016/j.scitotenv.2015.03.039.

Cañedo-Argüelles, M., Kefford, B., Piscart, C., Prat, N., Schäfer, R.B., and Schulz, C.J., 2013, Salinisation of rivers: An urgent ecological issue: Environmental Pollution, v. 173, no. 1, p. 157-167, doi 10.1016/j.envpol.2012.10.011.

Casey, R.E., Lev, S.M., and Snodgrass, J.W., 2013, Stormwater ponds as a source of long-term surface and groundwater salinization: Urban Water Journal, v. 10, no. 3, p. 145-153, doi 10.1080/1573062X.2012.716070.

Cooper, C.A., Mayer, P.M., and Faulkner, B.R., 2014, Effects of road salts on groundwater and surface water dynamics of sodium and chloride in an urban restored stream: Biogeochemistry, v. 121, no. 1, p. 149-166, doi 10.1007/s10533-014-9968-z.

David, M, Mitchell, C., Gentry, L., and Salemme, R., 2016, Chloride Sources and Losses in Two Tile-Drained Agricultural Watersheds: Journal of Environmental Quality, v. 45, no. 2, p. 341-348, doi 10.2134/jeq2015.06.0302.

Dugan, H., Bartlett, S., Burke, S., Doubek, J., Krivak-Tetley, F., Skaff, N., Summers, J., Farrell, K., McCullough, I., Morales-Williams, A., Roberts, D., Ouyan, Z., Scordo, F., Hanson, P., and Weathers, K., 2017, Salting our freshwater lakes: Proceedings of the National Academy of Sciences of the United States of America, v. 114, no. 17, p. 4453-4458, 10.1073/pnas.1620211114.

Edwards, M., and Triantafyllidou, S., 2007, Chloride-to-sulfate mass ratio and lead leaching to water: American Water Works Association, v. 99, no. 7, p. 96-109, doi N/A.

Evergreen Lake Watershed Planning Committee, 2006, Evergreen Lake Watershed Plan, https://web.extension.illinois.edu/lmw/downloads/22857.pdf, accessed on December 03 2017.

Gutchess, K., Jin, L., Lautz, L., Shaw, S.B., Zhou, X., and Lu, Z., 2016, Chloride sources in urban and rural headwater catchments, central New York: Science of Total Environment, v. 565, p. 462-472, doi 10.1016/j.scitotenv.2016.04.181.

Herlihy, A., Stoddard, J., and Johnson, C., 1998, The Relationship Between Stream Chemistry and Watershed Land Cover Data in the Mid-Atlantic Region, U.S.: Water, Air, and Soil Pollution, v. 105, no. 1-2, p. 377-386, doi 10.1023/A:1005028803682.

Hubbart, J.A., Kellner, E., Hooper, L.W., and Zeiger, S., 2017, Quantifying loading, toxic concentrations, and systemic persistence of chloride in a contemporary mixed-land-use watershed using an experimental watershed approach: Science of the Total Environment, v. 581-582, no. 1, p. 822-832, doi 10.1016/j.scitotenv.2017.01.019.

Illinois Environmental Protection Agency, 2006, Evergreen Lake Watershed TMDL Report, http://www.epa.illinois.gov/Assets/iepa/water-quality/watershed-management/tmdls/reports /evergreen-l ake/ap proved-report.pdf, Accessed on December 03 2017.

ISGS Staff, 2005, Quaternary deposits: Illinois State Geological Survey, ISGS 8.5 × 11 map series.

Jackson, R. and Jobbágy, E., 2005, From icy roads to salty streams: Proceeding of the National Academy of Science, v. 102, no. 41, p. 14487-14488, doi 10.1073/pnas.0507389102.

Kaushal, S.S., Likens., G.E., Pace, M.L., Haq, S., Wood, K.L., Galella, J.G., Morel, C., Doody, T.R., Wessel, B., Kortelainen, P., Räike, A., Skinner, V., Utz, R., and Jaworski, N., 2018, Novel 'chemical cocktails' in inland waters are a consequence of the freshwater salinization syndrome: Philosophical Transactions of the Royal Society B, v. 374, no. 1764, p. 1-11, doi 10.1098/rstb.2018.0017.

Kaushal S.S., Groffman P.M., Likens G.E., Belt K.T., Stack, W.P., Kelly, V.R., Band, L.E., and Fisher, G.T., 2005, Increased salinization of fresh water in the northeastern United States: Proceeding of the National Academy of Sciences of the United States of America, v.102, no. 38, p. 13517-13520, doi 10.1073/pnas.0506414102.

Kelly, W.R., Panno, S.V., Hackley, K.C., Hwang, H., and Martinsek, M.M., 2010, Using chloride and other ions to trace sewage and road salt in the Illinois Waterway: Applied Geochemistry, v. 25, no. 5, p. 661-673, doi 10.1016/j.apgeochem.2010.01.020.

Kelly, V., Lovett, G., Weathers, K., Findlay, S., Strayer, D., Burns, D., and Likens, G., 2008, Long-Term Sodium Chloride Retention in a Rural Watershed: Legacy Effects of Road Salt on Streamwater Concentration: Environmental Science & Technology, v. 42, no. 2, p. 410-415, doi 10.1021/es071391l.

Kinoshita, A.M., Hogue, T.S., Barco, J., and Wessel, C., 2014, Chemical flushing from an urban-fringe watershed: hydrologic and riparian soil dynamics: Environment Earth Sciences: v. 72, no. 3, p. 879-889, doi 10.1007/s12665-013-3011-x.

Kopáček, J., Hejzlar, J., Porcal, P., and Posch, M., 2014, A mass-balance study of chloride fluxes in a large central European catchment during 1900-2010L Biogeochemistry, v. 120, no. 1-3, p. 319-335, doi 10.1007/s10533-014-0002-2.

Lampo, L., 2017, Dynamics of Nitrate, Phosphorus, and Suspended Sediment Transport in Two Agricultural Streams in Central Illinois [M.S. thesis]: Illinois State University, 164 p.

Lax, S.M., Peterson, E.W., and Van der Hoven S.J., 2017, Stream chloride concentrations as a function of land use: a comparison of agricultural watershed to an urban agricultural watershed: Environmental Earth Sciences, v. 76, no. 708, p. 1-12, doi 10.1007/s12665-017-7059-x.

Lax, S.M. and Peterson, E., 2009, Characterization of chloride transport in the unsaturated zone near salted road: Environmental Geology, v. 58, no. 5, p. 1041-1049, doi 10.1007/s00254-008-1584-6.

Ledford, S.H, Lautz, L.K., and Stella J.C., 2016, Hyrdrogeologic Processes Impacting Storage, Fate, and Transport of Chloride from Road Salt in Urban Riparian Aquifers: Environmental Science & Technology, v. 50, no. 10, p. 4979-4988, doi 10.10 21/acs.est.6b00402.

Lilek, J., American Geosciences Institute, 2017, Roadway deicing in the United States, Factsheet 2017-003, https://www.americangeosciences.org/sites/default/files/CI_Factsheet_2017_3_Deicing_170712.pdf (accessed May 2019).

Ludwikowski, J.J., 2016, The Transport and Fate of Chloride within the Groundwater if a Mixed Urban Agricultural Watershed [M.S. thesis]: Illinois State University, 67 p.

McLean, M.M., Kelly M.D., and Riggs M.H., 1997, Thickness of Quaternary Deposits in McLean County, Illinois: Illinois State Geologic Survey, Scale 1:500,000, 1 sheet.

Meikle R.W. and Redemann C.T., 1966, Tracer Study of 6-Chloropicolinic Acid in Corn: Journal of Agricultural and Food Chemistry, v. 14, no. 2, p. 159-161, doi 10.1021/jf60144a018.

Nelson, S.S., Yonge, D.R., and Barber M.E., 2009, Effects of Road Salts on Heavy Metal Mobility in Two Eastern Washington Soils: Journal of Environmental Engineering, v. 135, no. 7, p. 505-510, doi https://doi.org/10.1061/(ASCE)0733-9372(2009)135:7(505).

Panno, S., Hackley, K., Greenberg, S., Krapac, I., Landsberger, S., and O'Kelly, D., 2006a, Characterization and Identification of Na-Cl Sources in Ground Water: Ground Water, v. 44, no. 2, p. 176-187, doi 10.1111/j.1745-6584.2005.00127.x.

Panno, S., Kelly, W.R., Martinsek, A.T., and Hackley, K.C., 2006b, Estimating Background and Threshold Nitrate Concentrations Using Probability Graphs: Ground Water, v. 44, no. 5, p. 697-709, doi 10.1111/j.1745-6584.2006.00240.x.

Peterson, E.W. and Benning, C., 2013, Factors influencing nitrate within a low-gradient agricultural stream: Environmental Earth Sciences, v. 68, no. 5, p. 1233-1245, doi 10.1007/s12665-012-1821-x.

Prosser, R.S., McInnis Q.R.R., Exall, K., and Gillis, P.L., 2017, Assessing the toxicity and risk of salt-impacted winter road runoff to early life stages of freshwater mussels in the Canadian province of Ontario: Environmental Pollution, v. 230, p. 589-597, doi 10.1016/j.e nvpol.2017.07.001.

Redemann, C.T., Meikle R.W., and Widofsky J.G., 1964, The Loss of 2-Chloro-6 (trichloromethyl)- pyridine from Soil: Agricultural and Food Chemistry, v. 12, no. 3, p. 207-209, doi 10.1021/jf60133a004.

Rivett, M.O., Cuthbert, M.O., Gamble, R., Connon, L.E., Pearson, A., Sheply, M.G., and Davis, J., 2016, Highway deicing salt dynamic runoff to surface water and subsequent infiltration to groundwater during severe UK winters: Science of the Total Environment, v. 565, p. 324-338, doi https://doi.org/10.1016/j.scitotenv.2016.04.095.

Rufatti, M., Supporting Scientist, Illinois State University, Personal Communication and Unpublished Survey, 2019.

Schulz, C.J. and Cañedo-Argüelles, M., 2018, Lost in translation: the German literature on freshwater salinization: Philosophical Transactions of the Royal Society B, v. 374 , no. 1764, p. 1-11, 10.1098/rstb.2018.0007.

Stets, E.G., Lee, C.J., Lytle, D.A., and Schock M.R., 2017, Increasing Chloride in rivers of the conterminous U.S. and linkages to potential corrosivity and lead action level exceedances in drinking water: Science of the Total Environment, v. 616-614, no. 1, p. 1498-1509, doi 10.1016/j.scitotenv.2017.07.119.

Stokes, J., Mclean County Engineer, Personal Communication, 2018.

Stripe, C.R., Cunningham, M.A., Menking, K.M., 2017, How will Climate Change Affect Road Salt Export from Watersheds?: Water, Air, & Soil Pollution, v. 228, no. 362, p. 1-15, doi 10.1007/s11270-017-3455-9.

Tyree, M., Clay, N., Polaskey, S., and Entrekin, S., 2016, Salt in in our streams: even small sodium addition can have negative effects on detritivores; Hydrobiologia, v. 775, no. 1, p. 109-122, doi 10.1007/s10750-016-2718-6.

United States Department of Agricutlrue, 2018, USDA's National Agricultural Statistics Service Illinois Field Office: https://www.nass.usda.gov/Statistics_by_State/Illinois/Publications/County_Estimates/ (accessed April 2019).

United States Environmental Protection Agency, 2011, 2011 Edition of the Drinking Water Standards and Health Advisories, U.S. Environmental Protection Agency, Washington, DC, EPA 820-R-11-002, 18 p.

APPENDIX A: WEEKLY FIELD AND MAJOR ION DATA

1. Dashes mean values are missing or were not measured
2. All ion concentrations are in mg/l
3. SpC - Specific Conductance
4. Q - Measured Stream or Tile Discharge

Table 1. Data from WS1.

Date	Q (m^3/s)	SpC (µS/Cm)	pH	F^-	Cl^-	Br^-	NO_3-N	PO_4-P	SO_4^{2-}	Ca^{2+}	Mg^{2+}	Na^+	K^+
2/17/18 9:30	-	1439.00	7.63	0.118	335.407	0.000	1.040	0.000	11.951	81.241	26.557	192.927	4.451
2/23/18 9:30	-	720.00	7.82	0.187	92.902	0.000	5.370	0.000	11.111	77.213	22.028	42.896	2.465
3/2/2018 9:30	-	719.60	7.74	0.218	76.202	0.000	6.605	0.000	10.320	72.440	18.158	25.204	1.164
3/9/2018 9:30	-	798.90	8.31	0.151	75.174	0.000	6.802	0.000	12.665	68.697	12.724	12.246	0.523
3/16/2018 9:30	0.192	782.50	8.45	0.161	71.718	0.000	6.481	1.978	13.424	58.442	10.125	8.331	0.658
3/23/2018 9:30	0.210	792.00	8.33	0.144	73.276	0.276	6.240	0.000	12.876	96.879	32.923	32.561	1.166
3/30/2018 9:30	1.189	700.10	7.91	0.149	62.167	0.268	9.362	0.000	9.444	87.693	27.878	28.671	2.895
4/6/2018 9:30	0.620	766.10	8.15	0.161	68.948	0.000	9.415	0.000	10.874	97.409	30.218	29.048	1.149
4/13/2018 9:30	0.349	752.00	8.21	0.133	61.552	0.000	8.954	0.000	11.236	97.733	33.762	26.614	1.124
4/20/2018 9:30	-	746.20	8.15	0.156	59.986	0.000	9.364	0.000	11.020	94.287	18.840	14.689	0.574
4/27/2018 9:30	0.343	739.00	8.18	0.144	56.729	0.000	9.213	0.000	11.285	96.347	33.958	23.945	1.000
5/4/2018 9:30	0.282	763.00	8.24	0.147	64.128	0.000	7.886	0.000	11.170	97.472	33.640	29.494	1.257
5/11/2018 9:30	0.204	731.00	8.02	0.158	51.105	0.000	7.739	0.000	11.339	95.779	35.313	21.067	1.049
5/18/2018 9:30	0.151	733.00	8.19	0.150	51.155	0.000	7.394	0.000	11.552	97.314	36.582	21.712	0.935
5/25/2018 9:30	0.138	721.00	7.95	0.178	46.792	0.000	6.719	0.000	11.878	93.610	36.148	18.943	0.946
6/1/2018 9:30	-	686.00	7.52	0.195	57.845	0.000	6.961	0.128	9.853	78.961	30.307	27.649	3.079
6/8/2018 9:30	0.182	723.00	7.75	0.165	46.525	0.000	7.499	0.000	10.857	98.533	34.653	19.605	0.967
6/15/2018 9:30	0.669	679.00	7.70	0.195	38.139	0.000	9.874	0.000	8.347	94.580	32.041	16.123	1.543
6/22/2018 9:30	-	449.00	7.40	0.244	33.172	0.000	5.444	0.377	5.504	49.350	17.560	17.567	3.233
6/29/2018 9:30	0.381	706.00	7.83	0.177	39.403	0.000	8.884	0.000	9.702	94.231	30.240	15.058	1.062
7/6/2018 9:30	0.182	721.00	8.02	0.191	40.924	0.000	7.391	0.000	10.680	94.014	33.202	17.119	1.131
7/13/2018 9:30	0.076	724.00	8.02	0.218	40.807	0.000	4.958	0.000	13.003	98.187	22.452	9.856	0.646
7/20/2018 9:30	0.045	737.00	8.05	0.224	44.260	0.000	2.914	0.000	14.250	94.908	30.996	19.385	1.127
7/27/2018 9:30	0.018	690.00	8.07	0.155	46.355	0.006	1.287	0.000	14.984	61.239	30.804	18.221	0.510
8/3/2018 9:30	0.006	666.00	7.90	0.163	37.653	0.000	0.904	0.000	15.885	82.276	33.805	14.632	0.803
8/10/2018 9:30	0.001	624.00	7.88	0.198	38.823	0.008	0.902	0.000	14.413	67.296	13.481	5.404	0.301
8/17/2018 9:30	0.089	586.00	7.76	0.183	36.099	0.003	0.719	0.000	13.275	61.609	18.855	8.711	0.967
8/24/2018 9:30	-	507.40	8.01	0.186	39.370	0.000	0.610	0.000	12.680	55.377	30.329	16.601	1.634
8/31/2018 9:30	0.023	439.36	7.94	0.151	45.768	0.000	0.763	0.000	7.349	47.549	15.397	25.784	2.850
9/7/2018 9:30	-	489.20	7.79	0.173	43.406	0.011	0.450	0.013	9.222	52.664	21.146	22.261	3.235
9/14/2018 9:30	-	610.00	8.08	0.182	69.077	0.046	0.703	0.000	10.374	59.102	23.009	37.998	2.772
9/21/2018 9:30	-	597.00	7.81	0.200	56.173	0.020	0.500	0.124	13.365	52.702	25.879	30.260	4.318
9/28/2018 9:30	-	603.90	8.03	0.150	60.936	0.052	0.388	0.000	10.406	53.388	26.642	29.533	4.176
10/5/2018 9:30	-	421.20	7.89	0.142	42.838	0.043	0.438	0.145	11.628	45.687	27.007	21.656	3.774
10/12/2018 9:30	0.140	647.20	7.94	0.169	59.249	0.046	1.710	0.105	10.610	63.120	26.666	32.290	2.609
10/19/2018 9:30	0.052	657.80	7.89	0.180	62.639	0.064	1.274	0.000	10.925	71.312	24.248	30.559	1.885
10/26/2018 9:30	0.033	740.00	7.58	0.152	64.662	0.069	0.838	0.019	14.722	78.789	25.692	24.425	2.016
11/2/2018 9:30	0.236	706.90	7.60	0.167	64.372	0.055	2.590	0.001	11.013	80.633	24.987	29.320	1.848
11/9/2018 9:30	0.106	799.90	7.46	0.135	69.315	0.065	2.371	0.000	13.153	83.836	29.551	33.932	1.547
11/16/2018 9:30	0.072	779.10	7.86	0.131	66.764	0.053	2.570	0.026	14.024	108.005	38.482	37.667	1.593
11/23/2018 9:30	0.084	851.00	7.88	0.150	88.279	0.065	2.810	0.004	14.220	106.372	31.918	39.568	1.227
11/30/2018 9:30	0.290	827.00	7.84	0.149	79.550	0.027	4.685	0.117	12.336	113.188	39.502	49.871	1.766
12/7/2018 9:30	0.423	794.80	7.81	0.155	65.226	0.010	6.347	0.049	11.794	120.446	41.576	37.907	1.539
12/14/2018 9:30	0.481	1042.00	7.50	0.107	173.887	0.060	4.526	0.075	10.792	112.636	34.612	120.483	3.191
12/28/2018 9:30	-	-	-	0.175	62.349	0.040	7.359	0.158	291.091	102.515	38.166	35.383	2.110
1/4/2019 9:30	0.873	714.70	7.56	0.147	50.793	0.024	8.679	0.069	10.888	110.856	41.479	26.124	1.472
1/11/2019 9:30	0.424	758.90	7.67	0.149	50.152	0.043	8.619	0.053	11.961	90.727	29.773	14.552	0.626
1/18/2019 9:30	0.320	887.00	7.69	0.154	93.900	0.067	7.861	0.013	12.193	109.403	45.520	62.566	1.366
1/25/2019 9:30	-	814.00	7.59	0.167	89.755	0.044	8.265	0.011	10.623	83.621	32.517	42.337	1.818
2/1/2019 9:30	-	842.00	8.30	0.175	72.016	0.020	8.515	0.043	11.694	81.138	28.706	23.583	0.865
2/17/2019 9:30	-	732.00	7.56	0.186	61.156	0.109	8.381	0.033	10.037	84.342	31.701	25.332	1.404

Table 2. Data from WS1.25.

Date	Q (m^3/s)	SpC (µS/Cm)	pH	F^-	Cl^-	Br^-	NO_3-N	PO_4-P	SO_4^{2-}	Ca^{2+}	Mg^{2+}	Na^+	K^+
7/27/2018 8:30	0.012	713.00	7.81	0.166	38.347	0.021	1.239	0.000	15.468	97.526	39.374	17.830	1.068
8/3/2018 8:30	0.005	732.00	7.64	0.180	41.314	0.008	0.409	0.000	14.752	96.708	31.305	13.528	1.127
8/10/2018 8:30	0.001	711.00	7.65	0.229	36.181	0.024	0.398	0.377	9.722	82.373	35.676	12.831	2.242
8/17/2018 8:30	0.048	530.00	7.62	0.254	48.414	0.007	0.559	0.120	10.844	54.948	25.108	23.690	3.991
8/24/2018 8:30	-	414.20	7.84	0.126	36.007	0.000	0.531	0.239	2.984	24.669	7.725	28.338	1.965
8/31/2018 8:30	0.009	570.00	7.83	0.199	65.368	0.040	0.418	0.048	12.415	61.312	21.420	34.292	3.357
9/7/2018 8:30	0.006	661.00	7.82	0.199	67.001	0.032	0.409	0.000	13.958	72.324	29.681	35.930	3.273
9/14/18 8:30	-	655.00	8.26	0.216	84.340	0.027	0.424	0.260	11.347	58.714	24.588	48.455	4.250
9/21/18 8:30	-	590.00	7.74	0.256	161.447	0.087	0.372	0.498	7.139	74.072	22.574	100.281	8.998
9/28/18 8:30	-	489.10	8.09	0.145	52.959	0.027	0.359	0.000	17.812	44.381	15.809	29.232	5.033
10/5/18 8:30	-	62.30	7.73	0.157	93.669	0.031	0.493	0.223	11.181	52.994	15.347	92.160	6.309
10/12/18 8:30	0.124	641.10	7.71	0.176	58.997	0.033	1.626	0.068	11.019	86.911	29.119	34.260	2.434
10/19/18 8:30	0.051	660.20	7.71	0.172	62.541	0.079	1.143	0.023	11.241	86.346	31.775	41.587	2.369
10/26/18 8:30	0.024	751.00	7.49	0.168	65.506	0.064	0.811	0.000	15.356	106.981	39.917	42.272	2.778
11/2/18 8:30	0.194	686.70	7.35	0.167	61.944	0.072	2.366	0.012	10.888	92.686	31.552	37.369	2.295
11/9/18 8:30	0.092	787.00	10.15	0.139	64.947	0.103	2.280	0.000	14.060	108.729	38.948	43.496	3.337
11/16/18 8:30	0.056	765.30	7.68	0.150	68.047	0.073	2.422	0.000	13.202	115.095	41.686	41.817	1.789
11/23/2018 9:00	0.065	827.00	7.65	0.243	81.049	0.000	2.726	0.004	14.334	113.152	40.949	51.472	1.798
11/30/2018 8:30	0.231	823.00	7.61	0.160	81.296	0.016	4.516	0.049	12.241	120.379	42.333	53.898	1.828
12/7/2018 8:30	0.318	802.80	7.47	0.172	68.870	0.050	6.107	0.104	12.058	105.787	37.951	38.340	1.541
12/14/2018 8:30	0.309	780.60	7.31	0.117	83.000	0.011	5.188	0.039	9.946	114.422	33.849	50.761	1.932
1/4/2019 8:30	0.606	716.20	7.16	0.167	50.528	0.000	8.384	0.142	10.514	103.035	37.427	24.822	1.529
1/11/2019 8:30	0.288	760.30	7.31	0.167	50.593	0.015	8.228	0.044	12.122	116.924	42.709	24.270	1.094
1/18/2019 8:30	0.213	993.00	7.34	0.163	126.384	0.094	7.457	0.027	12.164	122.514	43.337	82.042	1.469
1/25/2019 8:30	-	877.20	7.03	0.170	97.398	0.087	7.653	0.044	10.725	86.715	33.416	47.619	2.033
2/17/2019 8:30	-	740.00	7.60	0.187	62.609	0.045	8.325	0.134	10.036	81.030	32.057	26.214	1.407

Table 3. Data from WS2. Includes road salt runoff sample.

Date	Q (m^3/s)	SpC (µS/Cm)	pH	F^-	Cl^-	Br^-	NO_3-N	PO_4-P	SO_4^{2-}	Ca^{2+}	Mg^{2+}	Na^+	K^+
2/16/18 7:30	-	678.80	7.57	0.137	108.331	0.000	0.551	0.000	8.237	35.661	12.479	31.816	1.227
2/23/18 7:30	-	650.60	7.72	0.199	89.892	0.000	3.133	0.000	10.042	59.780	20.027	54.771	3.609
3/2/18 7:30	-	721.40	7.93	0.167	100.163	0.000	4.534	0.000	10.812	40.465	9.811	19.997	0.768
3/9/18 7:30	0.073	778.90	8.13	0.149	95.858	0.000	4.206	0.000	10.782	52.123	22.280	45.043	2.056
3/16/18 7:30	0.026	797.50	8.24	0.161	97.898	0.000	4.082	0.000	11.021	64.683	12.997	23.498	0.862
3/23/18 7:30	0.036	790.00	8.21	0.149	98.864	0.000	3.939	1.402	11.236	73.665	24.921	46.611	1.736
3/30/18 7:30	0.248	704.20	7.63	0.164	89.222	0.000	4.388	0.163	9.344	68.089	23.816	54.806	1.683
4/6/18 7:30	0.097	865.00	8.37	0.163	124.345	0.000	5.132	0.000	10.243	78.652	23.407	60.897	1.934
4/13/18 7:30	0.053	834.00	8.48	0.143	115.668	0.000	4.901	0.000	10.544	79.992	25.750	57.792	1.781
4/20/18 7:30	-	798.00	8.43	0.160	107.415	0.000	4.270	0.000	10.597	78.115	18.682	37.218	0.629
4/27/18 7:30	0.043	780.00	8.35	0.145	105.066	0.000	4.217	0.000	10.931	71.227	30.798	60.395	1.719
5/4/18 7:30	0.036	809.00	8.17	0.157	103.180	0.000	4.119	0.000	10.942	76.589	31.731	57.033	2.045
5/11/18 7:30	0.017	734.00	8.25	0.211	103.687	0.000	2.781	0.000	11.259	52.942	30.426	56.716	2.016
5/18/18 7:30	0.017	676.00	8.54	0.226	102.341	0.000	1.663	0.000	11.084	39.563	31.751	58.424	1.911
5/25/18 7:30	0.016	662.00	8.42	0.212	100.815	0.000	1.247	0.000	10.258	36.624	31.438	54.877	1.982
6/1/18 7:30	-	612.00	8.10	0.191	82.581	0.000	1.904	0.000	8.370	42.184	24.923	41.018	2.346
6/8/18 7:30	0.026	659.00	7.65	0.165	78.454	0.000	1.905	0.000	8.494	55.185	28.845	40.663	1.973
6/15/18 7:30	0.095	618.00	7.62	0.195	59.696	0.000	4.588	0.000	6.943	61.550	25.062	33.729	2.227
6/22/18 7:30	-	412.50	7.36	0.242	43.065	0.000	2.393	0.204	4.640	35.673	16.906	28.143	3.056
6/29/18 7:30	0.054	561.00	7.95	0.203	59.998	0.000	2.728	0.000	6.240	45.796	22.804	33.336	2.086
7/6/18 7:30	0.022	573.00	7.84	0.224	63.006	0.000	0.000	1.109	6.565	44.071	26.101	38.061	2.230
7/13/18 7:30	0.004	552.00	7.66	0.237	67.185	0.000	0.868	0.000	6.673	30.373	15.543	22.105	0.606
7/20/18 7:30	0.002	512.20	7.93	0.230	65.381	0.000	0.477	0.000	6.060	31.356	19.737	31.765	1.439
7/27/18 7:30	-	1193.00	6.74	0.159	129.529	0.257	0.409	0.000	11.436	142.509	49.448	56.826	1.900
8/3/18 7:30	-	1214.00	6.68	0.149	126.130	0.246	0.410	0.000	12.195	151.287	49.982	53.738	1.567
8/10/18 7:30	-	1218.00	6.72	0.206	129.903	0.243	0.419	0.000	12.331	148.252	35.468	39.403	0.960
8/17/18 7:30	-	1133.00	6.69	0.158	93.752	0.083	0.592	0.072	8.226	57.281	19.104	50.577	1.223
8/24/18 7:30	0.007	273.90	7.74	0.090	27.804	0.000	0.643	0.335	2.259	6.904	0.044	29.462	1.100
8/31/18 7:30	-	1176.00	6.82	0.221	74.277	0.087	0.525	0.000	5.325	58.094	23.206	37.437	0.705
9/7/18 7:30	0.001	290.80	8.03	0.114	44.576	0.000	0.736	0.579	2.568	10.333	1.487	48.624	1.564
9/14/18 7:30	-	1320.00	6.84	0.225	155.096	0.313	0.410	0.000	13.260	157.346	54.699	56.531	1.109
9/21/18 7:30	-	1138.00	6.83	0.221	106.160	0.169	0.454	0.023	8.750	92.084	32.917	48.950	2.788
9/28/18 7:30	-	1196.00	6.95	0.088	150.049	0.273	0.387	0.000	11.971	128.046	41.431	51.526	1.895
10/5/18 7:30	-	215.40	8.04	0.066	32.235	0.023	0.699	1.233	2.453	10.934	2.164	26.843	2.641
10/12/18 7:30	0.039	437.80	7.86	0.202	49.253	0.041	1.139	0.060	5.399	35.736	18.053	32.843	2.954
10/19/18 7:30	0.023	487.50	8.05	0.182	54.095	0.062	1.004	0.000	5.506	40.313	20.093	35.879	2.795
10/26/18 7:30	0.012	486.50	8.20	0.175	56.830	0.061	0.812	0.134	5.558	40.461	19.323	42.725	2.814
11/2/18 7:30	0.079	505.80	7.74	0.166	54.254	0.051	1.204	0.026	5.723	43.064	20.894	39.160	2.989
11/9/18 7:30	0.036	561.00	6.37	0.173	58.331	0.042	1.481	0.023	6.197	49.645	21.435	40.047	2.546
11/16/18 7:30	0.030	571.80	8.02	0.165	60.758	0.067	1.630	0.013	6.509	54.928	23.394	43.127	2.723
11/23/18 7:30	0.020	668.60	8.10	0.167	86.248	0.039	1.772	0.000	6.928	55.101	24.893	61.117	2.684
11/30/18 7:30	0.069	701.10	7.69	0.198	87.996	0.009	2.984	0.056	7.894	64.132	25.776	63.452	2.777
12/7/18 7:30	0.073	700.60	7.43	0.186	79.020	0.000	4.311	0.052	8.573	64.543	24.200	46.220	2.392
12/14/18 7:30	0.095	733.10	7.52	0.182	80.627	0.000	4.580	0.048	9.137	76.642	29.443	51.264	2.412
1/4/19 7:30	0.146	642.90	7.04	0.186	62.652	0.000	5.248	0.087	8.792	70.352	26.885	37.642	2.407
1/11/19 7:30	0.055	709.40	6.06	0.198	68.168	0.000	5.796	0.051	9.891	72.635	29.023	40.211	1.989
1/18/19 7:30	0.020	738.50	7.33	0.173	80.427	0.086	5.660	0.028	9.882	81.328	32.384	45.629	1.910
1/25/19 7:30	0.247	850.90	6.75	0.182	121.624	0.045	4.789	0.011	9.168	73.335	27.421	66.475	2.442
2/17/19 7:30	0.094	2394.00	8.12	0.190	636.773	0.111	5.055	0.110	7.929	61.423	23.004	356.851	4.795
Road Salt Runoff	-	86456.00	7.790	0.564	30997.975	2.115	4.710	0.349	21.525	73.552	1.370	17491.241	62.873

Table 4. Data from WS1.5.

Date	Q (m^3/s)	SpC (µS/Cm)	pH	F^-	Cl^-	Br^-	NO_3-N	PO_4-P	SO_4^{2-}	Ca^{2+}	Mg^{2+}	Na^+	K^+
2/16/2018 8:30	-	1558.00	7.64	0.102	346.635	0.172	0.437	0.000	12.077	80.867	27.663	220.441	4.052
2/23/2018 8:30	-	716.60	7.59	0.185	96.769	0.000	4.529	0.233	10.237	72.793	23.847	56.041	4.412
3/2/2018 8:30	-	712.20	7.69	0.172	70.355	0.000	4.958	0.097	9.558	84.607	24.986	38.054	2.650
3/9/2018 8:30	0.217	803.20	7.86	0.142	77.634	0.000	5.676	0.000	12.454	90.674	31.916	38.407	1.481
3/16/2018 8:30	0.106	818.00	8.16	0.140	77.966	0.000	5.314	0.000	13.252	92.508	18.348	19.555	0.277
3/23/2018 8:30	0.104	810.80	8.03	0.139	75.774	0.000	5.352	0.000	12.790	101.930	35.563	37.535	1.353
3/30/2018 8:30	0.730	709.80	7.68	0.175	67.756	0.000	7.944	0.000	9.366	85.538	28.753	35.476	2.100
4/6/2018 8:30	0.346	796.00	7.80	0.166	78.469	0.000	7.804	0.000	10.998	97.021	33.585	40.684	1.355
4/13/2018 8:30	0.162	788.00	7.81	0.135	71.679	0.000	7.257	0.000	11.479	103.467	36.012	36.211	1.186
4/20/2018 8:30	-	778.00	7.86	0.145	70.307	0.000	7.160	0.000	11.469	104.421	34.974	34.890	1.188
4/27/2018 8:30	0.168	772.00	7.74	0.129	65.714	0.000	7.255	0.000	11.411	104.840	37.401	32.664	1.216
5/4/2018 8:30	0.156	789.00	7.80	0.136	68.723	0.000	6.341	0.000	11.157	100.351	35.447	34.625	1.215
5/11/2018 8:30	0.090	766.00	7.70	0.131	59.684	0.000	6.484	0.000	11.543	100.666	37.810	28.072	1.056
5/18/2018 8:30	0.081	758.00	7.75	0.139	52.506	0.000	6.612	0.000	11.738	109.105	39.706	23.693	0.767
5/25/2018 8:30	0.058	756.00	7.59	0.144	49.178	0.000	0.420	0.000	11.800	107.164	38.491	21.625	0.894
6/1/2018 8:30	-	693.00	7.20	0.179	58.634	0.000	5.874	0.000	9.123	80.579	31.686	28.071	1.678

Table 5. Data from shallow T3 Well.

Date	F^-	Cl^-	Br^-	NO_3-N	PO_4-P	SO_4^{2-}	Ca^{2+}	Mg^{2+}	Na^+	K^+
5/16/2018	0.122	1.343	0.125	0.691	0.000	24.506	96.592	33.739	3.683	0.383
6/28/2018	0.161	3.021	0.296	0.748	0.000	27.338	117.738	36.660	4.782	0.390
7/25/2018	0.170	2.331	0.124	0.456	0.000	57.625	95.951	41.304	2.828	0.180
8/24/2018	0.213	2.315	0.104	0.431	0.088	35.875	105.252	44.844	5.954	1.799
9/27/2018	0.124	2.648	0.114	0.382	0.000	36.380	126.719	45.616	3.252	1.538

Table 6. Data from tile drains. T1 is the designation for the tile outside ELW.

Location	Date	Q (l/s)	SpC (µS/Cm)	pH	F^-	Cl^-	Br^-	NO_3-N	PO_4-P	SO_4^{2-}	Ca^{2+}	Mg^{2+}	Na^+	K^+
WS1	5/25/2018	0.231	699.00	7.37	0.186	41.781	0.000	19.428	0.000	11.592	99.211	37.132	4.732	0.454
WS1	6/8/2018	0.167	724.00	7.05	0.164	42.892	0.000	19.633	0.000	11.613	101.193	38.269	4.505	0.504
WS1	6/29/2018	0.301	749.00	7.15	0.181	40.567	0.000	19.837	0.000	11.141	105.072	40.384	4.758	0.552
WS1	11/23/2018	0.048	754.00	7.53	0.177	38.611	0.015	15.105	0.070	14.176	104.891	44.556	4.279	0.487
WS1	12/7/2018	1.100	698.70	7.42	0.157	33.933	0.000	15.395	0.042	13.141	98.125	39.897	4.505	0.448
WS1	1/4/2019	1.833	661.80	7.39	0.158	34.585	0.000	14.263	0.098	12.800	79.407	36.949	4.840	0.402
WS1	1/18/2018	0.611	670.00	7.19	0.240	32.536	0.033	15.494	0.053	11.980	90.289	37.457	2.727	0.371
WS1	1/25/2019	-	667.60	6.93	0.191	39.307	0.042	13.640	0.078	12.302	76.739	34.263	7.675	0.464
WS1	2/17/2019	-	640.00	7.61	0.201	38.573	0.033	13.473	0.121	12.403	74.900	32.527	5.443	0.635
WS1.25	11/2/2018	-	706.00	7.96	0.173	25.942	0.052	6.383	0.027	9.819	99.433	37.910	6.768	1.481
WS1.25	12/14/2018	-	684.50	7.03	0.165	29.763	0.017	8.700	0.048	10.856	102.621	37.541	3.370	1.317
WS1.25	12/14/2018	-	1899.00	7.10	0.176	464.015	0.000	4.184	0.333	8.364	111.595	37.294	268.838	5.133
WS1.25	1/4/2019	-	1191.00	7.36	0.160	166.898	0.018	7.910	0.143	9.738	132.716	52.660	75.793	0.848
WS1.25	1/18/2018	-	1880.00	7.81	0.156	408.925	0.091	9.274	0.041	10.507	137.059	56.463	224.548	1.533
WS1.25	2/17/2019	-	1128.00	7.40	0.164	155.270	0.106	7.805	0.017	8.156	110.286	44.134	60.836	0.889
WS2	5/18/2018	0.249	793.00	7.68	0.178	60.888	0.000	16.111	0.000	10.174	106.801	35.353	15.250	0.307
WS2	6/1/2018	0.623	785.00	7.23	0.204	48.254	0.000	21.677	0.050	9.960	109.340	38.302	13.953	1.377
WS2	6/15/2018	0.857	830.00	6.89	0.194	57.667	0.000	19.743	0.000	10.392	111.179	39.793	19.356	0.473
WS2	7/6/2018	0.071	965.00	7.31	0.173	89.587	0.000	16.259	0.000	11.835	122.629	33.913	24.801	0.423
WS2	11/30/2018	0.200	892.00	7.47	0.211	76.504	0.004	13.133	0.130	13.827	120.375	45.111	33.777	0.595
WS2	1/11/2019	0.458	860.00	6.88	0.167	67.675	0.001	14.953	0.089	12.749	118.571	45.007	26.906	0.481
WS2	2/17/2019	-	843.00	7.95	0.199	73.194	0.052	12.454	0.067	12.327	97.319	37.987	24.690	0.607
T1	2/21/2018	-	-	-	0.217	93.555	0.000	3.467	1.292	262.274	63.506	16.364	43.597	1.093
T1	2/21/2018	-	-	-	0.394	175.964	0.000	3.684	2.928	439.681	0.000	50.656	81.099	6.979
T1	2/21/2018	-	-	-	0.236	92.834	0.000	3.284	0.317	465.783	55.167	12.977	39.165	0.840
T1	2/22/2018	-	-	-	0.242	93.279	0.000	4.424	0.454	402.548	86.064	25.448	40.167	0.000
T1	2/23/2018	-	-	-	0.246	127.927	0.000	5.350	0.129	557.334	81.301	29.494	53.521	0.000
T1	2/23/2018	-	-	-	0.248	116.989	0.000	5.118	0.113	492.379	81.987	27.055	47.285	0.000
T1	2/24/2018	-	-	-	0.232	120.375	0.000	5.751	0.000	435.475	83.191	31.294	49.835	0.000
T1	2/25/2018	-	-	-	0.204	91.460	0.000	4.699	0.000	449.841	80.872	24.629	41.278	0.000
T1	2/26/2018	-	-	-	0.210	80.892	0.000	4.834	1.864	369.312	82.680	25.838	37.055	0.000
T1	2/27/2018	-	-	-	0.177	57.301	0.000	3.693	0.000	346.364	84.676	18.193	23.585	0.000
T1	3/2/2018	-	-	-	0.180	50.594	0.000	4.230	0.000	371.776	75.727	16.988	16.404	0.000
T1	3/3/2018	-	-	-	0.193	54.991	0.000	4.146	0.000	351.645	84.348	19.626	22.274	0.000
T1	3/4/2018	-	-	-	0.188	49.846	0.000	3.600	0.000	311.322	84.941	17.907	22.054	0.000
T1	3/5/2018	-	-	-	0.189	33.781	0.000	3.616	0.000	289.063	84.793	13.121	9.094	0.000
T1	5/23/2018	-	-	-	0.193	20.732	0.000	5.763	0.000	231.166	97.177	23.642	5.146	0.983
T1	5/26/2018	-	-	-	0.184	19.155	0.000	5.246	0.033	221.313	101.446	19.258	4.243	0.775
T1	5/25/2018	-	-	-	0.125	41.787	0.005	9.084	0.000	12.027	36.829	34.751	15.320	0.602
T1	5/29/2018	-	-	-	0.098	39.935	0.000	10.015	0.000	12.277	33.038	37.949	13.316	0.326
T1	6/1/2018	-	-	-	0.099	41.128	0.000	9.935	0.000	10.574	46.921	38.241	13.789	0.663
T1	6/1/2018	-	-	-	0.189	20.284	0.000	4.139	0.006	211.151	111.744	18.441	5.650	0.278
T1	6/4/2018	-	-	-	0.228	33.566	0.000	7.186	0.000	351.832	102.529	34.337	13.662	0.500
T1	6/6/2018	-	-	-	0.277	39.565	0.000	9.770	0.000	359.892	107.434	38.277	12.967	0.574
T1	6/9/2018	-	-	-	0.190	26.317	0.000	5.015	0.046	286.107	105.443	29.288	12.229	0.518
T1	6/10/2018	-	-	-	0.275	16.095	0.000	7.417	1.448	346.687	59.696	13.582	4.917	4.423
T1	6/10/2018	-	-	-	0.237	16.429	0.000	6.647	0.703	222.965	52.045	8.760	4.852	3.421
T1	6/12/2018	-	-	-	0.244	26.790	0.007	8.928	0.833	461.237	73.621	17.476	10.929	3.714
T1	7/9/2018	-	-	-	0.183	22.799	0.000	3.514	0.005	494.430	81.662	17.731	7.233	0.636
T1	7/15/2018	-	-	-	0.187	32.927	0.003	2.341	0.000	460.417	83.856	16.945	12.859	1.000
T1	8/28/2018	-	-	-	0.273	191.400	0.003	2.008	3.191	350.894	116.300	31.744	138.812	4.040
T1	9/8/2018	-	-	-	0.205	191.357	0.017	1.898	2.788	553.269	117.639	32.047	160.214	2.124
T1	10/7/2018	-	-	-	0.256	108.333	0.021	1.309	0.578	302.596	71.892	23.719	83.111	4.099
T1	10/8/2018	-	-	-	0.287	50.816	0.000	2.552	2.413	304.297	84.418	21.543	38.860	5.173
T1	10/8/2018	-	-	-	0.522	61.998	0.009	1.938	6.161	306.409	116.734	31.275	51.522	13.794
T1	10/9/2018	-	-	-	0.310	144.041	0.020	1.314	0.051	383.497	101.230	32.141	87.256	3.973
T1	10/14/2018	-	-	-	0.264	63.194	0.000	0.922	0.098	274.069	85.073	26.577	53.559	3.134
T1	10/25/2018	-	-	-	0.348	78.987	0.013	2.596	9.359	302.514	75.323	25.714	35.118	3.049
T1	10/31/2018	-	-	-	0.227	85.284	0.007	3.173	0.952	467.486	82.802	24.012	57.472	14.762
T3	5/16/2018	-	-	-	0.148	4.454	0.131	14.472	0.000	13.366	94.188	32.488	4.594	0.323
T3	6/28/2018	-	-	-	0.161	5.189	0.154	15.730	0.000	13.779	76.581	29.976	3.671	0.299
T3	7/25/2018	-	-	-	0.221	5.414	0.126	11.345	0.000	12.253	90.581	34.097	2.170	0.547
T3	8/24/2018	-	-	-	0.173	5.366	0.110	11.607	0.000	12.736	90.243	36.882	6.029	0.477
T3	9/27/2018	-	-	-	0.182	6.002	0.113	11.084	0.042	13.788	100.614	36.445	2.421	0.585

APPENDIX B: EVENT SAMPLE MAJOR ION DATA

1. Dashes mean values are missing or were not measured

2. All ion concentrations are in mg/l

Table 1. WS1 event sample data.

Date	F^-	Cl^-	Br^-	NO_3-N	PO_4-P	SO_4^{2-}	Ca^{2+}	Mg^{2+}	Na^+	K^+
2/19/2018 0:00	0.240	250.024	0.087	1.072	0.000	131.467	74.741	32.141	135.379	3.841
2/19/2018 1:30	0.278	250.300	0.079	1.031	0.000	136.654	75.155	25.126	110.755	2.821
2/19/2018 3:00	0.268	265.580	0.088	1.021	0.000	170.853	76.230	30.338	138.616	1.874
2/19/2018 4:30	0.259	291.060	0.099	1.052	0.000	155.924	77.511	33.370	154.324	4.224
2/19/2018 6:00	0.237	300.037	0.100	1.094	0.000	161.452	77.369	32.754	156.734	4.353
2/19/2018 7:30	0.243	345.644	0.112	1.185	0.000	188.424	75.526	24.702	134.031	3.233
2/19/2018 9:00	0.215	277.943	0.079	1.023	0.000	115.526	74.308	29.795	139.272	3.782
2/19/2018 10:30	0.179	264.254	0.070	0.994	0.000	90.603	70.804	29.531	138.586	3.977
2/19/2018 12:00	0.173	275.643	0.074	0.959	0.000	90.684	71.214	30.086	147.085	3.823
2/20/2018 15:30	0.188	149.719	0.000	2.048	0.498	59.960	54.752	23.829	67.627	6.499
2/20/2018 17:00	0.213	154.549	0.000	2.167	0.626	352.061	61.869	27.986	67.448	6.537
2/20/2018 18:30	0.236	128.289	0.000	2.481	1.002	389.434	80.646	34.334	58.504	6.429
2/20/2018 20:00	0.260	114.168	0.000	2.679	1.348	409.342	84.317	35.992	77.491	6.736
2/20/2018 21:30	0.224	107.047	0.000	2.604	1.162	372.209	72.845	29.774	66.274	6.662
2/20/2018 23:00	0.231	107.594	0.000	2.726	1.221	407.173	67.568	30.675	68.345	4.568
2/21/2018 0:30	0.189	106.434	0.000	2.870	1.113	345.155	55.065	24.544	66.955	6.475
2/21/2018 2:00	0.195	106.120	0.000	2.919	1.042	369.672	60.018	28.261	67.158	6.454
2/21/2018 3:30	0.204	98.494	0.000	3.092	1.119	342.805	65.561	29.415	62.411	6.364
2/21/2018 5:00	0.208	91.407	0.000	3.673	1.275	348.680	67.275	30.308	58.958	6.223
2/21/2018 6:30	0.234	88.451	0.000	3.376	1.214	364.979	62.952	26.936	52.341	5.976
2/21/2018 8:00	0.212	87.549	0.000	3.344	1.103	371.746	57.328	26.128	55.453	5.280
2/21/2018 9:30	0.197	86.657	0.000	3.460	0.971	47.600	49.217	21.700	55.643	5.816
2/21/2018 11:00	0.164	84.989	0.000	3.506	0.586	7.778	29.832	19.704	49.807	5.349
2/21/2018 12:30	0.167	83.352	0.000	3.632	0.582	8.283	28.807	20.686	51.468	2.760
2/21/2018 14:00	0.208	82.883	0.000	3.593	1.012	405.545	53.215	24.648	51.889	4.356
2/21/2018 15:30	0.214	81.396	0.000	3.740	1.014	421.739	51.267	21.209	44.987	4.473
2/21/2018 17:00	0.228	79.694	0.000	3.765	0.969	437.292	53.527	23.708	54.543	4.888
2/22/2018 19:00	0.210	93.343	0.000	4.878	0.505	442.495	57.824	26.126	46.516	3.760
2/22/2018 22:00	0.206	93.005	0.000	4.955	0.512	318.977	57.588	20.537	34.684	3.270
2/23/2018 1:00	0.197	92.578	0.053	4.991	0.491	392.311	62.223	27.624	47.297	3.449
2/23/2018 4:00	0.204	92.595	0.000	5.129	0.436	388.926	54.459	23.173	37.455	3.021
2/23/2018 7:00	0.222	93.327	0.000	5.230	0.387	397.873	57.967	26.834	45.193	3.455
2/23/2018 10:00	0.205	94.765	0.000	5.262	0.390	489.158	67.350	30.997	52.672	3.669
2/23/2018 13:00	0.208	108.530	0.000	5.185	0.302	445.306	71.150	32.319	64.861	4.201
2/23/2018 16:00	0.226	103.028	0.000	5.247	0.352	394.920	67.139	29.888	56.682	3.632
2/23/2018 19:00	0.211	102.712	0.000	5.298	0.340	502.144	58.850	21.793	36.918	2.362
2/23/2018 22:00	0.201	100.021	0.000	5.570	0.282	291.407	72.462	33.120	57.166	3.890
2/24/2018 1:00	0.203	97.390	0.000	5.588	0.283	252.386	71.140	33.617	56.629	3.661
2/24/2018 4:00	0.213	95.461	0.000	5.566	0.269	412.333	71.574	30.556	49.157	2.346
2/24/2018 7:00	0.207	93.942	0.000	5.609	0.302	459.028	72.507	32.282	49.838	2.773
2/24/2018 10:00	0.208	92.903	0.000	5.688	0.225	437.929	62.097	27.719	41.135	2.276
2/24/2018 13:00	0.221	94.038	0.000	5.681	0.188	418.709	67.140	31.950	49.591	3.214
2/24/2018 16:00	0.217	98.348	0.000	5.651	0.173	395.203	71.398	30.671	49.206	2.149
2/24/2018 19:00	0.216	102.749	0.000	5.620	0.211	332.391	70.792	30.658	53.413	2.993
2/24/2018 22:00	0.206	103.156	0.000	5.697	0.285	431.865	70.826	27.303	47.302	2.509
2/25/2018 1:00	0.198	104.861	0.000	5.692	0.207	374.304	73.794	33.190	62.340	3.287

Date	F^-	Cl^-	Br^-	NO_3-N	PO_4-P	SO_4^{2-}	Ca^{2+}	Mg^{2+}	Na^+	K^+
2/25/2018 4:00	0.209	104.373	0.000	5.821	0.392	372.174	70.175	18.780	33.994	1.887
2/25/2018 7:00	0.202	95.912	0.000	5.733	0.274	387.975	68.848	31.324	56.760	3.348
2/25/2018 10:00	0.202	96.758	0.000	5.880	0.319	447.899	70.938	32.180	56.715	3.178
2/25/2018 13:00	0.206	93.828	0.000	6.048	0.216	450.916	71.945	31.398	52.354	2.977
2/25/2018 14:10	0.225	92.682	0.000	5.842	0.226	933.104	70.059	32.211	52.360	2.942
2/25/2018 22:10	0.211	89.885	0.000	6.174	0.166	506.992	74.369	26.919	38.494	2.125
2/26/2018 6:10	0.217	89.995	0.000	6.214	0.175	473.851	76.594	35.670	49.929	3.087
2/26/2018 22:10	0.232	88.985	0.000	6.198	0.148	590.376	77.864	28.139	35.546	1.999
2/27/2018 14:10	0.225	89.145	0.000	6.316	0.000	407.808	80.076	35.533	45.547	2.281
2/28/2018 22:15	0.227	86.898	0.000	6.408	0.068	466.435	82.887	35.293	42.211	2.080
3/5/2018 21:15	0.247	72.268	0.045	7.192	0.000	430.839	76.232	21.717	21.513	1.165
3/6/2018 20:45	0.225	79.874	0.057	6.858	0.000	431.273	74.344	29.351	34.930	1.698
3/7/2018 23:00	0.223	84.438	0.059	6.615	0.000	421.967	65.267	30.806	36.698	1.659
3/13/2018 15:30	0.227	74.797	0.047	6.566	0.000	379.245	82.226	25.988	24.934	1.203
3/14/2018 11:00	0.238	73.959	0.052	6.674	0.000	368.713	79.453	31.655	29.656	1.267
3/15/2018 13:15	0.234	71.716	0.074	7.017	0.034	435.229	78.487	19.569	16.785	0.738
3/17/2018 4:45	0.196	76.664	0.054	5.898	0.000	433.305	74.084	20.671	22.662	1.051
3/17/2018 7:15	0.220	74.232	0.067	6.449	0.000	428.432	76.135	24.196	23.846	1.095
3/17/2018 10:15	0.217	104.580	0.064	4.462	0.099	417.594	63.027	17.405	36.527	1.291
3/17/2018 14:30	0.204	100.503	0.052	4.855	0.000	436.362	67.850	26.318	49.154	2.037
3/23/2018 15:15	0.182	57.099	0.051	4.752	0.000	360.442	74.349	23.001	20.708	0.832
3/25/2018 14:30	0.156	204.883	0.068	3.872	0.000	320.251	68.273	20.627	69.629	1.206
3/25/2018 19:15	0.161	199.481	0.064	4.220	0.000	341.908	71.262	28.471	78.125	1.693
3/26/2018 3:00	0.128	131.310	0.035	2.113	0.000	223.065	47.406	15.256	52.558	0.902
3/26/2018 12:30	0.139	141.001	0.053	2.996	0.000	305.022	72.159	17.300	59.396	1.028
3/26/2018 20:30	0.131	97.150	0.027	2.491	0.000	249.783	68.377	19.337	53.885	0.987
3/26/2018 22:45	0.154	146.698	0.034	3.777	0.074	349.381	72.195	26.071	78.573	1.742
3/27/2018 0:45	0.150	152.329	0.072	4.269	0.132	302.460	75.920	22.871	56.929	1.381
3/27/2018 3:15	0.192	104.060	0.037	5.890	0.846	429.189	71.847	24.806	51.201	1.308
3/27/2018 4:15	0.372	99.682	0.052	7.194	2.066	373.689	117.647	44.019	58.401	2.812
3/27/2018 4:45	0.367	81.702	0.019	6.341	1.802	421.038	147.409	41.773	45.153	2.862
3/27/2018 5:45	0.343	70.473	0.042	5.895	2.550	417.546	98.637	33.277	43.111	3.636
3/27/2018 7:15	0.307	43.925	0.033	4.535	1.906	321.096	95.213	28.521	22.430	2.729
3/27/2018 7:45	0.529	67.976	0.046	6.751	2.212	331.940	137.668	57.471	40.805	5.687
3/27/2018 12:30	0.532	64.114	0.042	6.386	4.843	1080.697	241.670	67.296	59.919	7.308
3/27/2018 17:15	0.374	71.712	0.048	7.183	1.420	292.601	138.258	54.735	37.752	3.271
3/27/2018 21:45	0.272	73.279	0.046	7.484	2.665	383.735	76.013	31.964	36.952	3.523
3/28/2018 7:00	0.370	66.384	0.040	8.339	1.419	326.451	164.081	59.145	31.610	2.900
3/28/2018 21:45	0.331	66.209	0.053	8.838	1.289	375.800	115.120	48.574	30.909	1.920
3/30/2018 8:45	0.302	63.623	0.041	9.251	1.727	405.752	114.426	51.546	29.249	1.347
3/30/2018 10:45	0.220	61.483	0.051	8.949	0.700	408.927	82.415	40.655	34.292	1.334
3/31/2018 20:45	0.192	52.874	0.046	7.707	0.208	343.215	72.998	31.062	22.720	0.933
4/3/2018 22:00	0.164	73.465	0.036	5.861	0.065	163.670	58.630	16.226	23.939	0.713
4/4/2018 8:45	0.158	73.092	0.051	6.555	0.058	270.007	45.839	16.087	22.683	0.762
4/10/2018 12:15	0.146	38.594	0.046	4.203	0.078	222.774	36.463	5.004	4.428	0.170
4/13/2018 10:00	0.151	42.512	0.028	5.783	0.000	264.358	50.037	15.474	10.077	0.560
4/14/2018 2:15	0.165	48.468	0.025	5.851	0.038	247.058	54.667	16.812	12.372	0.564
4/14/2018 3:00	0.232	64.355	0.026	7.941	0.098	313.898	72.378	18.061	13.671	0.665
4/14/2018 3:15	0.164	39.759	0.034	4.819	0.072	224.426	56.807	15.179	10.904	0.487
4/14/2018 5:00	0.177	52.644	0.031	3.952	0.154	209.058	59.563	12.081	18.280	0.811
4/14/2018 6:00	0.175	66.758	0.035	4.897	0.126	259.396	60.523	16.727	28.723	1.307
4/14/2018 7:30	0.231	89.136	0.053	6.677	0.306	314.468	69.893	21.813	35.830	2.024

Date	F^-	Cl^-	Br^-	NO_3-N	PO_4-P	SO_4^{2-}	Ca^{2+}	Mg^{2+}	Na^+	K^+
4/14/2018 8:00	0.233	88.215	0.050	5.221	0.438	323.883	65.506	20.191	44.616	2.348
4/14/2018 9:30	0.187	69.677	0.035	5.073	0.292	342.409	58.655	15.153	28.670	1.622
4/14/2018 10:45	0.202	74.523	0.028	6.588	0.110	384.586	60.463	18.222	32.142	1.810
4/14/2018 12:45	0.211	79.105	0.000	7.356	0.076	405.744	61.182	18.109	27.225	1.122
4/14/2018 17:00	0.225	91.529	0.060	8.221	0.026	352.919	66.847	19.094	31.781	1.312
4/15/2018 3:30	0.227	80.974	0.063	8.459	0.122	398.083	68.768	26.873	37.984	1.872
5/25/2018 12:15	0.183	34.036	0.000	4.604	0.124	306.871	75.079	27.055	12.489	0.773
5/25/2018 16:45	0.223	42.300	0.000	6.129	0.154	358.143	75.032	29.894	14.558	1.149
5/26/2018 0:15	0.181	29.323	0.000	4.082	0.121	235.471	62.691	20.990	10.042	0.665
5/26/2018 6:30	0.191	37.808	0.000	5.998	0.048	286.222	74.155	29.376	14.759	0.549
5/28/2018 13:45	0.218	49.375	0.000	6.038	0.108	354.649	76.012	25.890	14.023	1.055
5/30/2018 13:45	0.143	25.273	0.000	2.955	0.189	1024.145	70.437	16.677	8.698	0.735
5/30/2018 19:00	0.217	57.739	0.000	7.557	0.193	261.672	77.871	18.614	16.782	4.953
5/30/2018 19:15	0.411	38.069	0.000	2.497	1.778	1603.322	74.399	19.649	16.564	4.195
5/30/2018 19:30	0.296	36.161	0.000	4.748	1.667	1048.252	58.869	17.882	19.614	3.970
5/30/2018 20:30	0.273	29.947	0.000	4.590	1.181	640.778	55.295	16.413	15.545	3.621
5/30/2018 21:00	0.271	30.393	0.000	4.905	0.923	425.805	52.475	17.079	15.547	3.411
5/30/2018 21:30	0.240	30.134	0.000	5.231	0.867	364.793	-	-	-	-
5/31/2018 16:30	-	-	-	-	-	-	74.524	28.718	28.123	2.020
6/1/2018 4:15	0.217	56.376	0.000	6.676	0.283	223.063	65.707	26.795	23.743	2.078
6/1/2018 19:30	0.223	53.281	0.000	7.438	0.124	379.025	72.354	29.998	20.931	1.528
6/2/2018 11:45	0.226	49.867	0.000	8.045	0.115	292.938	77.629	32.125	19.345	1.267
6/8/2018 4:45	0.245	48.692	0.000	7.660	0.104	326.822	77.642	21.742	10.817	0.786
6/10/2018 6:45	0.203	53.644	0.000	5.832	0.206	377.738	72.082	29.912	22.226	1.579
6/10/2018 9:15	0.206	41.566	0.000	4.808	0.190	322.931	56.463	19.762	17.013	1.669
6/10/2018 11:00	0.190	44.678	0.000	6.031	0.380	348.536	66.547	25.995	20.175	2.356
6/10/2018 12:15	0.211	40.478	0.000	5.830	0.569	344.192	69.368	24.063	18.662	2.567
6/10/2018 12:45	0.232	40.364	0.000	6.119	0.760	361.442	70.934	23.991	18.057	1.560
6/10/2018 13:30	0.229	26.351	0.000	3.571	0.738	251.145	63.966	17.519	13.731	0.940
6/10/2018 14:15	0.220	21.514	0.000	3.080	0.764	235.925	62.228	13.956	8.450	2.032
6/10/2018 14:45	0.282	26.158	0.000	3.833	1.215	354.982	67.628	19.904	13.278	3.578
6/10/2018 15:30	0.286	20.101	0.000	3.780	1.302	290.911	67.936	19.209	8.547	1.957
6/10/2018 16:15	0.284	20.141	0.000	4.364	1.180	314.868	79.270	26.828	8.208	1.571
6/10/2018 18:30	0.284	19.165	0.000	4.626	1.283	283.543	78.292	24.415	7.053	4.079
6/10/2018 20:30	0.347	22.843	0.000	5.491	1.695	298.814	92.228	33.117	9.503	5.281
6/10/2018 21:45	0.299	32.002	0.000	5.683	1.457	315.971	79.851	26.774	11.645	4.079
6/10/2018 22:45	0.306	35.111	0.000	5.966	1.446	308.379	74.461	26.898	14.833	4.840
6/11/2018 11:30	0.319	22.406	0.000	5.158	1.101	151.007	104.919	37.605	8.511	2.508
6/11/2018 18:15	0.325	33.043	0.000	7.890	0.767	328.541	145.995	58.448	14.141	2.226
6/12/2018 2:30	0.333	34.865	0.000	8.512	0.829	231.093	131.094	47.798	13.549	1.770
6/19/2018 12:00	0.201	28.286	0.000	5.889	0.202	168.558	72.266	25.319	9.181	0.764
6/21/2018 4:00	0.174	24.461	0.000	4.679	0.240	223.435	55.731	18.754	8.619	0.682
6/21/2018 10:15	0.186	28.432	0.000	4.400	0.179	225.331	56.711	17.283	12.563	1.266
6/21/2018 16:15	0.187	29.937	0.000	4.153	0.347	261.641	63.789	18.408	13.709	0.627
6/21/2018 17:15	0.171	23.254	0.000	3.470	0.593	166.571	43.837	14.546	10.297	1.810
6/21/2018 18:15	0.246	24.880	0.000	4.654	1.053	346.370	60.788	21.206	11.230	3.117
6/21/2018 18:45	0.326	27.669	0.000	5.063	1.194	347.591	113.525	42.719	12.851	4.238
6/21/2018 19:00	0.265	20.952	0.000	3.815	1.403	180.966	90.959	29.055	8.204	4.024
6/21/2018 20:00	0.295	15.564	0.000	2.698	1.341	304.346	64.326	21.709	5.579	4.076
6/21/2018 23:30	0.274	17.370	0.000	3.067	1.397	308.899	49.701	16.519	5.998	1.563
6/22/2018 0:45	0.263	17.993	0.000	3.540	1.343	302.427	51.042	15.521	5.265	2.880
6/22/2018 3:30	0.300	24.511	0.000	3.974	1.353	272.677	71.989	23.505	10.911	4.297

Date	F^-	Cl^-	Br^-	NO_3-N	PO_4-P	SO_4^{2-}	Ca^{2+}	Mg^{2+}	Na^+	K^+
6/22/2018 8:30	0.279	33.546	0.000	5.060	1.002	339.917	71.808	28.678	16.118	4.573
6/22/2018 13:15	0.313	35.326	0.000	5.926	0.776	363.455	88.621	31.360	13.101	3.486
6/22/2018 22:00	0.283	35.827	0.000	6.263	0.830	342.182	80.660	30.995	14.771	2.246
6/23/2018 23:00	0.220	40.592	0.000	8.303	0.278	315.111	65.874	14.175	7.713	0.761
7/14/2018 9:00	0.245	37.189	0.000	4.296	0.211	388.356	74.629	32.151	13.016	1.635
7/14/2018 10:45	0.237	36.499	0.000	4.259	0.151	346.990	73.928	33.243	13.713	1.395
7/14/2018 11:00	0.242	38.053	0.000	4.251	0.169	364.433	74.313	33.105	14.413	1.395
7/14/2018 20:30	0.242	48.179	0.000	4.236	0.180	383.377	68.013	27.721	20.235	3.189
7/14/2018 22:30	0.226	48.194	0.000	2.826	0.316	353.106	49.850	17.955	22.465	4.282
7/15/2018 0:45	0.204	44.206	0.000	1.783	0.330	347.665	42.534	14.933	21.735	3.451
7/15/2018 4:45	0.220	45.392	0.000	2.817	0.160	355.587	58.013	22.153	21.329	1.729
7/16/2018 8:30	0.236	55.552	0.000	2.829	0.109	377.456	70.135	30.278	24.896	2.271
7/27/2018 4:30	0.241	47.352	0.031	1.370	0.084	373.334	54.284	11.436	4.605	0.534
7/30/2018 8:15	0.250	44.166	0.017	1.145	0.000	370.697	71.003	35.851	18.677	1.572
8/7/2018 3:00	0.211	32.716	0.000	0.968	0.045	377.635	56.402	23.774	8.459	1.312
8/9/2018 20:45	0.231	39.543	0.036	0.835	0.052	424.012	59.335	24.428	10.372	1.378
8/29/2018 7:30	0.257	34.125	0.003	0.568	0.266	286.179	46.359	23.604	16.497	3.170
8/29/2018 16:45	0.227	60.419	0.025	0.669	0.192	238.299	43.058	18.753	29.486	5.433
10/6/2018 8:00	0.106	36.031	0.035	0.602	0.438	271.945	27.029	8.205	16.696	3.575
10/6/2018 12:00	0.115	44.288	0.069	0.659	0.519	268.711	25.377	8.440	18.059	4.101
10/6/2018 14:30	0.097	27.603	0.020	0.542	0.255	141.336	23.978	6.642	13.538	2.615
10/6/2018 17:00	0.107	40.024	0.024	0.713	0.340	223.197	24.179	6.574	13.102	4.500
10/6/2018 19:15	0.134	48.590	0.039	0.706	0.399	273.864	31.864	10.160	28.626	4.377
10/6/2018 20:30	0.090	35.447	0.039	0.580	0.314	162.941	24.791	7.300	21.502	2.896
10/6/2018 22:45	0.171	76.834	0.098	0.662	0.347	256.590	49.486	18.586	44.155	4.958
10/7/2018 0:15	0.156	51.806	0.037	0.667	0.372	237.382	45.741	15.447	31.419	4.139
10/7/2018 4:45	0.133	33.828	0.000	0.683	0.614	303.857	30.009	8.594	18.870	4.070
10/7/2018 8:00	0.125	42.320	0.055	0.657	0.378	259.215	36.655	12.098	26.278	4.578
10/7/2018 12:30	0.163	48.607	0.032	0.597	0.192	242.846	41.977	12.029	24.949	2.907
10/7/2018 18:30	0.184	60.120	0.071	0.612	0.138	271.467	43.984	15.149	29.753	2.928
10/7/2018 20:30	0.167	55.471	0.059	0.656	0.316	266.023	41.203	14.464	27.667	2.941
10/7/2018 21:00	0.268	57.793	0.079	0.690	0.567	301.972	55.769	15.323	22.134	3.664
10/7/2018 22:30	0.295	32.107	0.042	0.606	0.691	268.309	48.020	15.316	19.774	4.196
10/7/2018 23:00	0.161	42.446	0.031	0.649	0.852	239.090	53.399	17.666	25.011	4.750
10/8/2018 1:00	0.185	45.981	0.055	0.843	0.829	230.004	60.130	19.040	24.400	4.852
10/8/2018 1:30	0.191	34.069	0.042	0.830	0.976	242.084	55.961	19.027	20.518	5.033
10/8/2018 2:15	0.161	24.734	0.023	0.703	0.975	263.286	40.166	9.348	9.720	3.146
10/8/2018 3:45	0.155	24.859	0.044	0.831	0.823	257.511	49.819	10.256	10.555	3.637
10/8/2018 5:00	0.154	28.859	0.038	0.921	0.850	226.210	38.437	9.664	13.274	3.972
10/8/2018 8:30	0.166	42.347	0.040	1.190	0.616	251.743	41.941	14.549	24.297	4.860
10/8/2018 12:00	0.155	48.339	0.061	1.218	0.439	282.819	39.507	15.967	28.425	4.439
10/10/2018 23:15	0.179	44.995	0.047	1.016	0.402	245.805	42.106	13.226	20.751	3.618
10/31/2018 4:00	0.172	44.465	0.062	0.730	0.614	223.932	44.936	11.301	17.889	2.935
10/31/2018 7:00	0.175	62.008	0.076	1.137	0.667	253.213	50.072	13.589	21.322	3.237
10/31/2018 7:30	0.108	32.265	0.041	0.790	0.533	164.061	40.569	6.827	10.470	1.627
10/31/2018 9:15	0.135	51.103	0.057	1.217	0.683	300.669	45.616	12.489	22.297	4.861
10/31/2018 10:30	0.076	25.428	0.023	0.817	0.521	103.666	26.655	8.179	13.825	3.076
10/31/2018 11:45	0.143	44.916	0.036	1.443	0.544	359.334	40.660	14.998	25.871	5.602
10/31/2018 12:45	0.141	45.674	0.033	1.614	0.392	313.184	42.048	13.828	23.498	4.724
11/25/2018 23:45	0.169	97.444	0.002	3.108	0.126	285.141	78.670	29.083	54.980	3.698
11/26/2018 1:45	0.159	96.401	0.000	3.231	0.284	299.970	74.121	26.831	54.947	4.176
11/26/2018 2:45	0.168	102.676	0.002	3.275	0.284	296.476	79.774	27.914	56.666	4.033

Date	F^-	Cl^-	Br^-	NO_3-N	PO_4-P	SO_4^{2-}	Ca^{2+}	Mg^{2+}	Na^+	K^+
11/26/2018 3:30	0.182	96.027	0.029	3.006	0.355	260.253	74.310	20.955	41.457	3.182
11/26/2018 5:15	0.164	87.809	0.022	3.143	0.284	279.588	67.396	23.677	51.537	4.063
11/26/2018 7:15	0.164	77.778	0.002	3.277	0.395	249.411	59.613	21.146	45.100	4.479
11/26/2018 8:45	0.159	74.592	0.001	3.609	0.170	305.390	60.425	12.645	24.369	2.174
11/26/2018 11:45	0.175	75.024	0.000	4.123	0.108	337.565	63.929	23.345	40.450	3.668
11/26/2018 16:30	0.191	86.796	0.008	4.437	0.131	332.392	69.357	25.896	49.836	3.542
12/1/2018 10:15	0.171	117.890	0.009	3.973	0.202	256.579	78.917	26.051	65.476	3.984
12/1/2018 10:45	0.163	103.715	0.000	4.029	0.371	333.387	70.687	24.683	55.270	3.661
12/1/2018 11:30	0.188	107.205	0.011	4.234	0.608	299.137	82.830	25.807	55.115	4.045
12/1/2018 13:00	0.208	106.075	0.013	4.419	0.692	246.656	92.543	30.060	59.440	4.886
12/1/2018 13:30	0.224	126.159	0.000	3.937	1.064	206.165	94.788	28.608	73.736	5.411
12/1/2018 14:30	0.216	92.919	0.000	3.432	1.257	283.006	85.976	27.806	54.023	5.918
12/1/2018 15:15	0.182	71.997	0.002	3.215	0.797	250.564	68.378	19.219	35.723	4.471
12/1/2018 16:00	0.203	68.092	0.005	3.850	0.890	318.600	70.411	22.228	33.255	4.329
12/1/2018 16:30	0.220	65.652	0.029	4.273	0.838	246.089	89.104	26.780	36.579	5.241
12/1/2018 18:30	0.181	57.789	0.002	5.053	0.582	263.926	63.016	22.303	29.264	3.784
12/1/2018 21:45	0.206	58.132	0.000	4.675	0.738	453.623	81.101	25.969	30.938	3.502
12/2/2018 8:15	0.206	69.443	0.001	5.561	0.766	345.127	86.970	29.512	37.499	3.902
12/2/2018 13:30	0.183	65.587	0.012	5.365	0.439	343.346	77.013	26.408	33.392	3.149
12/3/2018 7:30	0.193	68.865	0.001	5.981	0.166	252.140	83.665	30.605	35.880	2.888
12/13/2018 13:00	0.208	62.838	0.028	6.341	0.255	364.428	99.593	37.125	29.103	1.471
12/13/2018 21:30	0.191	60.912	0.005	6.456	0.042	324.181	97.395	30.817	23.800	1.214
12/13/2018 23:30	0.174	59.507	0.002	6.173	0.031	372.393	95.796	26.576	20.603	1.003
12/14/2018 16:45	0.194	129.117	0.018	6.201	0.035	292.655	92.473	27.500	53.576	2.001
12/14/2018 18:45	0.205	103.741	0.000	5.335	0.127	303.418	89.060	26.823	50.427	1.941
12/14/2018 22:30	0.223	107.574	0.000	5.883	0.034	245.044	91.146	33.571	60.630	2.425
12/27/2018 12:45	0.246	78.127	0.014	5.780	0.053	299.266	98.475	34.948	40.759	2.579
12/27/2018 14:00	0.184	70.675	0.000	5.394	0.111	264.437	85.865	23.901	29.438	1.720
12/27/2018 14:45	0.176	68.179	0.005	5.041	0.167	243.479	80.263	22.383	27.784	1.756
12/27/2018 16:30	0.194	79.583	0.008	6.133	0.468	266.789	89.866	26.167	33.518	1.928
12/27/2018 18:15	0.172	69.393	0.038	5.864	0.311	271.672	77.924	21.512	27.885	1.725
12/27/2018 19:30	0.175	69.557	0.001	5.776	0.269	279.232	75.182	20.331	26.643	1.746
12/27/2018 21:15	0.195	59.870	0.000	6.059	0.126	278.153	74.388	17.354	18.476	1.246
12/28/2018 1:45	0.195	61.438	0.000	7.568	0.095	280.665	83.824	22.965	20.837	1.415
12/28/2018 9:30	0.175	62.349	0.040	7.359	0.158	291.091	102.515	38.166	35.383	2.110
12/28/2018 12:15	0.201	66.218	0.000	7.517	0.087	353.779	86.116	33.631	32.452	2.095
12/31/2018 12:15	0.178	61.714	0.000	6.056	0.057	257.323	70.618	22.850	22.979	1.319
12/31/2018 13:00	0.183	63.408	0.000	6.533	0.130	254.753	56.154	18.763	17.701	1.075
12/31/2018 13:30	0.189	65.368	0.000	6.153	0.320	311.485	75.380	19.856	23.670	1.662
12/31/2018 14:30	0.179	57.003	0.011	5.624	0.363	267.450	52.170	17.271	18.119	1.619
12/31/2018 15:15	0.211	54.603	0.006	5.317	0.749	302.471	78.298	21.410	19.801	2.462
12/31/2018 16:15	0.232	44.574	0.000	5.263	0.920	281.475	99.038	26.271	19.780	3.561
12/31/2018 16:45	0.214	41.560	0.008	4.782	1.318	255.845	104.316	30.534	21.755	4.865
12/31/2018 18:00	0.225	33.266	0.000	4.431	1.515	267.022	95.478	26.298	12.450	6.780
12/31/2018 18:45	0.191	31.545	0.024	4.644	1.420	243.329	121.009	34.334	15.137	6.547
12/31/2018 19:45	0.203	31.577	0.000	4.921	1.391	294.715	41.497	16.184	7.728	6.314
12/31/2018 21:30	0.252	39.278	0.000	6.245	1.307	335.021	93.900	33.372	18.256	5.237
1/1/2019 1:00	0.226	46.403	0.000	6.864	0.790	253.014	71.823	27.409	22.256	4.142
1/1/2019 5:00	0.188	44.057	0.000	6.418	0.724	235.890	101.392	35.216	22.210	3.281
1/1/2019 12:00	0.294	47.140	0.005	6.932	0.532	251.919	82.986	30.564	22.164	3.408
1/2/2019 0:15	0.477	50.449	0.000	7.892	0.508	264.985	93.315	32.943	24.266	3.452
1/2/2019 7:00	0.349	49.375	0.003	8.040	0.981	275.787	94.190	33.745	23.657	3.024

Date	F^-	Cl^-	Br^-	NO_3-N	PO_4-P	SO_4^{2-}	Ca^{2+}	Mg^{2+}	Na^+	K^+
1/2/2019 17:30	0.422	51.073	0.000	8.686	1.396	286.799	130.869	40.589	19.758	2.184
2/6/2019 14:25	0.309	66.831	0.037	6.586	1.049	291.055	98.568	39.025	30.839	3.472
2/6/2019 18:30	0.238	54.657	0.059	6.543	0.826	263.926	75.714	26.462	21.164	2.810
2/7/2019 6:30	0.327	35.440	0.038	4.788	2.047	271.135	118.353	32.162	14.598	7.090
2/7/2019 14:25	0.217	45.037	0.048	5.335	1.160	229.284	59.813	20.077	17.586	3.951
2/7/2019 16:25	0.216	46.675	0.041	5.847	1.005	237.401	64.684	24.532	20.718	3.672
2/11/2019 10:40	0.179	91.535	0.044	5.472	0.593	218.137	75.586	27.019	47.474	3.018
2/12/2019 8:40	0.253	88.482	0.041	4.996	1.291	337.750	84.287	28.498	44.965	2.934
2/12/2019 12:35	0.186	112.017	0.044	5.549	0.547	286.411	78.999	28.926	59.226	3.042
2/12/2019 14:40	0.200	136.851	0.060	5.723	0.686	276.242	76.196	28.863	73.808	3.131
2/12/2019 16:40	0.203	155.749	0.037	5.927	0.690	270.279	69.250	19.881	60.188	2.164

Table 2. WS1.25 event data.

Date	F^-	Cl^-	Br^-	NO_3-N	PO_4-P	SO_4^{2-}	Ca^{2+}	Mg^{2+}	Na^+	K^+
2/19/2018 17:30	0.207	185.777	0.077	1.102	0.000	9.967	59.011	21.527	113.145	4.210
2/19/2018 19:00	0.148	142.489	0.000	0.978	0.000	7.112	43.433	15.004	87.902	3.815
2/19/2018 20:15	0.151	140.314	0.065	1.053	0.000	7.449	47.635	14.290	70.045	2.957
2/19/2018 21:45	0.136	166.031	0.070	1.435	0.000	8.767	55.439	18.245	100.020	4.876
2/19/2018 23:15	0.144	138.605	0.000	1.306	0.012	7.964	49.583	15.763	72.165	3.600
2/20/2018 0:45	0.144	161.951	0.067	1.463	0.042	9.108	52.634	18.173	88.782	4.910
2/20/2018 2:15	0.144	128.272	0.000	1.356	0.114	7.843	46.334	13.819	66.314	3.898
2/20/2018 3:45	0.148	140.308	0.061	1.593	0.105	8.502	48.301	15.849	73.190	3.840
2/20/2018 5:15	0.134	140.743	0.062	1.702	0.220	8.428	52.314	18.679	82.935	6.134
2/20/2018 6:45	0.140	135.018	0.060	1.792	0.077	8.463	50.575	17.721	77.837	5.980
3/26/2018 16:00	0.131	159.796	0.069	4.527	0.000	12.212	95.711	28.873	81.045	1.654
3/26/2018 18:30	0.105	267.521	0.087	3.531	0.000	10.819	88.622	19.178	108.077	1.051
3/26/2018 21:00	0.130	133.963	0.000	3.211	0.010	7.579	61.242	14.893	60.901	0.958
3/26/2018 23:30	0.127	126.034	0.054	5.662	0.000	8.074	65.579	21.869	73.374	1.089
3/27/2018 2:00	0.148	78.678	0.000	5.776	0.000	5.929	44.597	15.836	45.017	1.436
3/27/2018 4:30	0.185	93.490	0.000	5.934	0.597	6.922	52.425	16.763	46.777	2.086
3/27/2018 7:00	0.198	94.551	0.000	6.165	0.562	7.755	61.041	19.672	57.666	3.526
3/27/2018 9:30	0.206	89.428	0.000	6.135	1.146	7.347	50.632	18.514	47.811	2.432
3/27/2018 12:00	0.207	85.481	0.000	5.799	1.346	7.368	55.800	18.993	46.199	2.155
3/27/2018 17:00	0.202	91.436	0.000	6.022	0.975	8.262	60.740	20.227	45.993	3.609
3/27/2018 22:00	0.193	84.180	0.000	6.459	0.743	8.259	63.314	21.032	44.812	3.213
3/28/2018 5:30	0.191	71.851	0.000	7.176	0.657	8.369	66.324	20.485	34.862	1.296
3/28/2018 15:30	0.183	76.095	0.000	7.765	0.265	8.877	67.366	24.678	38.453	1.231
3/29/2018 1:30	0.179	71.666	0.000	8.018	0.185	8.969	83.984	25.813	35.883	1.891
3/29/2018 12:00	0.207	73.146	0.000	8.019	0.238	9.774	80.790	24.410	33.627	1.110
3/29/2018 20:00	0.200	66.983	0.000	7.380	0.215	9.068	68.124	23.551	31.030	1.415
3/30/2018 14:00	0.172	71.847	0.000	8.378	0.091	10.062	72.022	24.875	28.933	1.406
3/30/2018 22:00	0.168	67.851	0.000	7.737	0.000	9.603	63.870	10.740	15.683	0.494
5/3/2018 1:00	0.238	61.875	0.000	7.644	0.000	12.443	55.615	19.166	13.718	0.285
5/3/2018 3:30	0.158	59.041	0.000	6.788	0.000	11.226	84.611	16.472	11.050	0.252
5/3/2018 6:00	0.137	67.202	0.065	7.739	0.000	12.060	91.855	35.006	30.640	1.282
5/3/2018 8:30	0.157	78.804	0.000	6.075	0.000	12.039	93.963	31.384	33.835	1.341
5/3/2018 11:00	0.157	77.122	0.055	6.479	0.000	11.961	103.638	33.126	36.211	1.362
5/3/2018 13:30	0.140	75.479	0.061	6.153	0.000	11.406	83.965	16.301	15.775	0.555
5/3/2018 16:00	0.143	74.263	0.000	6.049	0.000	11.582	92.397	31.375	35.930	1.505

Table 3. WS1.5 event data.

Date	F^-	Cl^-	Br^-	NO_3-N	PO_4-P	SO_4^{2-}	Ca^{2+}	Mg^{2+}	Na^+	K^+
9/7/2018 9:00	0.335	68.911	0.048	0.419	0.000	14.138	68.450	29.471	36.891	4.578
9/7/2018 11:30	0.370	69.009	0.029	0.418	0.000	14.078	68.553	26.848	36.473	2.931
9/7/2018 14:00	0.316	75.873	0.035	0.406	0.000	14.975	67.166	26.311	41.000	4.943
9/7/2018 16:30	0.294	78.093	0.061	0.415	0.000	11.709	61.013	22.912	41.245	4.926
9/7/2018 19:00	0.253	82.373	0.143	0.424	0.045	11.506	60.378	20.772	43.798	5.753
9/7/2018 21:30	0.262	79.985	0.142	0.433	0.000	11.253	53.385	17.562	44.190	2.832
9/8/2018 0:00	0.199	79.512	0.096	0.530	0.000	10.309	50.428	15.584	46.266	4.032
9/8/2018 2:30	0.203	73.711	0.084	0.673	0.045	9.082	44.005	12.950	44.130	4.490
9/8/2018 5:00	0.168	58.811	0.032	0.709	0.000	7.332	17.618	9.472	36.623	3.860
9/8/2018 10:00	0.175	46.054	0.012	0.657	0.131	6.684	34.402	7.597	30.389	3.182
9/8/2018 15:00	0.166	54.968	0.037	0.660	0.113	7.401	39.864	9.910	36.042	1.951
9/8/2018 20:00	0.176	65.944	0.032	0.626	0.039	7.310	45.340	14.519	39.818	3.349
9/9/2018 3:30	0.216	53.613	0.013	0.565	0.062	6.059	47.542	14.508	31.225	3.227
9/9/2018 10:45	0.204	65.103	0.013	0.559	0.001	7.725	47.134	17.597	36.609	1.918